AD_____
(Leave blank)

Award Number: W81XWH-09-1-0200

TITLE: Nuclear Matrix Proteins in Disparity of Prostate Cancer

PRINCIPAL INVESTIGATOR: Asim B. Abdel-Mageed, D.V.M., MS, Ph.D.

CONTRACTING ORGANIZATION:
Tulane University School of Medicine
New Orleans, LA 70112

REPORT DATE: September 2013

TYPE OF REPORT:
Final

PREPARED FOR: U.S. Army Medical Research and Materiel Command
Fort Detrick, Maryland 21702-5012

REPORT DOCUMENTATION PAGE

Form Approved
OMB No. 0704-0188

1. REPORT DATE *(DD-MM-YYYY)*	2. REPORT TYPE	3. DATES COVERED *(From - To)*
1 Sept 2013	Final	1 July 2009-30Jun 2013

4. TITLE AND SUBTITLE
Nuclear Matrix Proteins in Disparity of Prostate Cancer

5a. CONTRACT NUMBER

5b. GRANT NUMBER
W81XWH-09-1-0200

5c. PROGRAM ELEMENT NUMBER

6. AUTHOR(S)
Asim B. Abdel-Mageed

email: amageed@tulane.edu

5d. PROJECT NUMBER

5e. TASK NUMBER

5f. WORK UNIT NUMBER

7. PERFORMING ORGANIZATION NAME(S) AND ADDRESS(ES)

Tulane University School of Medicine
New Orleans, LA 70112

8. PERFORMING ORGANIZATION REPORT NUMBER

9. SPONSORING / MONITORING AGENCY NAME(S) AND ADDRESS(ES)
U.S. Army Medical Research and Material Command
Fort Detrick, MD 21702-5015

10. SPONSOR/MONITOR'S ACRONYM(S)

11. SPONSOR/MONITOR'S REPORT NUMBER(S)

12. DISTRIBUTION / AVAILABILITY STATEMENT
Approved for public release: distribution unlimited.

13. SUPPLEMENTARY NOTES

14. ABSTRACT: African Americans(AA) have twice the incidence and mortality of prostate (PC) than Caucasian Americans (CA). While the disproportionate burden was partially explained by genetic, socioeconomic, and environmental factors, racial variation in the biology of prostate tumors was not investigated. We employed an unbiased functional genomics approach to identify genes differentially expressed in freshly procured prostate tumor cells of age- and tumor grade-matched AA and CA men. Microdissected (LCM)-procured *in vivo*-derived genetic materials of matched normal epithelium and PC cells were subjected to suppressive subtractive hybridization (SSH) to construct microarray chips encompassing two sets of race-based, PC-specific cDNAs. We demonstrate selective expression of the nuclear matrix proteins heterogeneous nuclear ribonucleoprotein H1 (hnRNP H1) and scaffold attachment factor B2 (SAFB2) in PC cells that correlate with disease progression and poor prognosis in AA men. SAFB2 and hnRNP H1 promote growth of PC cells via diverse mechanisms. Functional studies demonstrate that hnRNP H1 physically interacts with and induces AR transactivation in hormone dependent and independent manner. As an ERα co-repressor, SAFB2 potentially paves the way for activation of E2-ERβ axis, which in-turn promotes tumor growth through activation of AR signaling under hormone deprivation conditions. Our findings support a model in which hnRNPH1 is an auxiliary novel coactivator for AR and that activation of E2-ERβ axis in prostate tumors is a poor prognostic indicator of disease progression and survival. Collectively, both SAFB2 and hnRNPH1 have potential clinical utility as biomarkers, prognostic indicators and/or therapeutic targets in advanced PC, especially among AA-men.

15. SUBJECT TERMS
Prostate cancer, health disparity, differential gene expression, nuclear matrix proteins, SAFB2, hnRNPH1, progression.

16. SECURITY CLASSIFICATION OF:			17. LIMITATION OF ABSTRACT	18. NUMBER OF PAGES	19a. NAME OF RESPONSIBLE PERSON
a. REPORT	b. ABSTRACT	c. THIS PAGE			19b. TELEPHONE NUMBER *(include area code)*
U	U	U	UU	91	

Table of Contents

Introduction:

Racial make-up has been identified as one of many risk factors for PC with 50% higher incidence and mortality rates among AA men than CA counterparts (1). Earlier onset of the disease, high disease volume, aggressive metastatic disease, and poor survival rate are evident among AA males (2, 3). Although the disproportionate incidence and mortality cannot be fully explained by genetic, socioeconomic, and environmental factors (4, 5), chromosome 8q24 has recently been implicated in susceptibility of AA men to PC (6, 7). While a more biological aggressive phenotype has been proposed (8), little attention was focused on unraveling the underlying molecular mechanisms involved in racial disparity of PC.

Aberrant expression of AR has long been implicated in initiation and development of castration-resistant prostate cancer (CRPC) (9). Based on their physical interactions and ability to modulate transcription, a repertoire of intermediary transcriptional protein complexes (coactivators and corepressors) have been shown to be recruited by AR to modify chromatin and facilitate transcription of androgen-regulated genes (AGRs) in cell type-specific manner (10). Notably, the differential expression and pathophysiological significance of these cofactors in CRPC in AA men has not been established. These facts argue that aberrant expression and/or function of AR and its coregulators may contribute to disease progression and emergence of CRPC in AA men.

As a residual scaffolding of the nucleus to which repeated DNA sequences and actively transcribed genes are anchored (11), the nuclear matrix (NM), has recently sparked a surge of interest as being the molecular underpinning of cancer-specific markers (12). The family of heterogeneous nuclear ribonucleoproteins (hnRNPs) has more than 30 members of ubiquitously expressed NM proteins (13). hnRNPs complex with heterogeneous nuclear RNA (hnRNA) and modulate pre-mRNA biogenesis, metabolism, and transport (14). The hnRNP H/F is subfamily of hnRNPs encoded by different genes into subtype-naïve forms, including hnRNP H (hnRNP H1), hnRNP H' (hnRNP H2), hnRNP F, and hnRNP 2H9 (15). These proteins possess a modular and highly conserved structure encompassing two glycine-rich auxiliary domains and two or three repeats of RNA binding domain termed quasi-RNA recognition motif (qRRM). The hnRNP H/F members bind in concert to cognate G-rich intronic and exonic sequences in close proximity to the polyadenylation site to regulate both inhibitory and stimulatory alternative splicing of target genes (16). As a bona fide component of the NM, (17), the functional significance of hnRNP H1 is relatively unknown and only recently has evidence emerged related to its biological function. Although hnRNP H1 has been shown to be expressed in a number of human cancers (18), its functional significance in cancer development and/or progression has not been elucidated. The rapid reduction of hnRNP H1 transcripts in cells undergoing differentiation (19) underscores a potential role for this NM protein in tumor cell differentiation.

In the present study we identified by an *in vivo* functional genomics approach, encompassing a combined in tandem approach of LCM, SSH and custom cDNA microarray comparative analyses, the differential expression of hnRNP H1 in prostate tumor cells of AA men and further characterized its functional role in cell growth and development of therapeutic resistance through transcriptional regulation and activation of AR in hormone dependent and independent manner.

Body:

Task-1. To examine if hormone receptors mediate hnRNPH1 and SAFB2 induced growth and metastasis of PC cells *in vitro*. (*Months 1-12*).

Task-1a: siRNA silencing or ectopic expression strategies to determine if SAFB2 and/or hn-RNP-H1 gene(s) will modulate growth, colony-forming ability, cell cycle characteristics, and viability of PC cells.

Task-1b: Effects of target genes in modulating hormone receptor gene expression by qRT-PCR and western blot analysis.

Task1c: Effect of target genes on regulating promoter activities of hormone receptors (AR, ER) using reporter assays, EMSA and ChIP assays.

Task1d: Effect of target genes on binding to hormone receptor promoters using ChIP assay, and their protein-protein interactions by co-immunoprecipitation, and EMSA.

SAFB2 Gene

Our preliminary data show that SAFB2 or hnRNPH1 are selectively expressed in prostate tumors of AA-men, as opposed to CA-men. For Task-1a tests the hypothesis that silencing of either SAFB2 and/or hnRNPH1 inhibits growth of prostate cancer (PC) cell lines in vitro. As shown in Figure 1, siRNA silencing of either genes resulted in significant inhibition of AR-expressing MDA-PCa-2b PC cells *in vitro*. The data further attests to the tumor growth promoting ability of both nuclear matrix proteins, especially among AA-men.

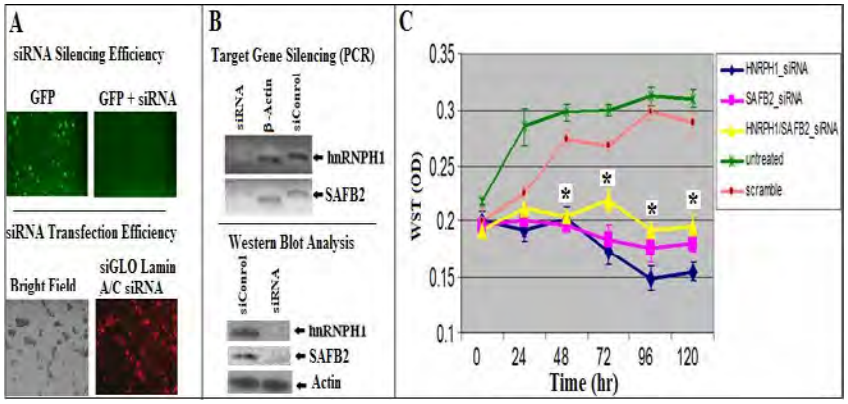

Fig. 1: optimization of silencing and transfection efficiencies of siRNA in PC cells using GFP and siGLO Lamin A/C siRNAs using serum-free Opti-MEM I, with Lipofectamine and RNase inhibitor. **B,** PCR and western blot analyses of hnRNPH1 and SAFB2 in MDA-PCa-2b cells 24hr after transfection with siCONTROL non-targeting siRNA, or target gene siRNAs (Dharmacon, Inc.). **C**, effects of siRNA silenced genes, alone or in combination, on growth of MDA-PCa-2b cells. Cells were grown in *complete* RPMI media. * denotes significant difference in comparison to siControl-transfected cells at 5% level (*t*-test).

Results: The growth of PC cells was significantly impaired when either of the target genes was silenced (72hr). **Pitfalls and Corrective Measures:** Unexpectedly silencing of SAFB2, unlike hnRNPH1, proved to be lethal to the PC cells (>96hrs), despite trying various experimental strategies. This unanticipated development hindered our ability to carry out long-term *in vitro* and *in vivo* experiments under silencing conditions. However, based on our proposed hypothesis that *SAFB2, as a selective co-repressor for ERα, paves the way for PC cell growth through activation of estrogens (E2)-ERβ axis in these cells*, we modified this approach to explore the functional significance of the down-stream target of SAFB2 (*E2-ERβ* signaling axis) in growth of PC cell both *in vitro* and *in vivo.*

For **task-1b**, we examined if activation of E2-ERβ signaling axis modulate expression of androgen receptor (AR) *in vitro*. As shown in Fig.2 (next page), the constitutive levels of AR are high in LNCaP and C4-2B cells, but undetectable in PC-3 and DU-145 cells (Fig.2A). In contrast, higher endogenous levels of ERβ were detected in PC-3 cells relative of AR-expressing cells (Fig 2B). However, ERβ levels are at least twice as high in C4-2B cells compared to LNCaP cells. Interestingly, we observed that E2 induces expression of AR (5 to 7-fold) in both AR-expressing cells, but to a higher extent in C4-2B cells (Fig. 2C).

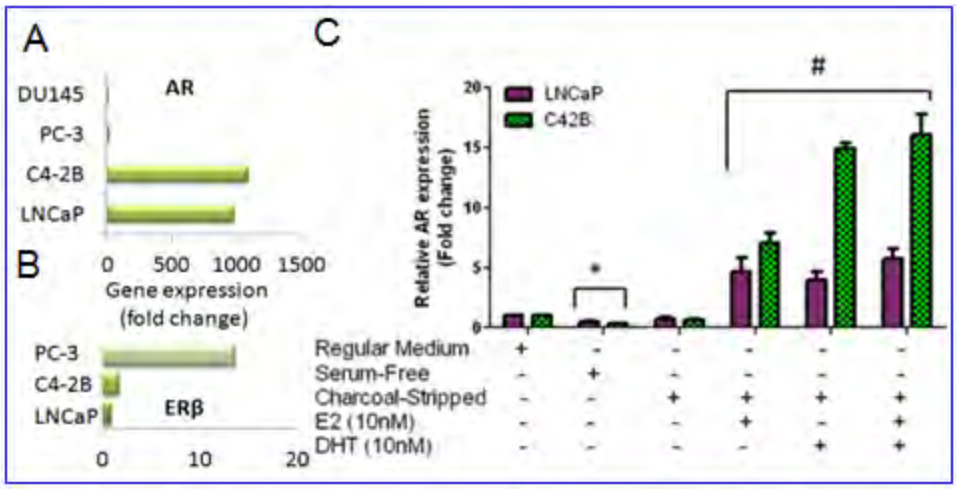

Fig. 2: Constitutive and induced expression of steroid hormones in PC cells. **A & B**, denote endogenous levels of AR and ERβ in a panel of PC cells (LNCaP, PC-3, DU145 and C4-2B). **C,** relative expression of AR in LNCaP and C4-2B cells. The cells were cultured in regular medium, serum-free medium or a medium containing charcoal-stripped FBS in presence or absence of E2 or DHT for 24 hrs. Cells were harvested and AR expression was measured by qRT-PCR. D, Western blot analysis of ERβ in PC cells. Data are expressed as mean ± SEM. Level of significance is calculated to *cells cultured in regular or # charcoal-stripped FBS medium at $p<0.05$.

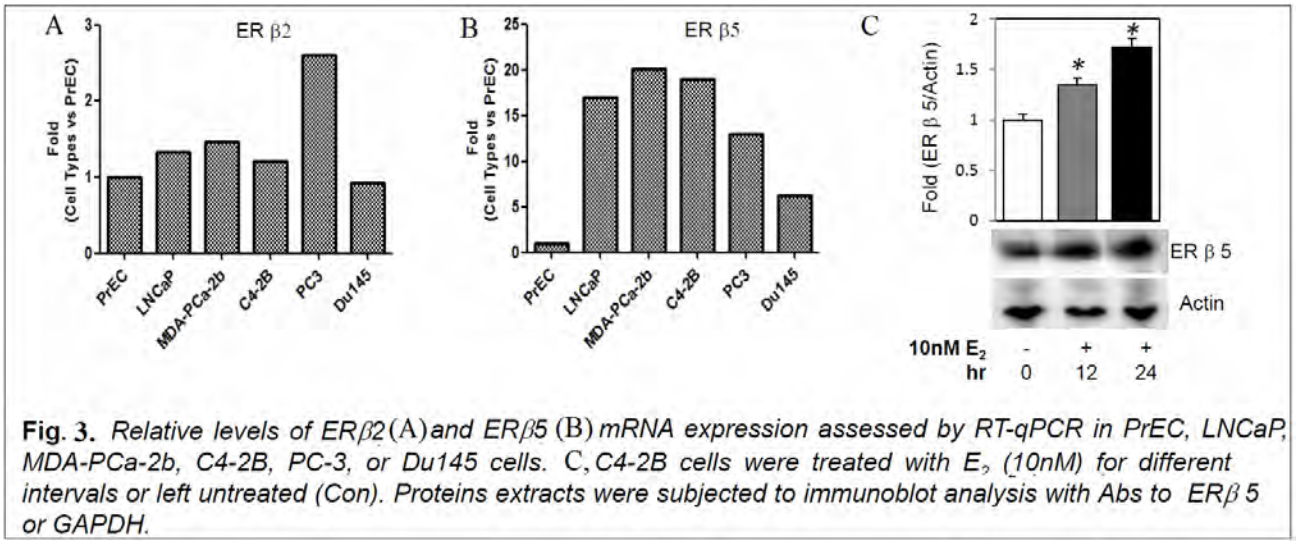

Fig. 3. *Relative levels of ERβ2 (A) and ERβ5 (B) mRNA expression assessed by RT-qPCR in PrEC, LNCaP, MDA-PCa-2b, C4-2B, PC-3, or Du145 cells. C, C4-2B cells were treated with E_2 (10nM) for different intervals or left untreated (Con). Proteins extracts were subjected to immunoblot analysis with Abs to ERβ 5 or GAPDH.*

Because ERβ exists in at least 5 isotypes, each with selective cellular functional role, we further identified isotypes detected in other types of cancers. Using qRT-PCR analysis, we demonstrate that the basal levels of ERβ5 (Fig 3B) are high in AR-expressing cells compared to AR-naïve cells. In contrast ERβ2 appears to be predominantly expressed in AR-naïve cells (Fig 3A). Interesting, the expression level of ERβ5 increases with E2 treatment in C4-2B cells. The results suggest that ERβ5 might be a direct down-stream target of E2 signaling in androgen independent PC cells.

Next, we examined if E2 induces growth of PC cells and whether such growth induction is influenced by the differential expression of ER subtypes in AR-expressing LNCaP cells (androgen dependent) and its isogenic androgen independent C4-2B cells.

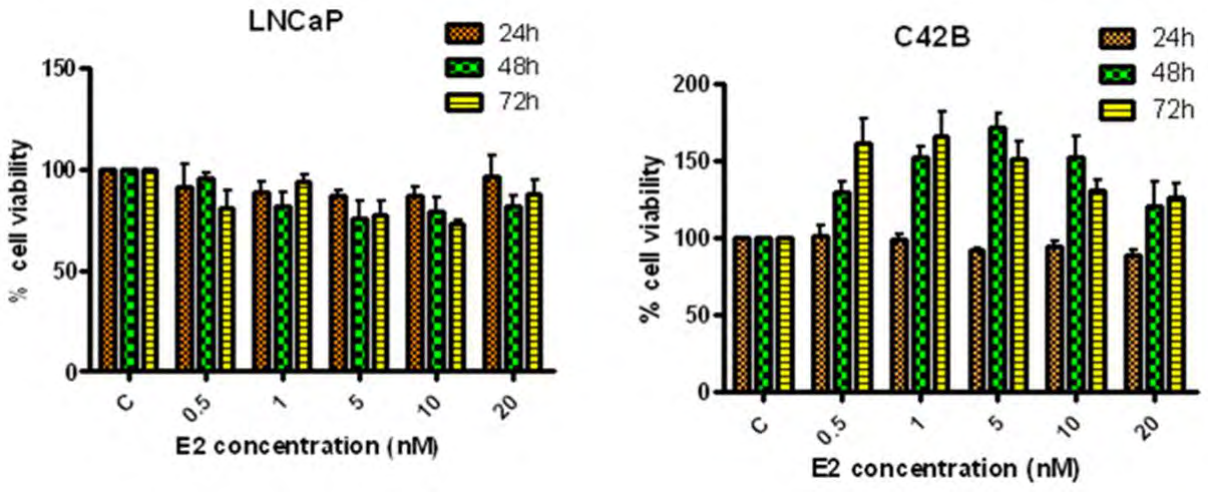

Fig. 4. LNCaP and C4-2B cells were cultured in phenol-free RPMI medium containing 10% charcoal-stripped FBS for up to 72 hr in presence or absence of various concentrations of E2. Cell growth was measured by a cell proliferation assay kit (WST-1). Results are represented as Mean ± SEM and significance is calculated at *p<0.05 relative to a vehicle control.

As shown in Figure 4, E2 selectively promoted growth of the androgen independent isogenic subline, C4-2B cells, but not the parental androgen dependent LNCaP cells. The results suggest that the differential E2 growth promoting ability in C4-2B may be attributed to differential high expression of ERβ subtype in these cells. The aforementioned results suggest that promotion of growth by SAFB2 in PC cells (Fig.1) is likely to be mediated through E2-mediated expression and/or activation of AR, presumably via activation of ERβ. To test this hypothesis, we examined by reporter assays if activation of E2 signaling induces transactivation of AR in this cell line (Task-1C).

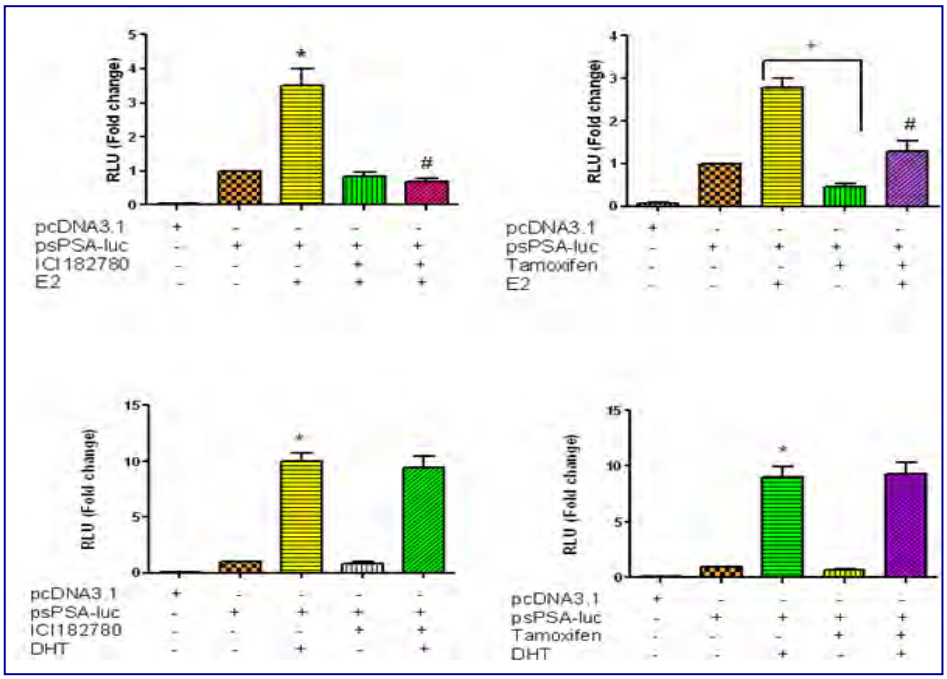

Fig. 5: Modulation of Androgen receptor (AR) transactivation by E2 in C4-2B cells, an isogenic androgen independent subline of the androgen dependent LNCaP cells. The psPSA-luc or control (pcDNA3.1) plasmids transfected cells were cultured in charcoal-stripped FBS medium containing E2 (10 nM) (upper panels) or DHT (10 nM) (lower panels) in presence or absence of ER antagonists; ICI 182,780 (1μM) or Tamoxifen (5μM). Luciferase activity was normalized to pRL-SV40 Renilla. The psPSA-luc plasmid encompasses truncated ARE sequences which drives expression of luciferase gene. All data are represented as Mean ± SEM and repeated at least 3 independent times in triplicates. *p<0.05 is calculated vs. psPSA-luc and # p<0.05 vs. E2-treated cells.

As shown in Fig. 5, E2 induced AR transactivation, as evidenced by PSA promoter activation, in C4-2B cells and the specificity of this effect was verified by ER antagonists. In contract, the DHT mediated AR activity was not affected by ER antagonists. Taken together, the data suggested that under androgen ablation therapy E2-ER signaling axis could induce AR transaction in AR-expressing androgen independent cells.

Next, we conducted additional experiments to determine if AR transactivation by E2 is mediated through activation of ERα or ERβ signaling axis. To this end, we examined if overexpression of either ER subtypes modulates activation of androgen regulated genes by E2 in COS-7 cells, hormone receptor naïve monkey kidney fibroblasts. Cells transfected with psPSA-luc, ERα, ERβ and/or AR were cultured in charcoal-stripped medium in presence or absence of E2 (10nM). The PSA promoter activity was measured with luciferase activity and results were normalized to pRL-SV40 Renilla as shown above. As shown in Fig. 6, E2 induces transactivation PSA promoter in COS-7 cells in presence of AR. Importantly, E2 mediated activation of PSA promoter is significantly induced by ERβ than by ERα in these cells. These findings further attests to the potential and crucial role of E2-ERβ axis in activation of AR signaling and disease progression especially in AA-men refractory to androgen ablation therapy. The results suggest that selective expression of SAFB2, an ERα co-repressor, could potentially inhibit ERα activation—thus paving the way for activation of E2- ERβ signaling axis to activate AR signaling, and, consequently, growth of prostate tumors in AA-men.

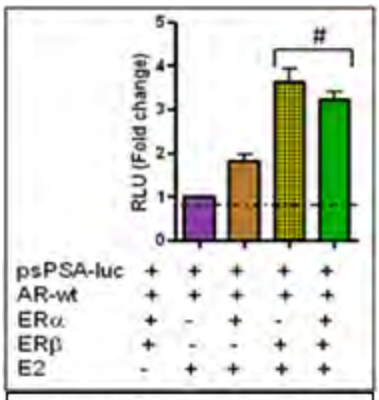

Fig. 6: Effect of ERα/β on psPSA-luc promoter activity showing ligand-independent effect of ER subtypes in COS7 cells. Cells were co-transfected with psPSA-luc, ERα, ERβ and or AR for 24 hrs and then treated in 10% charcoal-stripped FBS medium containing E2 (10 nM) for 24hrs. # denotes significance at $p<0.05$ vs E2-treated cells.

We examined if AR and androgen-regulated genes (ARGs) (PSA, Prostate Trans-membrane Protein, Androgen Induced (TMEPA1), and TMPRESS2) can be induced by E2 in PC cells under androgen deprived conditions. As shown in Figs. 7A & B, the expression of all examined ARGs was elevated in C4-2B cells in response to E2. However, no change in basal levels of AR or EGR (-ve control) was observed. The data was confirmed by Western blot analysis (Fig. 7c) . the results suggest that E2-ER axis induces AR transactivation as evidenced by increased expression of ARGs in PC cells.

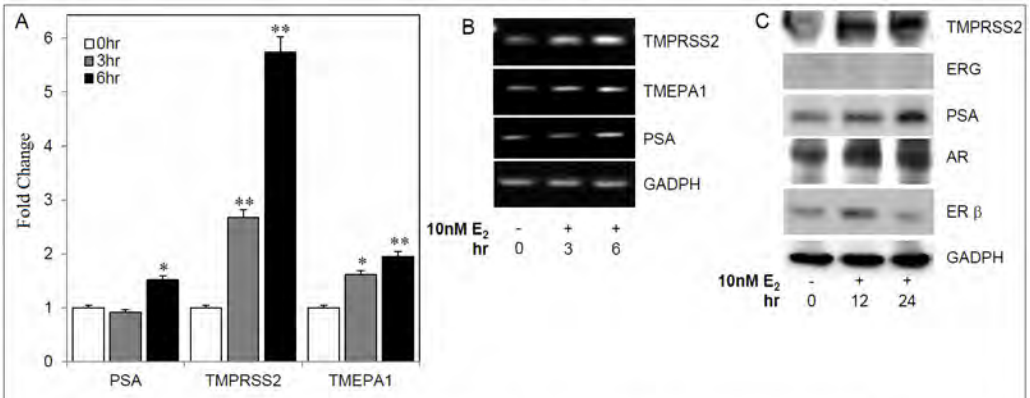

Fig. 7. *C4-2B cells was treated with E_2 (10nM) for 3hr or 6h in serum-free or charcoal stripped FBS medium and then followed by quantitative **(A)** or conventional **(B)** or PCR with primers specific to human TMPRSS2, TMEPA1, PSA or GADPH. * $p < 0.01$., or ** $p < 0.05$., different from respective untreated cells. **(C)** C4-2B cells were treated with E_2 (10nM) for different intervals or left untreated (Con). Proteins extracts were subjected to immunoblot analysis with Abs to TMPRSS2, ERG, PSA, AR, ERβ or GADPH.*

To determine if AR is required for E2-ERβ mediated expression and /or activation of ARGs, we tested the hypothesis that AR physically interacts with ERβ upon treating cells with E2. As shown in Fig 8, nuclear extracts were procured from C4-2B cells treated with E2 up to 60 min and subsequently subjected to Co-IP assay using AR specific antibody and ERβ pan-antibody. The input control (Fig 7a) depicts increased nuclear localization of both receptors. Reciprocal Co-IP assays (Figs 8B and C) demonstrate physical interaction between AR and ERβ. We also showed by Co-IP that molecular chaperon p23 and steroid receptor co-activator NCOA3 (SRC-3) are part of the AR-ERβ in the nucleus (*data not shown*).

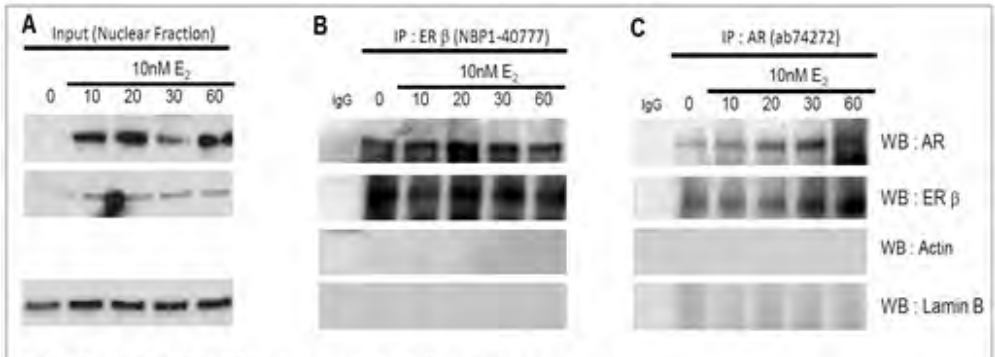

Fig. 8. *Analysis of AR–ERβ interaction by IP of nuclear cell fractions*
C4-2B cells were grown in 100mm dish for 24 h in RPMI-1640 supplemented with 10% FBS (v/v) and antibiotics. After that, the medium was replaced by free phenol red RPMI-1640 with10% charcoal stripped FBS(v/v), and antibiotics for another 48 h. Subsequently, cells were grown in the presence/absence of E_2 (10nM) for different intervals. Three hundred micrograms of nuclear protein extracts was subjected to immunoprecipitation (IP) using an antibody directed against ERβ or AR followed by Western blot analysis with anti-AR and anti-ERβ antibodies.

This notion was further confirmed by immunocytochemistry in C4-2B cells. Briefly, cells were cultured in chamber slides in a medium containing charcoal-stripped FBS and treated with 10 nM E2 (Fig. 9) or E2-Glow (Fig 10) for up to 60 min. Cells were then fixed and stained with antibodies against AR and ERβ and detected by fluorescently labeled secondary antibodies using fluorescence microscope.

The results shown in Figs 8 and 9 suggest that AR and ERβ co-localize along with E2 to the nucleus in androgen independent AR-expressing PC cells under androgen deprivation conditions, further attesting to the notion that E2 growth promoting ability may require AR as a heterodimeric partner with ERβ for transcriptional up- regulation of androgen regulated genes (ARGs), such as PSA. The potential binding of ERβ on ARE of ARGs, presumably through heterodimeric binding with AR, was examined with ChIP assays. C4-2B cells were treated with E2 (10 nM) and binding of ERβ to proximal prompter ARE-1 and II and enhancer element ARE-3 on PSA promoter region was examined with PCR analysis using ERβ specific antibody.

The results show that ERβ selectively binds to ARE-1 on PSA promoter and may thus explain in part the mechanism by which E2-ERβ axis increase the promoter activity of PSA in C4-2B cells (Fig 11).

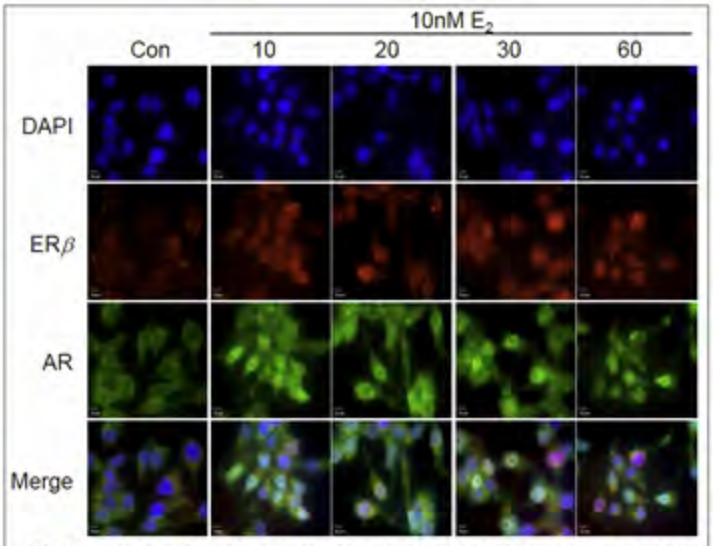

Fig. 9. *C4-2B cells grown in chamber slides were treated with 10 nM estrogen for the indicated times. The cells were then fixed and subjected to immunofluorescence staining with antibodies to AR, or ERβ. Con, control.*

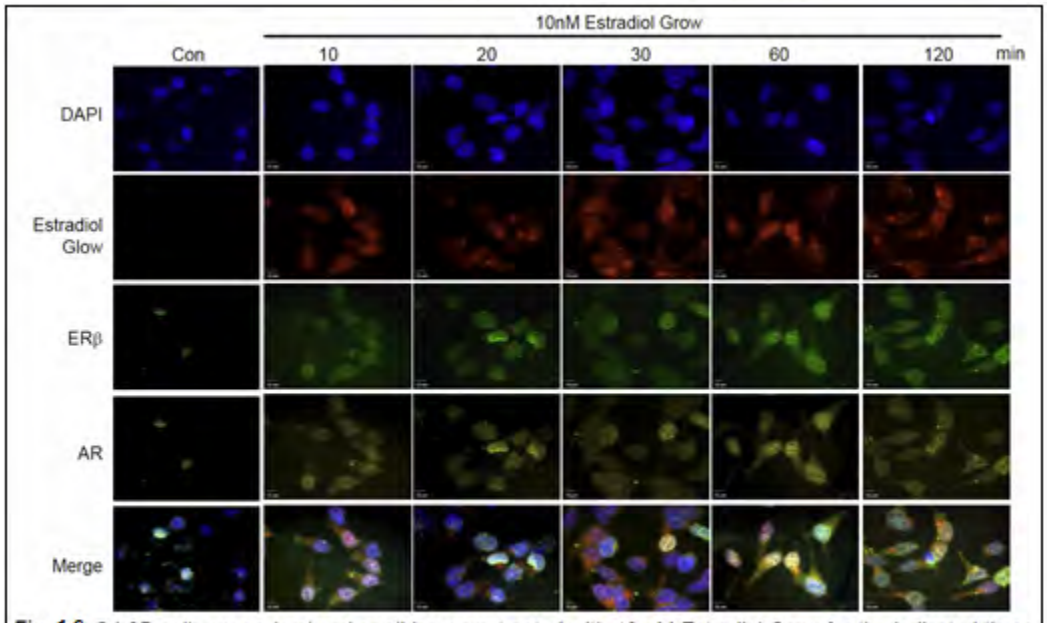

Fig. *10.* *C4-2B cells grown in chamber slides were treated with 10 nM Estradiol Grow for the indicated times. The cells were then fixed and subjected to immunofluorescence staining with antibodies to AR, or ERβ. Con, control.*

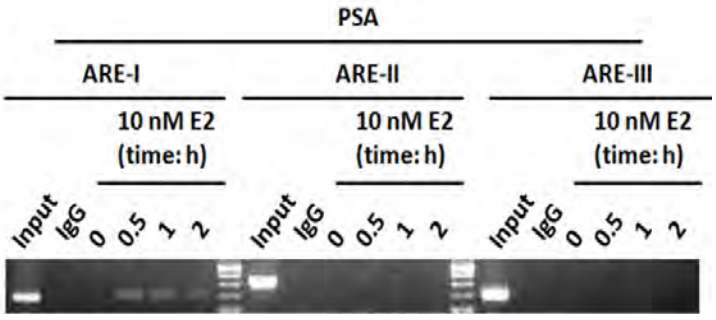

Fig. 11: E2 (10nM) mediates hormone dependent ERβ binding to AREs in C4-2b cells. ChIP assay performed using anti-ERβ and PCR amplification of sequences flanking AREs of PSA gene in presence or absence of E2 (*n*=3).

Conclusions: Collectively the data attests to the fact that up-regulation SAFB2, an ERα co-repressor, paves the way for activation of E2-ERβ signaling axis in prostate tumor cells. The latter enables activation AR signal leading to expression of ARGs under hormone castration conditions and presumably disease progression especially among AA-men.

Task-2. To assess efficacy of down regulation of target gene(s) in inhibiting tumorigenic growth and metastatic potential of AA-derived CaP cells *in vivo (Months 13-36).*

- The tumorigenicity and metastatic potential of SAFB2 shRNA-silenced PC cells in castrated or gonadally intact athymic mice in presence or absence of estrogen pellets will be examined.

Because silencing of SAFB2 is lethal to PC cells, we were not able to pursue the proposed in vivo experiments. However, since we *hypothesized* that SAFB2 overexpression is associated with activation of E2-ERβ signaling axis in prostate tumor cells, we opted to examine if this signaling axis stimulates prostate tumor growth under hormone (androgen castrate conditions). Briefly, athymic nude mice (n=5/group)were castrated or underwent sham surgery. Gonad-intact mice were used as another control group. Seven days later slow release 90-day E2 or placebo pellets were implanted s.c. Forty eight hrs later, mice were transplanted s.c. with C4-2B cells in Matrigel (1:1 ratio) and tumor formation (volume) and body was monitored and recorded weekly over a 5-week period. E2 blood levels were measured by enzyme immunoassay. As shown in Fig 12A, B tumor formed in gonad-intact sham-operated group. However, larger tumors (3-fold) formed in castrated mice compared to castrated placebo control and gonad-intact mice.

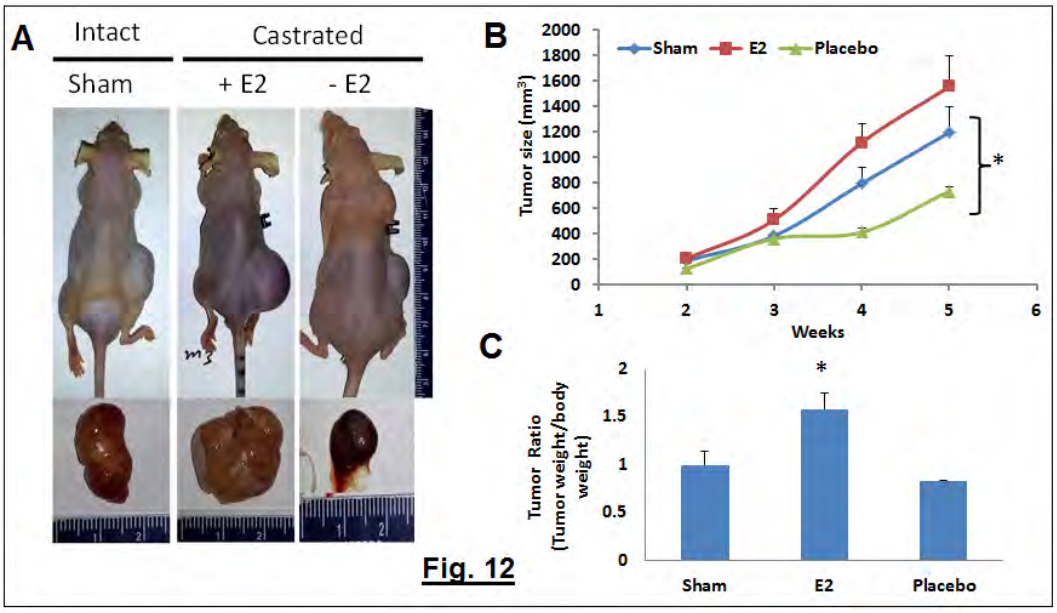

Fig. 12

These findings corroborate our in vitro data further attesting to the tumor growth promoting ability of E2-ER signaling axis under androgen deprivation conditions.

** above data shown in tasks 1 and 2 were presented at the AACR meeting (abstract attached) and the manuscript under preparation.

Task-3. To establish the clinical utilities of target gene(s) as biomarkers and/or prognostic indicators of disease progression in AA men (*Months 24-36*).

- Using NCI designed tissue microarrays and immunohistochemical (IHC) analysis; we will investigate if expression of target genes alone or in combination with hormone nuclear receptor (ER isoforms and AR) can serve as biomarkers or prognostic indictors of PC progression in AA men.

Using blood samples from AA and CA men and TMA tumor cores (NCI ethnicity-based TMA-4 with 150 patients each per race group), we performed comparative analysis of circulating E2 and prostate tumor expression of ERβ in both race groups. *In situ* ERβ expression was validated by quantitative reverse transcription–PCR in matched microdissected normal prostate epithelium and tumor cells and datasets extracted from independent cohorts. In comparison with normal age matched subjects, circulating E2 levels were significantly elevated in all PCa patients. Further analysis demonstrates an increase in blood E2 levels in AA men in both normal and PCa in comparison with age- and stage-matched counterparts of CA decent. Histochemical score analysis reveals intense nuclear immunoreactivity for ERβ in tumor cores of AA men than in CA men. Gene expression analysis in microdissected tumors corroborated the biracial differences in ERβ expression. Gene expression analysis from independent cohort datasets revealed correlation between ERβ expression and PCa progression. However, unlike in CA men, adjusted multivariate analysis showed that ERβ expression correlates with age at diagnosis and low prostate-specific antigen recurrence-free survival in AA men. Taken together, our results suggest that E2-ERβ axis may have potential clinical utility in PCa diagnosis and clinical outcome among AA men.

***The data was presented at two AACR meetings and was published in Carcinogenesis Journal (2013 May 8; PMID: 23658372)*

hnRNPH1 Gene

All three tasks were implemented as proposed for hnRNPH1 gene. The data is presented as manuscript initially submitted and reviewed by Nature Medicine, but the paper was rejected after new reviewers suggested additional experiments. The revised manuscript (attached) will be submitted to Cancer Discovery this month. The summery of the findings is as follow:

Background Despite recent decline, prostate cancer (PC) incidence and mortality rates still remain significantly higher in African-American (AA) men than Caucasian Americans (CA) and other ethnic minority groups. While the causes remain elusive, little is known about the contributory role of the underlying biology in the disproportionate clinical manifestation and outcome of PC among AA men.

Methods We employed an unbiased functional genomics approach to identify genes differentially expressed in freshly procured prostate tumor cells of age- and tumor grade-matched AA and CA men. Laser capture microdissected (LCM)-procured *in vivo*-derived genetic materials of matched normal epithelium and PC cells were subjected to suppressive subtractive hybridization (SSH) to construct microarray chips encompassing two sets of race-based, PC-specific cDNAs. Validation in independent cohorts and functional assays of target genes were performed.

Results Herein we identified in microdissected tumors of African American (AA) men selective expression of heterogeneous nuclear ribonucleoprotein H1 (hnRNPH1) in comparison to Caucasian American (CA) men. The hnRNPH1 expression correlates with androgen receptor (AR) expression, PC progression and development of castration resistant PC (CRPC). The aberrant expression of hnRNPH1 is attributed to promoter methylation and down-regulation of miRNA-22 and miR-212 in prostate tumors in AA-men. Whereas expression promotes tumor formation in *vivo*, hnRNPH1 siRNA silencing confers growth arrest and sensitizes AR-expressing PC cells to the anti-androgen bicalutamide. The hnRNPH1 is a transcriptional target of androgens that upregulates AR transcription through a positive feedback loop in PC cells. Functional studies demonstrate that hnRNPH1 physically interacts with and enhances ligand-dependent and independent AR *trans*activation through recruitment of steroid receptor coactivator-3 (SRC-3) to its cognate DNA elements on promoters of androgen-regulated genes.

Conclusions Our data support a model in which hnRNPH1 is a novel auxiliary coregulator for hormone dependent and independent AR *trans*activation in prostate tumor cells. The AR-hnRNPH1 axis represents a previously uncharacterized mechanism potentially involved in disease progression, development of therapeutic resistance and ethnic disparity of PC.

Discussion

Our studies clearly demonstrate differential expression of nuclear matric proteins (NMPs) hnRNPH1 and SAFB2 in prostate tumors of AA-men as opposed to CA-men. Based on its known co-repressor effect of ERα, we demonstrate that SAFB2 mediates its prostate tumor cell growth, presumably through activation of AR activation through estrogen-ERβ signaling axis in prostate tumor cells, especially among AA-men.. Our demonstration of high circulating estrogens and selective expression of ERβ in prostate tumor cells of AA-men, as opposed to CA-men, further attests and strengthens this notion. Additionally, we demonstrate that high expression of another NMP, hnRNPH1, in prostate tumors of AA-men is associated with increased expression and activation of AR signaling and androgen regulated genes in prostate tumor cells, independent of SAFB2. The selective upregulation of hnRNPH1 in prostate tumor cells is associated with hypermethylation of promoter region and down-regulation of miRNA-22 and miR-212 in prostate tumor cells in AA-men. The expression of hnRNPH1 correlates with disease progression, relapse and poor clinical outcome, especially among AA-men.

Key Research Accomplishments

- We demonstrate selective expression of nuclear matrix proteins, SAFB2 and hnRNPH1 in prostate tumors of independent cohorts AA-men compared to CA-men
- Expression of SAFB2 enables activation of E2-ERβ axis in tumor cells under hormone deprivation conditions
- The latter enables activation of AR signaling, expression of androgen regulated genes in prostate tumor growth both in vitro and in vivo under hormone deprivation conditions
- High levels of circulating E2 and tumor expression of ERβ were detected in AA-men compared to CA men
- The tumor expression of ERβ correlates with disease progression and recurrence in AA-men
- Activation of E2-ERβ signaling in prostate tumors of AA-men may be associated to the disproportionate disease progression and relapse in this ethnic group of patients
- Aberrant expression of hnRNPH1 in prostate tumors tumor growth, both *in vitro* and *in vivo*.
- The growth inducing ability of hnRNPH1 is mediated through interaction with AR, in presence of SRC-3 in a ligand dependent and independent manner, suggesting that hnRNPH1 is a novel AR co-activator.

Reportable Outcomes:

1. **Presentations:** The outsome of the study was presented orally (invited speaker) at the Innvovative Minds in Prostate Cancer Today (IMPact) meeting in FL, March 9-12, 2011 (*attached*)
2. **Abstracts:** AACR annual meeting (2012) and the Sixth AACR Conference: The Science of Cancer Health Disparities in Ethnic Minorities and the Medically Underserved, Atlanta, GA, November, 2013 (*attached*)
3. **Manuscripts:**
   a. One publication pertaining to SAFB2 on "Role of Estrogen-ERβ Axis in Racal Disparity of Prostate Cancer" was published in Carcinogenesis; 2013 Sep;34(9):2017-23. PMID: 23658372 (*copy attached*)
   b. Another manuscript initially considered by Nature Medicine will be submitted to Cancer Discovery Journal. (*copy of the manuscript is appended*)
   c. E2-ERβ Signaling Axis Promotes Prostate Tumor Growth Through Activation of AR signaling (*manuscript under preparation*)

Conclusions: African Americans (AA) have twice the incidence and mortality of prostate (PC) than Caucasian Americans (CA). While the disproportionate burden was partially explained by genetic, socioeconomic, and environmental factors, racial variation in the biology of prostate tumors was not investigated. Our studies clearly demonstrate differential expression of nuclear matric proteins (NMPs) hnRNPH1 and SAFB2 in prostate tumors of AA-men as opposed to CA-men. The functional significance of these NMPs in modulating disease progression through activation of nuclear receptors (AR and ERβ) attests to the fact that the underlying biology of prostate cancer differs in AA-men in comparison to CA-men, and possibly other ethnic minority groups. Our results argue that the disproportionate incidence, progression and mortality among AA-men may be partially attributed to differences in biology of prostate cancer, and consequently response to therapy. Since we demonstrate that the two NMPs acts through modulation of nuclear receptors (AR and ER), it may of utmost importance to establish therapeutic targeting strategy of personalized medicine, rather than conventional medicine, based on screening and expression profiles of these genes in prostate tumors among AA-men.

References:

1. Horner MJ, Ries LAG, Krapcho M. et al. SEER Cancer Statistics Review, 1975-2006, National Cancer Institute. Bethesda, MD; 2009.
2. de Vere White RW, Deitch AD, Jackson AG. Radical differences in clinically localized prostate cancers of black and white men. *J Urol.* 1998;159(6):1979-1983.
3. Powell IJ, Banerjee M, Novallo M, et al. Prostate cancer biochemical recurrence stage for stage is more frequent among African American than white men with locally advanced but not organ-confined disease. *Urology.* 2000;55(2):246-251.
4. Whittemore AS, Wu AH, Kolonel LN, et al. Family history and prostate cancer risk in black, white, and Asian men in the United States and Canada. *Am J Epidemiol.* 1995; 141(8):732-740.
5. Cher ML, Lewis PE, Banerjee M, et al. A similar pattern of chromosomal alterations in prostate cancers from African-Americans and Caucasian Americans. *Clin Cancer Res.* 1998;4(5):1273-1278.
6. Haiman CA, Patterson N, Freedman ML, et al. Multiple regions within 8q24 independently affect risk for prostate cancer. *Nat Genet.* 2007;39(5):638-641.
7. Yeager M, Orr N, Hayes RB, et al. Genome-wide association study of prostate cancer identifies a second risk locus at 8q24. *Nat Genet.* 2007;39(5):645-649.
8. Epstein JI, Pizov G, Walsh PC. Correlation of pathologic findings with progression after radical retropubic prostatectomy. *Cancer.* 1993;71(11):3582-3593.
9. Chen CD, Welsbie DS, Tran C, et al. Molecular determinants of resistance to antiandrogen therapy, *Nat Med.* 2004;10(1):33-39.
10. Heemers HV, Tindall DJ. Androgen receptor (AR) coregulators: a diversity of functions converging on and regulating the AR transcriptional complex. *Endocr Rev.* 2007; 28(7):778-808.
11. Small D, Nelkin B, Vogelstein B. Nonrandom distribution of repeated DNA sequences with respect to supercoil loops and the nuclear matrix. *Proc Natl Acad Sci, USA*. 1982;79(19):5911-5915.
12. Leman ES, Getzenber RH. Nuclear structure as a source of cancer specific biomarekers. *J Cell Biochem.* 2008;104(6):1988-1993.
13. Krecic AM, Swanson MS. hnRNP complexes: composition, structure, and function. *Curr Opin Cell Biol*. 1999;**11(3):**363–371.
14. Siomi MC, Eder PS, Kataoka N, et al. Transporin-mediated nuclear import of heterogeneous nuclear RNP proteins. *J Cell Biol.* 1997;138(6):1181-1192.
15. Honoré B, Rasmussen HH, Vorum H, et al. Heterogeneous nuclear ribonucleoproteins H, H′, and F are members of a ubiquitously expressed subfamily of related but distinct proteins encoded by genes mapping to different chromosomes. *J Biol Chem.* 1995;**270(48):**28780–28789.
16. Alkan SA, Martincic K, Milcarek C. The hnRNPs F and H2 bind to similar sequences to influence gene expression. *J Biochem*. 2006;393(Pt1):361-371.
17. Holzmann K, Korosec T, Gerner C, et al. Identification of human common nuclear-matrix proteins as heterogeneous nuclear ribonucleoproteins H and H' by sequencing and mass spectrometry. *Eur J Biochem.* 1997;244(2):479-86.
18. Honoré B, Baandrup U, Vorum H. Heterogeneous nuclear ribonucleoproteins F and H/H' show differential expression in normal and selected cancer tissues. *Exp Cell Res.* 2004;294(1):199-204.
19. Liu J, Beqai S, Yang Y, et al. Heterogeneous nuclear ribonucleoprotein-H plays a suppressive role in visceral myogenesis. *Mech Dev*. 2001;104(1-2):79-87.

Appendices

Accepted Abstract (##53352_1): Presented at the Sixth AACR Conference: The Science of Cancer Health Disparities in Ethnic Minorities and the Medically Underserved, Atlanta, GA, November, 2013.

Estradiol-ERβ Signaling Axis in Disparity of Prostate Cancer in African American-Men

Zakaria Y. Abd Elmageed[1], Hogyoung Kim[1], Raju Thomas[1], Krishnarao Moparty[1]and Asim B. Abdel-Mageed[1].

[1]Departments of Urology, Tulane University Health Science Center, New Orleans, LA, USA

ABSTRACT

Our study showed that high circulating estrogens and estrogen receptor beta (ERβ) may be implicated in prostate cancer (PCa) progression, and had higher expression level in African American (AA) than Caucasian American (CA) men. However, the underlying mechanisms remain elusive. The objective of this study was to investigate the signaling cross-talk between ERβ and AR *in vitro* and *in vivo* levels. Prostate cancer cells; LNCaP, C4-2B and PC3 were treated with different concentrations and at different time points with 17β-Estradiol (E2) and 5α-dihydrotestosterone (DHT) and examined for cell proliferation by WST assay, promoter activity by luciferase assay, DNA-protein interaction by electrophoretic mobility shift assay (EMSA) and chromatin immunoprecipitation (ChIP) assay. After E2 or DHT treatment, the translocation of ERβ and AR in PCa cells was also examined using fluorescence microscope.

Our results show that ERβ was stimulated by treatment of cells with 10nM DHT and AR was also induced by treating PCa cells with10nM E2. These results were confirmed by promoter activity of truncated psPSA-luc in either PCa cell lines or Cos-7 cells. The predesigned Androgen Response Element (ARE) was bound to the protein's receptor after E2 induction. ChIP experiment corroborated the cross-talk between AR and ERβ after treating C4-2B cells with 10nM E2 for 30 min up to 1.5 hr. Immunofluorescence depicted co-localization of AR and ERβ in the nucleus after 30 min from E2 treatment. To our knowledge, this is the first report demonstrating crosstalk between ERβ and AR signaling in PCa in response to E2 treatment. Our results implicate potential therapeutic application by targeting AR and ERβ in castration-resistant PCa (CRPC).

Keywords: Prostate cancer, Androgen receptor, Estrogen receptor beta, E2, receptor interaction.

Cancer Research: April 15, 2012; Volume 72, Issue 8, Supplement 1
doi: 10.1158/1538-7445.AM2012-438
Proceedings: AACR 103rd Annual Meeting 2012-- Mar 31-Apr 4, 2012; Chicago, IL

Poster Presentations - Metastasis Biomarkers

Abstract 438: The importance of estrogen-ERβ axis in racial disparity of prostate cancer

Zakaria Y. Abd Elmageed[1], Krzysztof Moroz[1], Sudesh K. Srivastav[1], Byron E. Crawford[1], Krishnarao Moparty[1], Raju Thomas[1], and Asim B. Abdel-Mageed[1]

[1]Tulane University School of Medicine, New Orleans, LA

Purpose: The role of estrogens and estrogen receptors (ERs) in the disproportionate incidence and mortality of prostate cancer (PCa) has not been established. Although ERβ has been implicated in PCa progression, its ethnic-based expression and underlying mechanisms are not fully understood. The aim of this study is to establish correlation between estrogen-ERβ axis and clinical outcome in African American (AA) in comparison to Caucasian American (CA) men. Patients and Methods: 17β-Estradiol (E2) was determined in the blood procured from normal (n=30) and PCa patients (n=50) by ELISA. The expression of ERβ was assessed using an NCI-designed ethnicity-based tissue microarray (TMA) slide encompassing 150 each of AA and CA PCa tissue cores, 17 BPH, 13 normal biopsies, and 3 PCa cell lines (LNCaP, DU-145 and PC-3). Validation of ERβ in situ was validated by qRT-PCR in matched microdissected tumors and normal glands from both populations. Results: In comparison to normal subjects, circulating E2 levels were significantly (p=0.0160) elevated in AA-men than in CA-men with PCa. Additionally, a significant difference in E2 blood levels (p=0.0015) was observed between AA and AA PCa patients. Histoscore analysis demonstrate intense nuclear immunoreactivity (p=0.0018) against ERβ in tumors of AA than CA men. This notion was further validated by qRT-PCR on LCM-procured tumor cells (p=0.0315). In the adjusted multivariate analysis there was no correlation between ERβ expression and any clinical parameters in PCa tissues. In AA, there was a positive correlation between Gleason score (GS) and age but a negative correlation was found between GS, age and PSA-recurrence free. However, no correlation was found in CA. Conclusion: Together, high circulating levels of blood estrogens and mRNA levels coupled with a differential expression of ERβ in PCa tissues suggest a potential role for estrogen-ERβ axis in the development of castrate-resistant prostate cancer in AA men. Key words: E2, ER beta, mRNA, TMA, histoscore, African Americans, health disparities.

Citation Format: {Authors}. {Abstract title} [abstract]. In: Proceedings of the 103rd Annual Meeting of the American Association for Cancer Research; 2012 Mar 31-Apr 4; Chicago, IL. Philadelphia (PA): AACR; Cancer Res 2012;72(8 Suppl):Abstract nr 438. doi:1538-7445.AM2012-438

Carcinogenesis vol.34 no.9 pp.2017–2023, 2013
doi:10.1093/carcin/bgt156
Advance Access publication May 8, 2013

High circulating estrogens and selective expression of ERβ in prostate tumors of Americans: implications for racial disparity of prostate cancer

Zakaria Y.Abd Elmageed[1], Krzysztof Moroz[2], Sudesh K.Srivastav[3], Zhide Fang[4], Byron E.Crawford[2], Krishnarao Moparty[1], Raju Thomas[1,5] and Asim B.Abdel-Mageed[1,5,*]

[1]Department of Urology, [2]Department of Pathology and [3]Department of Biostatistics and Bioinformatics, Tulane University Health Science Center, New Orleans, LA 70112, USA, [4]Biostatistics Program, School of Public Health, LSU Health Sciences Center, New Orleans, LA 70112, USA and [5]Tulane Cancer Center, Tulane University Health Science Center, New Orleans, LA 70112, USA

*To whom correspondence should be addressed. Department of Urology, Tulane University School of Medicine, 1430 Tulane Avenue, New Orleans, LA 70112, USA. Tel: +504 988 3836; Fax: +504 988 5059;
Email: amageed@tulane.edu

Although estrogen receptor beta (ERβ) has been implicated in prostate cancer (PCa) progression, its potential role in health disparity of PCa remains elusive. The objective of this study was to examine serum estrogens and prostate tumor ERβ expression and examine their correlation with clinical and pathological parameters in African American (AA) versus Caucasian American (CA) men. The circulating 17β-estradiol (E2) was measured by enzyme immunoassay in blood procured from racially stratified normal subjects and PCa patients. Differential expression profile analysis of ERβ was analyzed by quantitative immunohistochemistry using ethnicity-based tissue microarray encompassing 300 PCa tissue cores. *In situ* ERβ expression was validated by quantitative reverse transcription–PCR in matched microdissected normal prostate epithelium and tumor cells and datasets extracted from independent cohorts. In comparison with normal age-matched subjects, circulating E2 levels were significantly elevated in all PCa patients. Further analysis demonstrates an increase in blood E2 levels in AA men in both normal and PCa in comparison with age- and stage-matched counterparts of CA decent. Histochemical score analysis reveals intense nuclear immunoreactivity for ERβ in tumor cores of AA men than in CA men. Gene expression analysis in microdissected tumors corroborated the biracial differences in ERβ expression. Gene expression analysis from independent cohort datasets revealed correlation between ERβ expression and PCa progression. However, unlike in CA men, adjusted multivariate analysis showed that ERβ expression correlates with age at diagnosis and low prostate-specific antigen recurrence-free survival in AA men. Taken together, our results suggest that E2-ERβ axis may have potential clinical utility in PCa diagnosis and clinical outcome among AA men.

Introduction

Estrogen is a steroidal hormone involved in regulation of growth and differentiation in many target tissues (1,2). Estrogen is also implicated in many pathological disorders including osteoporosis and cancers of breast, endometrial, colon and prostate (3–7). The active form of estrogen is 17β-estradiol (E2) while estrone and estriol are weakly bound to estrogen receptors (ERs) (8). The two ERs, ERα and ERβ, belong to the nuclear receptor family of transcription factors. The tissue-specific effects of ERs are dependent on ligand binding, heterodimerization, transactivation or activity of estrogen-response element. Notably, diverse biological response to E2 is dependent on tissue type and the synchronization between ERα and ERβ signaling pathways (9).

The incidence and mortality of PCa is significantly high among AA men in comparison with CA men (10,11). In 2007, Rohrmann *et al.* (12) reported that circulating estrogen, but not testosterone, levels are considerably high among AA men than CA men. The decreased androgen to estrogen ratio may be a risk factor for PCa (13). Estrogens not only induce growth and differentiation of normal prostate glands but also involved in pathogenesis of PCa (4). Although the underlying mechanisms remain elusive, E2 has been shown to be a risk factor for prostate carcinogenesis in animal models (14). A recent study has suggested that E2 may abrogate ERβ- and KLF5-mediated signaling and promote cellular proliferation (15). The human prostate progenitor cells appear to be estrogen targets, whereas E2, when combined with testosterone, acts as a carcinogen in human prostate epithelium (16).

The aberrant expression of ERs may affect transcription of target genes, which in turn demarcate estrogen effects on PCa tissues (17). Unlike ERα expression in prostate stroma (18), ERβ is expressed in normal prostatic epithelium (19–21). However, the role of ERβ in PCa growth and progression is still a matter of conjecture. ERβ activation appears to inhibit cell proliferation directly or through ERα blockage, suggesting PCa-suppressive function for ERβ (17,22,23). However, Lai *et al.* (19) have reported that ERβ is expressed in PCa metastases and may be a relevant target for treatment of advanced PCa. Indeed, recent evidence on pivotal involvement of ERβ in the carcinogenesis of non-classical estrogen target tissues, including PCa, suggests targeted ERβ therapies may be effective in PCa (24). To our knowledge, this is the first study to examine the potential role of estrogen-ERβ axis in health disparity of PCa patients.

Abbreviations: AA, African American; AAD, age at diagnosis; BPH, benign prostatic hyperpasia; CA, Caucasian American; CRPC, castration-resistant PCa; E2, 17β-estradiol; ERβ, estrogen receptor beta; GS, Gleason score; HS, H-Score, histochemical score; PCa, prostate cancer; PRF, PSA recurrence-free; PSA, prostate-specific antigen; TMA, tissue microarray.

Materials and methods

Study subjects and measurement of serum estrogens

All information on research subjects was handled in accordance with an approved IRB protocol (Biospecimen Core, Louisiana Cancer Research Consortium; www.lcrc.info). Blood samples were collected from AA and CA PCa patients at Tulane University Hospital, New Orleans, LA. Normal serum samples were purchased from BioReclamation (LLC, NY) after informed consents from donors. Blood was collected from either normal or PCa participants and serum was isolated by centrifugation at 1500 r.p.m. for 5 min, then all sera were aliquoted and stored at −80°C for hormonal analysis. The analysis of circulating E2 was performed in serum samples procured from AA and CA patients with matched age (~ 54 years), body mass index (BMI; 26 kg/m^2), PSA (6 ng/ml) and tumor grade [Gleason score (GS) < 7]. For comparative interracial baseline analysis, the E2 levels were also monitored in serum derived from age-matched normal subjects representing AA and CA (Supplementary Table 1, available at *Carcinogenesis* Online). E2 was measured in diluted serum (1:2) by an enzyme immunoassay kit according to the manufacturer's protocol (Cayman Chemical Co., MI). The E2 enzyme immunoassay kit is a competitive assay between serum E2 and E2-acetylcholinesterase for a limited amount of E2 antiserum.

Tissue microarray analysis

The differential expression of ERβ in prostate tumors in the biracial population was performed by immunohistochemical analysis using an ethnicity-based tissue microarray (TMA-4). Designed by the National Cancer Institute, the TMA-4 provides high statistical power to investigate possible differences in PCa marker prevalence between AA and CA men. The tissue cores encompass four neoplastic tissue samples from 150 each of AA and CA biopsies, 17 benign prostatic hyperpasia (BPH) cores, 13 normal cores and 3 cell line cores (LNCaP, DU-145 and PC-3). The clinical annotations of PCa patients include age at diagnosis (AAD), race, PSA at diagnosis, tumor size, TNM stage, GS and grade,

PSA recurrence, PSA recurrence-free (PRF) and vital status (Supplementary Table 2, available at *Carcinogenesis* Online). Although the TMA-4 is lacking metastatic cores, it contains tissue cores encompassing GS range from 6 to 9. The TMA-4 information and maps can be retrieved at http://cpctr.cancer.gov/cpctr_tma.html#tma2. For immunohistochemical analysis, the TMA slides were deparaffinized, rehydrated and immunostained using Biocare reagents in a Biocare Nemesis 7200 automated system (Biocare Medical, Concord, CA). The endogenous biotin and H_2O_2 were quenched by sequential incubation in 3% H_2O_2 (5 min) and avidin–biotin blocking solution (10 min). Antigen retrieval (Biocare BORG solution) and non-specific site blocking (Sniper block solution) were followed by addition (1:100 dilution) of mouse monoclonal anti-ERβ antibody (abcam, Cambridge, MA) for 45 min. The ERβ antibody was raised against a recombinant 6-His fusion protein encoding amino acids from 1–153, a specific peptide for human ERβ. The antigen–antibody complex was revealed using horseradish peroxidase–conjugated secondary antibody (10 min) and visualized by diaminobenzidene substrate–chromogen solution. The slides were counterstained by hematoxylin and bluing solution. Negative controls were prepared in the absence of the primary antibody. Immunoreactivity of ERβ was scored using high-resolution digital images (NanoZoomer, UK) at ×20 magnification with a web-based interface and Distiller software (SlidePath Ltd, Dublin, Ireland). A histochemical score (H-score) was used to assess the intensity of ERβ and the percentage of stained cells as reported previously (25). H-score was calculated according to the following formula: H-score = (% negative nuclei × 0) + (% weak staining nuclei × 1) + (% moderate nuclei × 2) + (% strong nuclei × 3). The TMA slides were also independently examined and scored under light microscopy by two pathologists from Tulane University (K.M. and B.E.C. Jr). The agreement between the software and observers was excellent with interclass correlation scores >0.85. The final score of the AA and CA tissue cores was expressed as mean ± standard error.

Laser capture microdissection and quantitative reverse transcription–PCR

Thirty frozen PCa sections provided by the Louisiana Cancer Research Consortium Biospecimen Core were subjected to laser capture microdissection. Clinical annotations of these samples are provided in Supplementary Table 4 (available at *Carcinogenesis* Online), including age, GS, PSA and tumor grade. Briefly, after thawing at room temperature for 10 s, the slides were fixed in 70% ethanol for 10 s, then stained in hematoxylin (40 s), bluing solution (20 s) and eosin (20 s), followed by dehydration twice in 95% ethanol and 100% ethanol for 15 s. The sections were then incubated in xylene, air dried and microdissected using PixCell II system and CapSure LCM caps (Arcturus Engineering, Mt. View, CA). Matched normal prostate epithelium and tumor cells in each section were laser capture microdissection procured using ~2000 pulses, spot diameter of 15 µm and 35–45 mW laser power. Total RNA was extracted from captured cells by TRI Reagent (Molecular Research Centre, Cincinnati, OH), mixed with RNA carrier GenElute™ Linear Polyacrylamide (Sigma, St Louis, MO) and treated with RQ1 RNase-free DNase (Promega Corporation, Madison, WI). The RNA yield and integrity were determined using an Agilent 2100 bio-analyzer (Agilent Technologies, Palo Alto, CA). The complementary DNA was synthesized and subjected into quantitative reverse transcription–PCR analysis (Thermal Cycler, Bio-Rad, CA) using primers for ERβ (forward, 5′-GGCAGAGGACAGTAAAAGCA-3′; reverse, 5′-GGACCACACAGCAGAAAGAT-3′) and glyceraldehyde 3-phosphate dehydrogenase (forward, 5′-AGAAGGCTGGG GCTCATTTG-3′; reverse, 5′-AGGGGCCATCCACAGTCTTC-3′).

ERβ expression profile in independent cohorts of PCa

We extracted and analyzed microarray data encompassing prostate tumor messenger RNA expression profiles in two independent cohorts. The first set was extracted from Gene Expression Omnibus (GEO; GSE 6919) profiled by Affymetrix HG-U95av2 and consists of four probe-set IDs (34431_at, 31437_r_at, 31436_s_at, 1442_at) with PCa gene expression, including ERβ. The arrays include 171 samples; 18 normal samples, 63 normal adjacent to the tumor, 65 primary tumors and 25 metastatic tumors as reported previously (26). The raw microarray data were preprocessed by Robust Multi-array Analysis procedure with quantile normalization method (27). ERβ gene expression was expressed in $\log_2$ scale. A heat-map was employed to investigate any changes in the pattern of ERβ gene expression at different grades of PCa. For each probe set, the median of ERβ gene expression in each group was used for the analysis. The second set of data was extracted from Oncomine Web site (www.oncomime.org), including 139 human microdissected samples procured from AA (n = 24) and CA (n = 115), and all descriptive details of these samples were reported before (28).

Statistical analysis

Statistical significance was analyzed using one-way analysis of variance method for comparing multiple groups, followed by Dunnett's post hoc multiple comparison test to evaluate differences with respect to a control group. Cancer-specific survival rates were evaluated on the basis of a Cox proportional hazard model, and statistical significance was determined with corresponding Wald's tests. The Pearson correlation coefficient was used to test the correlation among different variables. The study hypotheses were tested on the 5% level of significance throughout the analysis. All statistical summaries and analyses were performed using SAS software (version 9.1 or higher in Windows) and R/Bioconductor.

Results

Clinicopathological analysis

For serum E2 study, the average age of normal subjects was 54.9 ± 3.9 and 54.7 ± 5.1 years old and the BMI was 25.4 ± 3.9 and 27.3 ± 5.9 for AA and CA men, respectively. The average age of PCa patients was 57.5 ± 7.1 years for AA and 62.8 ± 5.5 years old for CA men. BMI was 30.2 ± 4.2 for AA regarding 29.3 ± 4.8 for CA men. PSA levels were 7.52 ± 7.6 and 5.55 ± 2.3 ng/ml in AA and CA men, respectively (Supplementary Table 1, available at *Carcinogenesis* Online). The ERβ TMA study involved analysis of four neoplastic tissue samples from each of the 150 AA and CA tumor tissue cores. The average AAD was 59.5 ± 6.3 and 62.8 ± 6 years old for AA and CA men, respectively. Sixteen percent of AA patients have a GS ≥ 8, compared with 24% of CA. PRF was 37.04% (n = 50) in AA compared with 44.91% (n = 66) in CA. Other patient clinicopathological characteristics are summarized in Supplementary Table 2 (available at *Carcinogenesis* Online).

Circulating levels of E2 are elevated in AA men

The E2 concentration (pg/ml) was measured by enzyme immunoassay method in the sera of AA versus CA men in normal (n = 41) and PCa patients (n = 50). Circulating E2 levels in normal subjects were influenced by the race with higher levels among AA men (P = 0.0332) (Figure 1a). Significant elevation of circulating E2 levels was detected in AA (P = 0.0011), but not in CA (P = 0.1814), with PCa compared with their corresponding age- and race-matched normal subjects (Figure 1b and c). Inter-racial analysis demonstrates a significant increase (P < 0.0046) in circulating E2 levels in AA (30.97 ± 14.99 pg/ml) compared with CA men (19.01 ± 9.51 pg/ml) with PCa (Figure 1d and Supplementary Table 1, available at *Carcinogenesis* Online).

Regardless of race, there was no correlation between E2 levels and age (r = −0.024; P = 0.894) or BMI (r = −0.071, P = 0.690) in normal patients (Table I). The remarkable increase of E2 blood level in AA men did not show any correlation with AAD (r = −0.148, P = 0.557), BMI (r = 0.006, P = 0.986) or PSA concentration (r = 0.007, P = 0.980) in PCa patients (Table I).

ERβ is selectively expressed in prostate tumors of AA men

The specificity of ERβ antibody was examined by western blot analysis. For immunohistochemical analysis, appropriate dilution of the ERβ antibody was optimized on human breast, ovarian and prostate cancer tissue sections and examined by the pathologist (K.M.). Nuclear immunoreactivity to ERβ was detected in 45.33% (136/300) of PCa patients compared with normal patients (50.0%) and the BPH (45.75%) of prostatic tissues (Figures 2 and 3a–b). Interestingly, a high frequency of nuclear immunostaining of ERβ (57.33%; 86/150) was observed in AA compared with CA men (33.3%; 50/150) (Figure 2 and Supplementary Table 3, available at *Carcinogenesis* Online). Further analysis revealed that 30.66% of stained nuclei had weak, 16.0% moderate and 10.66% strong immunostainings in tumors of AA patients. In contrast, although 16.66% and 10.66% had weak and moderated staining, respectively, only 6.0% of the tumor nuclei were found to have a strong staining intensity in CA men. As positive controls, both LNCaP and DU-145 PCa cell lines revealed an intense immunoreactivity to ERβ (Figure 2e–h). Overall, the average H-score of ERβ showed a significant increase (P < 0.05) in PCa patients (n = 296) compared with normal cores (n = 28) (Figure 3a). Notably, the H-score of ERβ was also higher (P < 0.005) in AA (n = 148) than in CA (n = 150) of PCa patients (Figure 3b). When the data were stratified based on GS, there was a significant increase in H-score of ERβ at Gleason 7 in AA compared with CA men (P < 0.05) (Figure 3c).

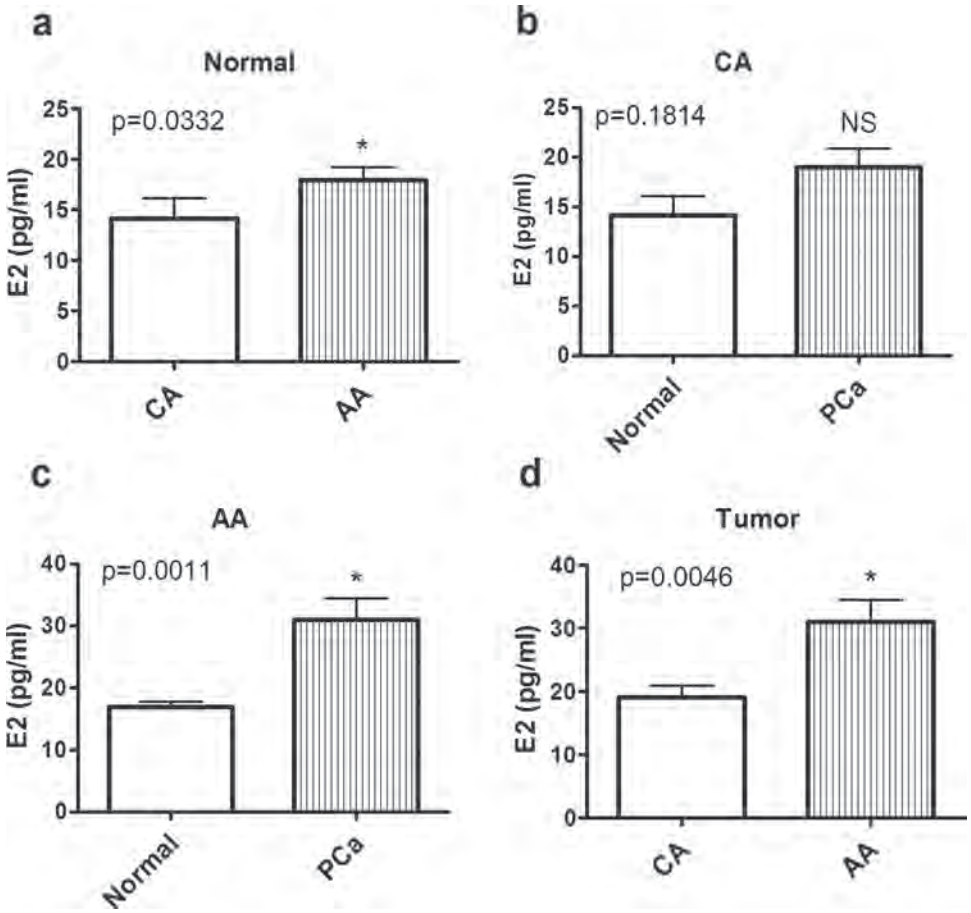

Fig. 1. Circulating E2 levels in normal and PCa patients. Blood was collected from 40 normal subjects and 50 PCa patients. Samples were equally divided into AA and CA. Based on race, the blood level of E2 (pg/ml) was measured in the normal versus PCa patients (**a–d**). *$P < 0.05$ is considered significant regarding normal or CA men. NS, nonsignificant.

Correlation of ERβ histochemical score with clinical parameters of PCa patients

The correlation of ERβ expression with PRF survival in AA and CA men was examined using a Cox proportional hazard model. The potential impacts of other factors such as ERβ-HS were considered when fitting the model by selecting the histochemical score (HS) of 5, 15 and 25 as, respectively, low, medium and high expression intensity of ERβ (Supplementary Table 3, available at *Carcinogenesis* Online). The final significant models we obtained are ones pertaining to race ($P < 0.0106$), the squared root of ERβ-HS ($P < 0.0299$) and ERβ-HS ($P < 0.0595$) as the covariates. Other factors such as AAD and GS do not have significant impact to the PRF survival. This may be attributed to high correlation between age and ERβ-HS in AA group. The PRF survival curves stratified by the degree of intensity (HS) of ERβ immunostaining is illustrated in Figure 3d. In this model, a significant negative correlation ($P < 0.0106$) was observed between ERβ, regardless of HS, and PRF survival in AA men versus CA men. The data imply that ERβ nuclear immunoreactivity can serve as a prognostic indicator of disease progression and poor clinical outcome in this ethnic group of patients.

Consistent with PRF, the ERβ-HS was found to be correlated with the AAD in AA men ($r = 0.3596$, $P = 0.0418$). Aside from AAD, there was no correlation between ERβ-HS and any of other clinical parameters related to AA patients. In contrast, no correlation was observed between ERβ-HS and GS ($r = 0.126$, $P = 0.125$), AAD ($r = 0.071$, $P = 0.3906$) or PRF ($r = 0.005$, $P = 0.9696$) in CA men (Table II). Nevertheless, a positive correlation was found between AAD and GS ($r = 0.191$, $P = 0.008$) as race-independent factor (Table II).

Validation of ERβ gene expression in independent cohort of PCa patients

Next, we validated the differential gene expression of ERβ in 30 microdissected prostate tumors as oppose to their matched normal glands. In general, the ERβ transcripts were found to be approximately 3-fold higher in PCa than in normal glands ($P < 0.01$), regardless of race. When race stratified, the ERβ transcripts are expressed at significantly higher levels ($P < 0.05$) in prostate tumors derived from AA than in CA men (Figure 4a). A positive correlation was detected between ERβ expression and GS ($r = 0.576$, $P = 0.04$) in AA men, as well as between ERβ expression and tumor grade in both AA ($r = 0.649$, $P = 0.016$) and CA ($r = 0.660$, $P = 0.004$) men. The sample clinical annotations and analysis of their correlation with ERβ gene expression are depicted in Supplementary Tables 4 and 5, available at *Carcinogenesis* Online. Moreover, we also validated ERβ gene expression in two independent cohorts of PCa using pre-existing datasets extracted from 171 samples (GEO/PubMed), as well as 139 samples (Oncomine), as described in the Methods section. In the first dataset, the ERβ gene expression was detected at significantly higher levels in metastatic tumors ($P = 0.015$) and the heat-map showed a positive correlation between ERβ transcript and PCa progression (Figure 4b and c). In the second cohort encompassing samples procured from 24 AA and 115 CA as reported before (28), the ERβ transcript levels are significantly elevated in metastatic versus primary tumors (data not shown). However, no significant difference was identified based on the race or age in CA ($P = 0.481$) or AA men ($P = 0.869$) (Figure 4d–f), possibly due to sample size difference between the two groups.

Table I. Correlation of E2 with age, BMI, GS and PSA of normal and prostate cancer of AA and CA men subjected for E2 measurement (pg/ml serum)

			AA					CA					Total				
			Age	BMI	E2			Age	BMI	E2			Age	BMI	E2		
Normal ($n = 41$)	Age	*r*	1.000	0.037	−0.004			1.000	−0.430	0.114			1.000	−0.228	−0.024		
		P		0.885	0.989				0.096	0.673				0.195	0.894		
		N	21	21	21			20	20	20			41	41	41		
	BMI	*r*		1.000	−0.126				1.000	0.059				1.000	−0.071		
		P			0.620					0.828					0.690		
		N		21	21				20	20				41	41		
	E2	*r*			1.000					1.000					1.000		
		P															
		N			21					20					41		
			Age	BMI	E2	GS	PSA	Age	BMI	E2	GS	PSA	Age	BMI	E2	GS	PSA
Tumor ($n = 50$)	Age	*r*	1.00	−0.082	−0.148	0.218	0.285	1.000	−0.025	−0.006	0.416	0.094	1.000	−0.071	−0.218	0.299	0.082
		P		0.799	0.557	0.385	0.285		0.926	0.976	**0.043**	0.613		0.720	0.165	0.054	0.639
		N	25	25	25	25	25	25	25	25	25	25	50	50	50	50	50
	BMI	*r*		1.00	0.006	0.003	−0.102		1.000	−0.080	−0.005	−0.185		1.000	−0.005	0.012	−0.062
		P			0.986	0.992	0.779			0.759	0.986	0.565			0.979	0.951	0.783
		N		25	25	25	25		25	25	25	25		50	50	50	50
	E2	*r*			1.00	0.398	0.007			1.000	−0.042	0.090			1.000	0.091	0.143
		P				0.127	0.980				0.864	0.713				0.605	0.413
		N			25	20	25			25	20	25			50	40	50
	GS	*r*				1.00	0.75				1.000	0.296				1.000	0.083
		P					0.783					0.218					0.634
		N				25	25				25					50	50
	PSA	*r*					1.000					1.000					1.000
		P															
		N					25					25					50

Pearson correlation coefficient (*r*) is calculated among groups and number in bold indicates significance at $P < 0.05$.

Discussion

The causes of disproportionate incidence and mortality of PCa among AA men, in comparison with CA and other ethnic minorities, are not fully understood. Although initially responsive to androgen ablation therapy, prostate carcinomas inevitably progress to castration-resistant PCa (CRPC) for which no efficacious treatment is currently available. Deregulated growth and survival signaling is a characteristic of CRPC, suggesting that factors other than androgens contribute to PCa progression. However, several experimental and epidemiological studies have suggested a potential role for estrogens in the pathogenesis of PCa. Consistent with other studies (12), our ethnicity-based study revealed selective elevation of serum E2 levels in AA compared with CA men and corresponding race-, and age-matched normal subjects. Estradiol increases cell proliferation in LNCaP cell line (29) and induces carcinoma *in situ* and adenocarcinoma in the prostates of transgenic mice (30). Likewise, E2 metabolism has been shown to play a key role in prostate carcinogenesis (31). In contrast, low circulating E2 has been detected in Japanese men, known to have a low risk of PCa (32). Moreover, serum levels of testosterone, dihydrotestosterone, prolactin, follicular stimulating hormone, luteinizing hormone, estron and estradiol do not correlate with PCa risk (33,34). However, older men with high estrogen to testosterone ratio are at increased risk of PCa (35). Conversely, a positive correlation between testosterone to E2 ratios and PCa risks was found in young CA but not in AA men (36). On the blood level and regardless of race, our study revealed no correlation of E2 with BMI, AAD, PSA level or GS in PCa patients. Furthermore, the fact that in the Cox model, the race variable (1 for AA, 0 for CA) has a positive coefficient is consistent with the report that AA men have more aggressive disease at early age in comparison with CA men and as a result, die at an earlier age. The aforementioned findings argue that high circulating estrogens may pose risk for PCa in aging populations, especially at young age among AA men.

The expression and functional significance of ERβ in prostate tumorigenesis is still a matter of conjecture. The ERβ subtype has been shown to be expressed in most metastatic PCa, suggesting that therapeutic targeting this receptor may be effective in late-stage PCa (19,22). This notion was further strengthened by the fact that ER antagonists inhibit growth and/or induce apoptosis in PCa cells expressing either ERβ or both ER subtypes (37,38). Although ERβ expression has been documented in PCa, its expression as influenced by race remains elusive. We demonstrate high histochemical score for ERβ nuclear immunostaining in adenocarcinomas in PCa patients in comparison with normal subjects. Inter-racial analysis demonstrates a significant increase in both ERβ transcripts and protein levels in tumors of AA as opposed to CA men. The biracial differential expression of ERβ was validated in microdissected tumors procured from an independent cohort at the gene transcription level by quantitative reverse transcription–PCR. Dataset extracted from another independent cohort study revealed increased ERβ transcripts in metastatic tumors, although it is not clear if these metastatic tumors are castration resistant.

Consistent with our data, detection of ERβ in high-grade prostate tumors has been reported, regardless of race (19,39). In the same study, the authors reported that ERβ is predominantly expressed in lymph nodes and PCa bone metastasis. Significant levels of ERβ in primary and metastatic adenocarcinoma suggest that tumor cells may exploit estrogen-ERβ-mediated pathway for survival. Conversely, ERβ downregulation in high-grade prostatic intraepithelial neoplasia

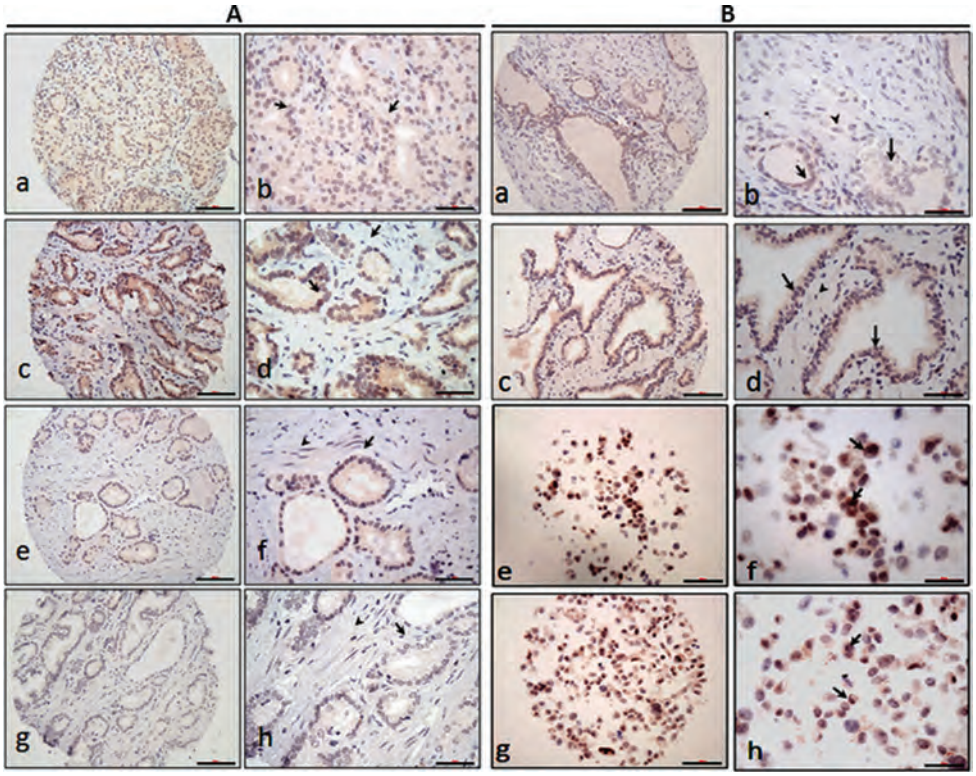

Fig. 2. Immunostaining of ERβ in ethnicity-based PCa TMA: TMA encompasses 300 prostate tumor cores with 150 each from AA and CA men, 17 BPH cores, 13 normal cores and 3 PCa cell lines. A strong intensity of ERβ was observed in malignant cells (nuclear staining denoted by arrows) compared with adjacent stroma (arrows head) as depicted in (**A**). (A) The immunostaining of ERβ in AA (**a–d**) was higher in AA than in CA men (**e–h**). (**B**) The immunoreactivity of ERβ was detected in 27 samples of BPH (**a–b**) and normal prostate glands (**c–d**). LNCaP and DU-145 PCa cell lines stained positive with ERβ antibody (**e–h**) and were used as positive controls. Scale bars represented as 100 µm (a, c, e and d) and 50 µm (b, d, f and h).

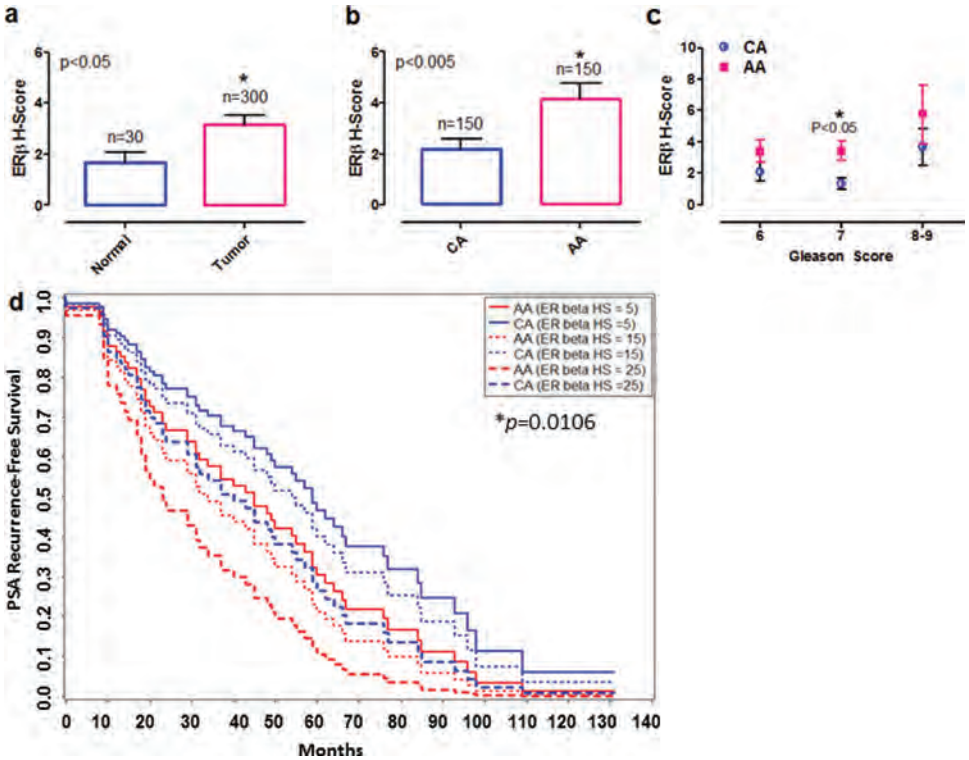

Fig. 3. HS of ERβ protein expression in ethnicity-based PCa TMA: ERβ-HS was calculated as indicated before. ERβ-HS was calculated in normal versus PCa men (**a**), CA versus AA men (**b**) or based on GS in AA and CA men (**c**). Kaplan–Meier survival curve was stratified according to the effect of ERβ-HS on PRF in AA (red color) versus CA men (blue color) at selected HS of 5 (considered low HS), 15 (considered medium HS) and 25 (considered high HS) (**d**). *$P < 0.05$ is considered significant.

Table II. Correlation of ERβ-HS with GS, AAD and PRF of AA and CA prostate cancer patients

Parameters		AA				CA				Total			
		GS	AAD	PRF	ERβ-HS	GS	AAD	PRF	ERβ-HS	GS	AAD	PRF	ERβ-HS
GS	*r*	1.000	0.3326	–0.409	–0.0613	1.0000	0.0291	0.0039	0.1258	1.0000	0.1918	–0.1456	–0.0085
	P		**0.0001**	**0.0031**	0.4557		0.7238	0.9753	0.1251		**0.0008**	0.1188	0.8826
	N	150	150	50	150	150	150	66	150	300	300	116	300
AAD	*r*		1.0000	–0.307	0.3596		1.0000	0.1137	0.0706		1.0000	–0.0199	0.0108
	P			**0.0303**	**0.0418**			0.3632	0.3906			0.8321	0.8512
	N		150	50	150		150	66	150		300	116	300
PRF	*r*			1.0000	0.0391			1.000	0.0048			1.000	–0.0011
	P				0.7877				0.9696				0.9910
	N			50	50			66	66			116	116
ERβ-HS	*r*				1.0000				1.0000				1.000
	P												
	N				150				150				300

Pearson correlation coefficient (*r*) is calculated among groups and $P < 0.05$ is considered significant (bold numbers).

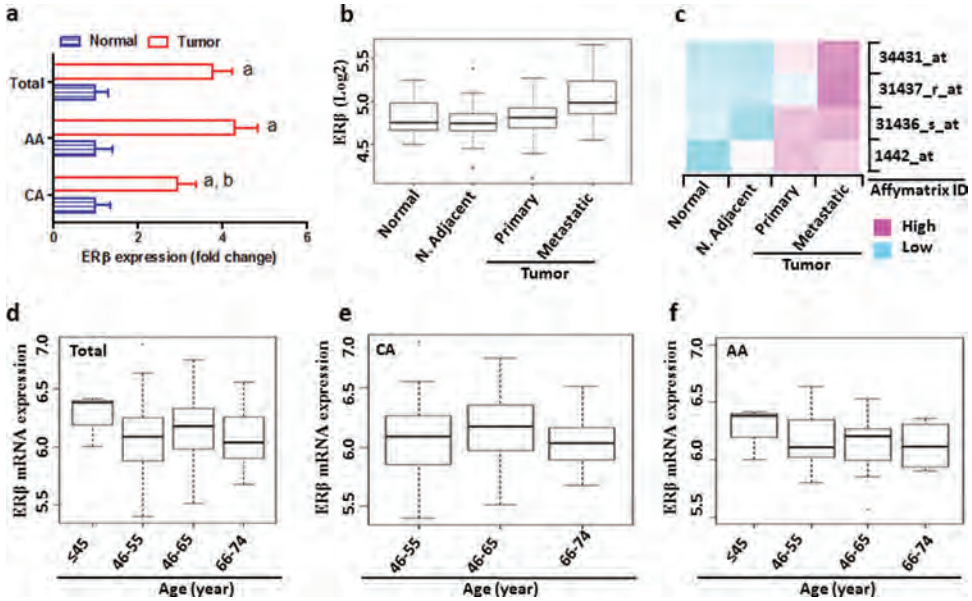

Fig. 4. ERβ gene expression profile in normal and PCa tissues. (**a**) ERβ messenger RNA level in normal and PCa microdissected samples was assessed by quantitative reverse transcription–PCR. Total RNA was extracted from 30 tissue sections procured by laser capture microdissection from matched normal glands and tumors of PCa patients. Data are expressed as fold change normalized to glyceraldehyde 3-phosphate dehydrogenase. *$P < 0.05$ is considered significant to normal subjects (a) or CA men (b). To study the expression profile of ERβ in independent cohorts, data were extracted from 117 samples including normal and PCa tumor and the expression was expressed as $\log_2$ (**b**). The heat-map of the median ERβ expression in these 117 normal and human PCa samples ($n = 18$ for normal, $n = 63$ for normal adjacent, $n = 65$ for primary tumor and $n = 25$ for metastatic tumor) was generated using different Affymatrix IDs (**c**). Red color represents the highest value while blue color represents the lowest value. The second dataset was extracted from other cohort including 139 samples ($n = 24$ for AA and $n = 115$ for CA). Correlation analysis between ERβ expression and AAD is illustrated (**d–f**).

(39) is consistent with its potential protective effects. Leav *et al.* (22) reported that prostatic carcinogenesis is characterized by the loss of ERβ expression at high-grade dysplasia, followed by reappearance at grade 3 cancers and then rarely detected at grade 4/5 neoplastic tissues. Inhibition of PCa growth by selective ER modulators through ERβ induction further strengthens this notion (38,40–42). Mechanistically, ERβ is required to impede epithelial-to-mesenchymal transition through destabilization of HIF-1α and inhibition of vascular endothelial growth factor-mediated Snail nuclear localization (43). The controversy of ERβ staining in aggressive PCa tissue may also be attributed to differential control of gene transcription by methylation (37,44), a shift in estrogen to androgen ratio in CRPC patients, induction of non-classical androgen receptor pathways in CRPC patients (15) or the specificity of antibodies used in tissue immunostaining.

Our adjusted multivariate analysis shows that ERβ expression correlates with AAD and low PRF survival in AA men in comparison with CA men. Gene expression analysis in datasets derived from independent cohort revealed significant upregulation of ERβ in prostate tumors and that this expression correlates with disease progression. In view of these findings, we can infer that prostate tumor expression may be a novel predictor of disease progression, poor prognosis and clinical outcome, especially among AA men. Similar findings of poor survival rates in hormone refractory patients was associated with high expression of aromatase and BRCA1 and a weak immunoreactivity against ERα in stromal cells (45). Taken together, our study implicates a pivotal role of estrogen-ERβ axis in PCa risk, progression and poor prognosis, especially among AA men. The mechanism(s) of E2-ERβ signaling axis in disease progression and development of CRPC in AA men certainly warrants further investigation.

Supplementary material

Supplementary Tables 1–5 can be found at http://carcin.oxfordjournals.org/

Funding

National Institutes of Health (U01CA149204-01A1 to A.B.A); the Department of Defense (PC081598 to A.B.A.); American Cancer Society (RSGT-09-248-01-CCE to A.B.A.).

Acknowledgements

The authors thank Ms Grace Kelly for support in scoring analysis of TMAs by SlidePath image software (SlidePath Ltd, Dublin, Ireland). The authors also thank Ms Jennifer Cvitanovic from LCRC Biospecimen core for providing human PCa tissue sections and serum samples.

Conflict of Interest Statement: None declared.

References

1. Couse,J.F. *et al.* (1999) Estrogen receptor null mice: what have we learned and where will they lead us? *Endocr. Rev.*, **20**, 358–417.
2. Gustafsson,J.A. (2003) What pharmacologists can learn from recent advances in estrogen signalling. *Trends Pharmacol. Sci.*, **24**, 479–485.
3. Chang,E.C. *et al.* (2006) Impact of estrogen receptor beta on gene networks regulated by estrogen receptor alpha in breast cancer cells. *Endocrinology*, **147**, 4831–4842.
4. Ho,S.M. *et al.* (2006) Estrogens and antiestrogens as etiological factors and therapeutics for prostate cancer. *Ann. N. Y. Acad. Sci.*, **1089**, 177–193.
5. Horowitz,M. *et al.* (1993) Effects of norethisterone on bone related biochemical variables and forearm bone mineral in post-menopausal osteoporosis. *Clin. Endocrinol. (Oxf).*, **39**, 649–655.
6. Jongen,V. *et al.* (2009) Expression of estrogen receptor-alpha and -beta and progesterone receptor-A and -B in a large cohort of patients with endometrioid endometrial cancer. *Gynecol. Oncol.*, **112**, 537–542.
7. Konstantinopoulos,P.A. *et al.* (2003) Oestrogen receptor beta (ERbeta) is abundantly expressed in normal colonic mucosa, but declines in colon adenocarcinoma paralleling the tumour's dedifferentiation. *Eur. J. Cancer*, **39**, 1251–1258.
8. Kuiper,G.G. *et al.* (1997) Comparison of the ligand binding specificity and transcript tissue distribution of estrogen receptors alpha and beta. *Endocrinology*, **138**, 863–870.
9. Liu,M.M. *et al.* (2002) Opposing action of estrogen receptors alpha and beta on cyclin D1 gene expression. *J. Biol. Chem.*, **277**, 24353–24360.
10. Krieg,M. *et al.* (1993) Effect of aging on endogenous level of 5 alpha-dihydrotestosterone, testosterone, estradiol, and estrone in epithelium and stroma of normal and hyperplastic human prostate. *J. Clin. Endocrinol. Metab.*, **77**, 375–381.
11. Harris,R. *et al.* (2002) Screening for prostate cancer: an update of the evidence for the U.S. Preventive Services Task Force. *Ann. Intern. Med.*, **137**, 917–929.
12. Rohrmann,S. *et al.* (2007) Serum estrogen, but not testosterone, levels differ between black and white men in a nationally representative sample of Americans. *J. Clin. Endocrinol. Metab.*, **92**, 2519–2525.
13. Briganti,A. (2009) Oestrogens and prostate cancer: novel concepts about an old issue. *Eur. Urol.*, **55**, 543–545.
14. Leung,Y.K. *et al.* (2011) Estrogen receptor β: switching to a new partner and escaping from estrogen. *Sci. Signal.*, **4**, pe19.
15. Nakajima,Y. *et al.* (2011) Estrogen regulates tumor growth through a nonclassical pathway that includes the transcription factors ERβ and KLF5. *Sci. Signal.*, **4**, ra22.
16. Hu,W.Y. *et al.* (2011) Estrogen-initiated transformation of prostate epithelium derived from normal human prostate stem-progenitor cells. *Endocrinology*, **152**, 2150–2163.
17. Carruba,G. (2007) Estrogen and prostate cancer: an eclipsed truth in an androgen-dominated scenario. *J. Cell. Biochem.*, **102**, 899–911.
18. Adams,J.Y. *et al.* (2002) Expression of estrogen receptor beta in the fetal, neonatal, and prepubertal human prostate. *Prostate*, **52**, 69–81.
19. Lai,J.S. *et al.* (2004) Metastases of prostate cancer express estrogen receptor-beta. *Urology*, **64**, 814–820.
20. Latil,A. *et al.* (2001) Evaluation of androgen, estrogen (ER alpha and ER beta), and progesterone receptor expression in human prostate cancer by real-time quantitative reverse transcription-polymerase chain reaction assays. *Cancer Res.*, **61**, 1919–1926.
21. Linja,M.J. *et al.* (2003) Expression of ERalpha and ERbeta in prostate cancer. *Prostate*, **55**, 180–186.
22. Leav,I. *et al.* (2001) Comparative studies of the estrogen receptors beta and alpha and the androgen receptor in normal human prostate glands, dysplasia, and in primary and metastatic carcinoma. *Am. J. Pathol.*, **159**, 79–92.
23. Pasquali,D. *et al.* (2001) Loss of estrogen receptor beta expression in malignant human prostate cells in primary cultures and in prostate cancer tissues. *J. Clin. Endocrinol. Metab.*, **86**, 2051–2055.
24. Gallo,D. *et al.* (2012) Estrogen receptor beta in cancer: an attractive target for therapy. *Curr. Pharm. Des.*, **18**, 2734–2757.
25. McCarty,K.S. Jr *et al.* (1985) Estrogen receptor analyses. Correlation of biochemical and immunohistochemical methods using monoclonal antireceptor antibodies. *Arch. Pathol. Lab. Med.*, **109**, 716–721.
26. Chandran,U.R. *et al.* (2007) Gene expression profiles of prostate cancer reveal involvement of multiple molecular pathways in the metastatic process. *BMC Cancer*, **7**, 64.
27. Irizarry,R.A. *et al.* (2003) Exploration, normalization, and summaries of high density oligonucleotide array probe level data. *Biostatistics*, **4**, 249–264.
28. Taylor,B.S. *et al.* (2010) Integrative genomic profiling of human prostate cancer. *Cancer Cell*, **18**, 11–22.
29. Arnold,J.T. *et al.* (2005) Comparative effects of DHEA vs. testosterone, dihydrotestosterone, and estradiol on proliferation and gene expression in human LNCaP prostate cancer cells. *Am. J. Physiol. Endocrinol. Metab.*, **288**, E573–E584.
30. Wang,Y. *et al.* (2000) Sex hormone-induced carcinogenesis in Rb-deficient prostate tissue. *Cancer Res.*, **60**, 6008–6017.
31. Lord,R.S. *et al.* (2002) Estrogen metabolism and the diet-cancer connection: rationale for assessing the ratio of urinary hydroxylated estrogen metabolites. *Altern. Med. Rev.*, **7**, 112–129.
32. Bosland,M.C. (2000) The role of steroid hormones in prostate carcinogenesis. *J. Natl Cancer Inst. Monogr.*, **27**, 39–66.
33. Hsing,A.W. *et al.* (1993) Serological precursors of cancer: serum hormones and risk of subsequent prostate cancer. *Cancer Epidemiol. Biomarkers Prev.*, **2**, 27–32.
34. Roddam,A.W. *et al.* (2008) Endogenous sex hormones and prostate cancer: a collaborative analysis of 18 prospective studies. *J. Natl Cancer Inst.*, **100**, 170–183.
35. Griffiths,K. (2000) Estrogens and prostatic disease. International Prostate Health Council Study Group. *Prostate*, **45**, 87–100.
36. Tsai,C.J. *et al.* (2006) Sex steroid hormones in young manhood and the risk of subsequent prostate cancer: a longitudinal study in African-Americans and Caucasians (United States). *Cancer Causes Control*, **17**, 1237–1244.
37. Lau,K.M. *et al.* (2000) Expression of estrogen receptor (ER)-alpha and ER-beta in normal and malignant prostatic epithelial cells: regulation by methylation and involvement in growth regulation. *Cancer Res.*, **60**, 3175–3182.
38. Kim,I.Y. *et al.* (2002) Raloxifene, a mixed estrogen agonist/antagonist, induces apoptosis in androgen-independent human prostate cancer cell lines. *Cancer Res.*, **62**, 5365–5369.
39. Fixemer,T. *et al.* (2003) Differential expression of the estrogen receptor beta (ERbeta) in human prostate tissue, premalignant changes, and in primary, metastatic, and recurrent prostatic adenocarcinoma. *Prostate*, **54**, 79–87.
40. Dondi,D. *et al.* (2010) Estrogen receptor beta and the progression of prostate cancer: role of 5alpha-androstane-3beta,17beta-diol. *Endocr. Relat. Cancer*, **17**, 731–742.
41. Kim,H.T. *et al.* (2002) Raloxifene, a mixed estrogen agonist/antagonist, induces apoptosis through cleavage of BAD in TSU-PR1 human cancer cells. *J. Biol. Chem.*, **277**, 32510–32515.
42. Rossi,V. *et al.* (2010) Raloxifene induces cell death and inhibits proliferation through multiple signaling pathways in prostate cancer cells expressing different levels of estrogen receptor alpha and beta. *J. Cell Physiol.*, **226**, 1334–1339.
43. Mak,P. *et al.* (2010) ERbeta impedes prostate cancer EMT by destabilizing HIF-1alpha and inhibiting VEGF-mediated snail nuclear localization: implications for Gleason grading. *Cancer Cell*, **17**, 319–332.
44. Sasaki,M. *et al.* (2003) Hypermethylation can selectively silence multiple promoters of steroid receptors in cancers. *Mol. Cell. Endocrinol.*, **202**, 201–207.
45. Celhay,O. *et al.* (2010) Expression of estrogen related proteins in hormone refractory prostate cancer: association with tumor progression. *J. Urol.*, **184**, 2172–2178.

Received November 21, 2012; revised April 12, 2013; accepted May 5, 2013

hnRNPH1 Promotes Prostate Tumorigenesis and Hormone Resistance Through Transcriptional Upregulation and Activation of Androgen Receptor: Potential Role in Racial Disparities of Prostate Cancer

Yijun Yang*[1], Dingwu Jia*[1], Zakaria Y. Abd Elmageed[1], Hogyoung Kim[1], Kommu N. Mohan[1], Rodney Davis[6], Sudesh Srivastav[7], Krzysztof Moroz[2,5], Byron E. Crawford[2], Krishnarao Moparty[1,8], Raju Thomas[1,5], Robert S. Hudson[9], Stefan Ambs[9] and Asim B. Abdel-Mageed[1,3,5**]

[1]Department of Urology, [2]Department of Pathology, [3]Department of Pharmacology, [4]Department of Medicine, and [5]Tulane Cancer Center, Tulane University School of Medicine, New Orleans, LA 70112
[6]Department of Urology, University of Arkansas for Medical Sciences, Little Rock, Arkansas 72205
[7]Department of Biostatistics, Tulane University School of Public Health and Tropical Medicine, New Orleans, LA 70112
[8]Division of Urology, Southeast Louisiana Veterans Health Care System (SLVHCS), New Orleans, LA 70112
[9]Laboratory of Human Carcinogenesis, National Cancer Institute, NIH, Bethesda MD, 20892-4258

* Y. Y. and D. J. contributed equally to this work

**** Corresponding author:**
Asim B. Abdel-Mageed, DVM, Ph.D.
Department of Urology, SL-42,
Tulane University Health Sciences Center
1430 Tulane Ave
New Orleans, LA 70112
Tel: 504-988-3634
Fax: 504-988-5059
e-mail: amageed@tulane.edu

Background Despite recent decline, prostate cancer (PC) incidence and mortality rates still remain significantly higher in African-American (AA) men than Caucasian Americans (CA) and other ethnic minority groups. While the causes remain elusive, little is known about the contributory role of the underlying biology in the disproportionate clinical manifestation and outcome of PC among AA men.

Methods We employed an unbiased functional genomics approach to identify genes differentially expressed in freshly procured prostate tumor cells of age- and tumor grade-matched AA and CA men. Laser capture microdissected (LCM)-procured *in vivo*-derived genetic materials of matched normal epithelium and PC cells were subjected to suppressive subtractive hybridization (SSH) to construct microarray chips encompassing two sets of race-based, PC-specific cDNAs. Validation in independent cohorts and functional assays of target genes were performed.

Results Herein we identified in microdissected tumors of African American (AA) men selective expression of heterogeneous nuclear ribonucleoprotein H1 (hnRNPH1) in comparison to Caucasian American (CA) men. The hnRNPH1 expression correlates with androgen receptor (AR) expression, PC progression and development of castration resistant PC (CRPC). The aberrant expression of hnRNPH1 is attributed to promoter methylation and down-regulation of miRNA-22 and miR-212 in prostate tumors in AA-men. Whereas expression promotes tumor formation in *vivo*, hnRNPH1 siRNA silencing confers growth arrest and sensitizes AR-expressing PC cells to the anti-androgen bicalutamide. The hnRNPH1 is a transcriptional target of androgens that upregulates AR transcription through a positive feedback loop in PC cells. Functional studies

demonstrate that hnRNPH1 physically interacts with and enhances ligand-dependent and independent AR *trans*activation through recruitment of steroid receptor coactivator-3 (SRC-3) to its cognate DNA elements on promoters of androgen-regulated genes.

Conclusions Our data support a model in which hnRNPH1 is a novel auxiliary coregulator for hormone dependent and independent AR *trans*activation in prostate tumor cells. The AR-hnRNPH1 axis represents a previously uncharacterized mechanism potentially involved in disease progression, development of therapeutic resistance and ethnic disparity of PC.

In the United States, race has been identified as one of many risk factors for PC with more than 50% higher incidence and mortality rates among AA men than CA counterparts (1). Earlier onset of the disease, high disease volume, aggressive metastatic disease, and poor survival rate are evident among AA males (2, 3). Although the disproportionate incidence and mortality cannot be fully explained by genetic, socioeconomic, and environmental factors (4, 5), chromosome 8q24 has recently been implicated in susceptibility but not the aggressiveness of PC in AA men (6, 7). While a more biological aggressive phenotype has been proposed (8), little attention was focused on unraveling the underlying molecular mechanisms involved in racial disparity of PC.

Aberrant expression of AR has long been implicated in initiation and development of CRPC (9). Based on their physical interactions and ability to modulate transcription, a repertoire of intermediary transcriptional protein complexes (coactivators and corepressors) have been shown to be recruited by AR to modify chromatin and facilitate transcription of androgen-regulated genes (AGRs) in cell type-specific manner (10). Notably, the differential expression and pathophysiological significance of these cofactors in CRPC in AA men has not been established. These facts argue that aberrant expression and/or function of AR and its coregulators may contribute to disease progression and emergence of CRPC in AA men.

As a residual scaffolding of the nucleus to which repeated DNA sequences and actively transcribed genes are anchored (11), the nuclear matrix (NM), has recently sparked a surge of interest as being the molecular underpinning of cancer-specific markers (12). The family of heterogeneous nuclear ribonucleoproteins (hnRNPs) has more than 30 members of ubiquitously expressed NM proteins (13). hnRNPs complex with heterogeneous nuclear RNA (hnRNA) and modulate pre-mRNA biogenesis, metabolism, and transport (14). The hnRNP H/F is subfamily of hnRNPs encoded by different genes into subtype-naïve forms, including hnRNPH

51204(hnRNPH1), hnRNP H' (hnRNP H2), hnRNP F, and hnRNP 2H9 (15). These proteins possess a modular and highly conserved structure encompassing two glycine-rich auxiliary domains and two or three repeats of RNA binding domain termed quasi-RNA recognition motif (qRRM). The hnRNP H/F members bind in concert to cognate G-rich intronic and exonic sequences in close proximity to the polyadenylation site to regulate both inhibitory and stimulatory alternative splicing of target genes (16). As a bona fide component of the NM, (17), the functional significance of hnRNPH1 is relatively unknown and only recently has evidence emerged related to its biological function. Although hnRNPH1 has been shown to be expressed in a number of human cancers (18), its functional significance in cancer development and/or progression has not been elucidated. The rapid reduction of hnRNPH1 transcripts in cells undergoing differentiation (19) underscores a potential role for this NM protein in tumor cell differentiation.

In the present study we identified by an *in vivo* functional genomics approach, encompassing a combined in tandem approach of LCM, SSH and custom cDNA microarray comparative analyses, the differential expression of hnRNPH1 in prostate tumor cells of AA men. Functional analysis depicted a previously uncharacterized role for hnRNPH1 in promoting growth and development of therapeutic by CRPC cells through transcriptional upregulation as well as ligand dependent and independent AR transactivation, possibly via recruitment of coactivator SRC-3, also known as nuclear coactivator-3 (NCOA3).

Methods

Patients and Prostate Cancer Specimens

Fresh, flash-frozen specimens were obtained from age- (50 to 60 yrs) and tumor grade-matched (Gleason score 6) AA and CA prostate cancer patients. All patients received no prior therapy, presented with palpable prostate tumors, and underwent radical prostatectomy. Following surgical removal of the prostate, part of the specimens were excised, embedded in Tissue-Tek® OCT Compound (Jed Pella Inc., Redding, CA), snap-frozen in liquid nitrogen, and stored at -80ºC until processing. In addition, histopathological sections were made from the rest of the specimens for confirmation, staging, and grading of PC. IRB approval was obtained prior to conducting the experiments.

LCM and RNA Preparation

Using a Minotome Plus™ cryostat microtome (Triangle Biomedical Sciences, Inc., Durham, NC), frozen specimens were sectioned (6 μm thick), mounted onto uncoated glass slides, and store in -80ºC until used. For LCM, frozen sections were thawed at room temperature for 10 s, fixed in 70% ethanol for 10 s, and stained in Hematoxylin (40 s), bluing solution (20 s) and Eosin (20 s), followed by dehydration twice in 95% ethanol and 100% ethanol for 15 s. The sections were then incubated in Xylene, air dried, and microdissected using PixCell II system and CapSure LCM caps (Arcturus Engineering, Mountain View, CA, USA). Using replica sections, matched normal prostate epithelium and tumor cells in each section were LCM procured using 2,000~3,000 pulses, spot diameter of 15 μm, and 25-35 mwatt laser power. Total RNA was extracted from pooled captured cells in a 500 μl nuclease-free Eppendorf tube containing 400μl of TRI Reagent (Molecular Research Centre, Inc., Cincinnati, OH) mixed with

1µl of 10µg/µl of RNA carrier GenElute™ Linear Polyacrylamide (Sigma, St. Louis, MO), as per manufacturer's instructions. After recovery of RNA pellet, a DNase treatment step was performed for 2 hr at 37°C using 2 unit of RQ1 RNase-free DNase (Promega Corporation, Madison, WI), followed by re-extraction and precipitation. The RNA yield and integrity were determined using Agilent 2100 bioanalyzer (Agilent Technologies, Palo Alto, CA) with RNA LabChip (Ambion Inc., Austin, TX, USA).

Construction of Race-Based PC-Specific SSH cDNA Libraries

First-strand cDNA synthesis was performed according to the SMART™ PCR cDNA Synthesis kit (Clontech Laboratories, Inc., Palo Alto, CA). For the long-distance (LD)-PCR, 200ng of total RNA from matched LCM captured prostate tumor cells or normal prostate epithelium of each section were reverse transcribed using CDS primer (5'-AAGCAGTGGTAACAACGCAGA $GTACT_{(30)}N_{-1}N$-3') and SMART II oligonucleotide (5'-AAGCAGTGGTAACAACGCAGAG TACGCGGG-3'). The first-strand cDNAs were amplified by 18 to 22 cycles of LD-PCR, as determined by the parallel control tubes, and then purified by ammonium chloride-ethanol precipitation method followed by *Rsa*I digestion to generate shorter, blunt-ended ds cDNA fragments. The purified cDNAs were dissolved with 1 × TE buffer a final concentration of 300 ng/µl. The SSH analysis was performed using CLONTECH PCR-Select™ cDNA Subtraction kit (Clontech Laboratories, Inc., Palo Alto, CA). Briefly, the cDNAs of normal prostate cells (*driver*) and tumor cells (*tester*) were subjected to forward and reverse subtractions. Using T4 DNA ligase, aliquots of the *tester* cDNAs were ligated to Adaptor1 and Adaptor 2R separately. Ligation efficiency was performed using G3PDH 3' primer and PCR primer 1 followed by two rounds of hybridization. In the first hybridization, the *Rsa*I-digested *driver* cDNA was mixed

with either Adaptor1-ligated *tester* cDNA or Adaptor2R-ligated *tester* cDNA. In the second hybridization the two reactions from the first hybridization were mixed and processed for a second hybridization in the presence of freshly denatured *driver* cDNAs to further enrich the differentially expressed transcripts. The missing strands of the adaptors were then filled to create a template for PCR primer 1. To enrich the differentially expressed target sequences, PCR amplification was performed using nested PCR primers 1 and 2R (5'-TCGAGCGGCCGCCCGGGCAGGT-3'; 5'-AGCGTGGTCGCGG CCGAGGT-3') using 10-12 cycles of 94°C for 10 s (denaturing), 68°C for 30 s (annealing), and 72°C for 1.5 min (extension). Subtraction efficiency analysis was determined using β-actin to confirm the reduced relative abundance of the housekeeping gene after SSH. The SSH nested PCR products were cloned using pCR®2.1 vector TA Cloning® Kit (Invitrogen™ Life Technologies, Carlsbad, CA). Hundreds of colonies were analyzed for DNA inserts by direct colony PCR using M13 forward and reverse amplimer set and high fidelity platinum *Taq*® DNA polymerase (Invitrogen™ Life Technologies, Carlsbad, CA) in a thermal cycle conditions of 95°C, 5 min (denaturing) followed by 30 cycles of 94°C for 30 s, 48°C for 30 s, and 72 °C for 2 min (annealing/extension), and a final extension at 72°C for 7 min. The PCR products were resolved onto a 1.2% agarose/EtBr gel and fragment sizes of less than 200 bp or multiple bands were considered negative and were excluded from study.

Custom Construction of Race-Based PC-Specific cDNA Arrays

To generate PC-specific cDNA arrays for AA and CA patients, PCR amplification of the selected clones was carried out using nested PCR primers in 96-well plates then purified by Montage™ PCR_{96} Cleanup Kit (Millipore Corporation, Bedford, MA). Briefly, nested PCR reaction of selected clones was carried out in 96-well plates encompassing 1 μl of diluted

template (1:200 dilution of colony PCR), 36.8 μl of H_2O, 5.0 μl of 10 × high Fidelity PCR buffer, 2.0 μl of 50 mM MgSO4, 2.0 μl of 10 μM Nested PCR primer 1, 2.0 μl of 10 μM Nested PCR primer 2R, 1.0 μl of 10 mM dNTP mix, and 0.2 μl of High Fidelity Platinum *Taq*® DNA polymerase. The thermal cycle conditions included a denaturing step at 94°C, 2 min; followed by 27 cycles of 94°C for 10 s, 68°C for 30 s, and 72 °C for 1.5 min, and by the final extension repair at 72°C for 7 min. The products were resolved onto 1.2% agarose/EtBr and the nested PCR products were then purified by Montage™ PCR_{96} Cleanup Kit (Millipore Corporation, Bedford, MA). Briefly, $MultiScreen_{96}$ PCR plates containing nested PCR products were cleaned using a vacuum manifold, then washed once with 100 μl of H_2O. Samples were eluted in nuclease-free water and transferred to the 384-well plates. DNA concentrations were determined spectrophotometrically and plates were then lyophilized and tightly sealed. For microarray spotting, the cDNAs (750/race group) were individually reconstituted in 150 mM phosphate buffer (pH 8.5) with a DNA concentration of 1 μg/ml. Each cDNA was subsequently printed (Virtek Chipwriter Pro) and pooled to construct two supergrids (one for AA and another for CA) onto GAPS II amino-silane coated glass slides (Corning Inc, Corning, NY). The microarray printer relies on Telechem split pin technology to deliver equally sized spots with low variability of DNA concentration. Additionally, negative and positive controls (housekeeping genes) from the Ambion™ ArrayControls™ Set were included, and each cDNA on the array was double spotted for reliable data interpretation.

Gene Array Analysis

Total RNA isolated from LCM-procured normal epithelium and tumor cells from flash-frozen sections of matched (50 to 60 yrs; Gleason score 6) tissue sections of AA and CA patients was amplified using MessageAmp™ aRNA Kit according with the manufacturer's instruction

(Ambion Inc., Austin, TX). Microarray probes were prepared by *in vitro* RNA transcription followed by reverse transcription of the aRNA in presence of aminoallyl-dUTP, and coupled to Cyanine-3 (Cy3) or Cyanine-5 (Cy5) dye. Briefly, 200 ng of RNA was mixed with T7 Oligo(dT) primer, denatured at 70°C and snap cool on dry ice. Reverse transcription master mix was then added and subsequently incubated at 42°C for 2 hr in an air incubator. The *in vitro* aRNA transcription step was performed using MEGAscript® T7 High-yield Transcription Kit at 37°C overnight in an air incubator. The amplified RNA was then treated with DNase I to remove the cDNAs and subsequently purified using RNeasy® Micro Kit (Qiagen, Inc., Valencia, CA). A second round of amplification was performed using second round primers as shown above. The final concentration of aRNA was determined spectrophotometrically and its quality was determined by denatured RNA gel electrophoresis. The aRNA was then aliquoted and stored at -80°C until for microarray analysis. Probe preparation was performed by reverse transcribing 5 μg of aRNA in presence of 6 μg of random primers (Invitrogen™ Life Technologies, Carlsbad, CA), 500 μM each of dATP, dCTP, and dGTP, 200 μM of 5-aminoallyl- dUTP (Ambion Inc., Austin, TX), 300 μM of dUTP, 10 mM dithiothreitol, and 400 unit of Superscript II (Invitrogen™ Life Technologies, Carlsbad, CA) at 42°C for 3 hours. The reaction was stopped by addition of EDTA and NaOH followed by heating at 65°C for 15 min; reactions were then neutralized with HCl. The cDNA was purified using QiaQuick PCR Purification Kit (Qiagen, Inc., Valencia, CA), vacuum-dried, and resuspended in sodium carbonate buffer (pH 9.0). The coupling reaction was performed by addition of NHS ester of Cy3 or Cy5 dye (Amersham Pharmacia Biotech Inc., Piscataway, NJ) at RT for 1 hr in the dark, quenched by the addition sodium acetate (pH 5.2), and the unincorporated dye was removed using QIAquick PCR

Purification Kit. The labeled cDNAs were vacuum-dried, re-suspended in 1× SlideHyb buffer (Ambion Inc., Austin, TX), mixed (1:1 ratio) and stored at –70^{o}C until used.

The custom race-, PC-based cDNA microarray slides were re-hydrated over steam of boiled water for 5 sec and then dried on a heat block for 5 sec. After UV cross-linking, the slides were washed in 1% SDS for 2 min, incubated in 95°C water for 2 min, dipped in 95% ethanol 20 times, and spun dry by centrifugation. For hybridization, probes prepared from normal and prostate tumors of each patient was denatured at 98°C, mixed at 1:1 ratio and loaded onto the slide in an automated GeneTAC^{TM} Hybridization station (Genomic Solutions Inc., Ann Arbor, MI). An over-night step-down temperature hybridization program (65^{o}C for 3 hr with agitation; 55^{o}C for 3 hr with agitation; 50^{o}C for 12 hr with agitation) was performed followed by medium- (2 cycles at 55^{o}C), high-stringency (2 cycles at 42^{o}C), and post-wash buffer (2 cycles at 42^{o}C) washes. The hybridized slides were scanned by GeneTAC^{TM} UC-IV microarray scanner (Genomic Solutions Inc., Ann Arbor, MI, USA). The quality of the images and visualization of the spatial homogeneity of the hybridization was assessed by histogram plots techniques. The foreground spot intensities formed the primary data for all subsequent analyses and were corrected by subtracting the background intensities. All spots with background intensities higher than the foreground intensity were excluded.

Analysis of hnRNPH1 Expression in Independent Cohorts of PC Patients

Affymetrix Human Genome U133 Plus 2.0 Array data set GSE17386 was downloaded from NCBI GEO and analyzed with BRB array tools (http://linus.nci.nih.gov/BRB-ArrayTools.html). Raw CEL files were pre-processed using MAS.5, median array normalized, and filtered for probe sets with default settings. Log transformed triplicate data was averaged and used for expression analysis.

For evaluation of hnRNPH1 expression in prostate tissues data sets oncomine (ww.oncomine.com) was used to find informative hnRNPH1 expression data as identified using over-expression ranking of hnRNPH1 among three independent datasets. Affymetrix Human Genome U133 Plus 2.0 Array datasets have complete patient demographics and variable hnRNPH1 expression in prostate tumors and normal glands. The hnRNPH1 expression data was extracted as log2 median centered intensity and compared using student t-test, one way ANOVA and Pearson correlation.

Tissue Microarray (TMA) Analysis

Differential expression of hnRNPH1 in prostate tumor cells was validated by immunohistochemical (IHC) analysis using an ethnicity-based TMA (TMA-4). Designed by the National Cancer Institute (NCI), TMA-4 provides high statistical power to investigate possible differences in PC marker prevalence between AA and CA men. The tissue cores of TMA-4 include 4 neoplastic tissue samples from each of 150 AA and CA biopsies, 17 BPH cores, 13 normal cores, and 3 cell line cores (LNCaP, DU-145, PC-3) on each side of the 4-slide set. The clinical annotation and array maps of the TMA can be retrieved at http://cpctr.cancer.gov/cpctr_tma.html#tma2 and Supplementary Table 1 (available online).

For IHC analysis, the TMA slides were deparaffinized, rehydration, and immunostained using Biocare reagents in a Biocare Nemesis 7200 automated system (Biocare Medical, Concord, CA). The endogenous biotin and H_2O_2 were quenched by sequential incubation in 3% H_2O_2 (5 min) and avidin-biotin blocking solution (10 min). Antigen retrieval was achieved by incubation in Biocare BORG solution and the non-specific sites were blocked by Sniper block solution for 10 minutes, followed by addition of anti-hnRNPH1 antibody (1:2,000) (Bethyl Laboratories, Inc., Montgomery, TX) for 45 min. The hnRNPH1 antibody is highly specific since it was raised

against a peptide representing a portion of the C-terminus. The antigen-antibody complex was revealed using secondary and tertiary HRP-conjugated antibodies (10 min each) and visualized by beta-DAB substrate-chromagen solution for 1 min. The slides were then counterstained by hematoxylin and blueing solution and dried up for mounting. For negative controls, the entire IHC method was performed on sections in the absence of primary antibody.

The TMA slides were independently examined and scored under light microscopy by two pathologists (B.E.C. and K.M.), who were blinded to all clinical information as described (20, 21). The extent of immunoreactivity in tumor and adjacent non-tumor cells was graded using a two-score system. In the first score system, the prostate tumor cell staining intensity of hnRNPH1 in each tissue core was assigned a score of 0=0 (no staining); 1=1+ (weak); 2=2+ (moderate); and 3=3+ (strong). In addition, the antigen expression was designated a score of 0 to 3 (0=0%; 1=<25%; 2=25-50%; or 3= >50%) based on the percentage of stained tumor cells in each of these categories of tissue microarray cores examined. The score of cells in each stain-intensity category was multiplied by the corresponding percent staining to obtain a score on a scale of 0 to 9; (0 = no staining; 1-2 = weak; 3-6 = moderate; 7-9 = strong staining). In the second score system, the antigen staining was scored +1, 0, or -1 if intensity in tumor glands was greater, equal or less than the adjacent normal tissue, respectively. A net immunoscore value was obtained by adding the scores of the two systems to give a final value ranging from 0 to10. The final score of the AA and CA tissue cores was expressed as Mean ± SE.

Cell Lines and Plasmids

All cell lines were obtained from American Type Culture Collection and maintained at 37°C in a humidified atmosphere at 5 % CO_2. PC-3 was cultured in F-12K medium (Invitrogen Corporation, Carlsbad, CA) whereas COS-7 and CV-1, an SV40 transformed African green

monkey kidney cells were maintained in DMEM (GIBCO). MDA-PCa-2b, an AA bone marrow-derived metastatic PC cell line, was maintained in BRFF-HPC1 medium (Athena Environmental Sciences, Inc, Baltimore, MD) supplemented with 20% FBS and 50 μg/ml gentamicin. C4-2B cells, an isogenic subline of LNCaP cells obtained from Dr. L. W. Chung (Emory University, Atlanta, GA), was cultured in RPMI medium supplemented with 10% FBS. Normal prostate epithelial RWPE1 cells were maintained in keratinocyte-serum-free medium (Life Technologies) supplemented with 50 μg/ml bovine pituitary extract, 5 ng/ml epidermal growth factor, antibiotic and antimycotics. Unless otherwise indicated, all cells were cultured in RPMI medium supplemented with 10% FBS for comparative analysis while DHT treated PC cells were cultured in phenol red-free RPMI-1640 media supplemented with 10% charcoal stripped FBS (Atlanta Biologicals, Lawrenceville, GA), and antibiotics.

The human hnRNPH1 expression plasmid, pcDNA3.1/V5-His-TOPO-HNRPH1, was constructed by subcloning a cDNA of the hnRNPH1 gene (Genbank accession # BC001348) into a pcDNA3.1/V5-His-TOPO© expression kit in accordance with the manufacturer's instructions (Invitrogen™ Life Technologies, Carlsbad, CA). cDNAs derived from hnRNPH1-expressing MDA-PCa-2b cells was used as a template to amplify a 1373 bp fragment encompassing the OFR of the gene with 30 PCR cycles using a primer set (sense, 5'-GTAAGAGACGATGTTGGG-3'; antisense 5'-GCTCCTTGGTTACCTATGC-3') a high-fidelity platinum® *Taq* DNA polymerase (Invitrogen™ Life Technologies, Carlsbad, CA) at 94°C for 1 min (denaturing), 53°C for 1 min (annealing) and 70°C for 2 minutes (extension). The target sequence was amplified by PCR and fused in-frame into a pcDNA3.1/V5-His©TOPO® TA expression plasmid to generate pCMV-hnRNPH1. Insertion and orientation of DNA was verified by colony PCR, restriction digest map, and PCR amplification using

hnRNPH1 specific sense primer and the plasmid flanking BGH reverse primer. The pcDNA3.1(+)AR (pCMV-AR), a human wt-AR expression plasmid was kindly provided by Dr. X-B Shi (University of California at Davis). The supra PSA/pGL3-luc (psPSA-luc), a luciferase reporter gene driven by truncated PSA promoter sequences encompassing AREs, was obtained from Dr. L. W. Chung (Emory University).

Promoter Methylation Analysis

We analyzed methylation of the hnRNPH1 promoter-CpG island by combined bisulfite restriction analysis (COBRA) and bisulfite sequencing by following our previously described methods (22). Briefly, ~1 μg each of genomic DNA from normal prostate epithelial cells and RWPE-1 and MDA PCa-2b cell lines was treated with bisulfite using the Epitect bisulfite kit (Qiagen, USA) and amplified with primers specific to 6 overlapping domains within the CpG island. Sequences of the PCR primers and the conditions for amplification are given in **Supplementary Table 2 (available online)**. The amplified products were purified from agarose gels using MinElute gel extraction kits, digested with *Bst*UI and run on agarose gels to identify digestion fragments to identify potential regions that show a difference in the levels of DNA methylation. In these experiments, presence of digestion products indicates methylation of the region amplified by the primers. For bisulfite genomic sequencing, PCR products were gel purified, cloned in PCRII-Topo vectors (Invitrogen, USA) and multiple recombinant clones were sequenced to identify methylated CpG sites. To examine if promoter methylation influence hnRNPH1 gene expression, MDA PCa2b cells were grown to 30% confluence and then treated with 5-Aza-2′-deoxycytidine (Sigma, St Louis; final concentration = 2μM) for six days. The levels of hnRNPH1 transcripts were quantified by qRT-PCR analysis.

Quantitative RT-PCR

Briefly, RNA was extracted from matched LCM procured normal epithelium and tumor cells of age-, tumor grade-matched flash-frozen sections (*n*=24) of AA and CA patients or PC cells using Tri-Reagent kit or RNeasy kit (Qiagen, Inc., Valencia, CA), respectively and subsequently reverse transcribed using SuperScript II RT and oligo dT primers. First-strand cDNAs were then analyzed by qRT-PCR using specific amplimer set for hnRNPH1, AR and β-actin genes (Icycler iQTM, Bio-Rad, Hercules, CA). The primers for hnRNPH1, designed using Primer Express Software Version 2.0 (Applied Biosystems), AR (23) and PSA (24) are shown in Supplementary Table 3 (available online), and were PCR amplified using a SYBR® GREEN PCR Master Mix and iTaq^{TM} DNA polymerase at 95°C 5 min for 1 cycle followed by 40 cycles of denaturation at 95°C for 30 s, annealing at 60°C for 30 s (hnRNPH1) or 55°C for 45 s (AR and PSA), and extension 72°C for 30 s, and a final hold at 72°C for 10 min. The primer specificity for each gene was determined by a melting curve graph using selected max emission dye family fluorophore FAM-490. Serial dilutions of the input samples were used to make a standard curve. Data was analyzed using the comparative C_T method and the amount of each amplicon was normalized to a house-keeping gene, β-actin or GAPDH. Gene expression was calculated using CFX-qPCR Version 1.5 (Bio-Rad, Hercules, CA). Data was represented by three independent experiments in triplicates for each treatment condition and primer set.

Cell Growth and Drug Sensitization Analysis

To examine whether **s**iRNA-silencing of hnRPH1 gene modulates mitogenic response MDA-PCa-2b and PC-3 cells were plated in RPMI medium supplemented with 10% FBS at 5 x 10^3 cells/well in 96-well plates for 48 hr and subsequently transfected with 50 nM hnRNPH1 siRNA duplex (5'-UGAAAAGGCUCUAAAGAAAUU-3') or non-targeting siControl sequences

(Dharmacon, Inc., Lafayette, CO). In another set of experiments, sensitization to the nonsteroidal antiandrogen Bicalutamide (BIC) (0 to 20 μM) was examined in hnRNPH1 siRNA-silenced and siControl-transfected MDA-PCa-2b and C4-2B cells in presence or absence of DHT (10^{-8}M). Transfection was performed by mixing siRNAs in serum-free Opti-MEM I medium with Lipofectamine™ 2000 (Invitrogen Corporation, Carlsbad, CA). Transfection efficiency was tested with siGLO Lamin A/C siRNA (Dharmacon, Inc., Lafayette, CO) and pCMV-SFP in presence or absence of GFP siRNA using fluorescence microscopy. Target gene silencing was determined 24 hr post-transfection by RT-PCR and western blot analyses. The effect of hnRNPH1 siRNA-silencing on cell growth (0 to 120 hr) and sensitization to BIC (24 hr) was monitored by WST-8 assay as per manufacturer's instructions (Alexis Biochemicals, San Diego, CA). Data was expressed as Mean ± SE as a percent of control.

Transactivation Analysis

The CV-1, COS-7, C4-2B and MDA-PCa-2b cells (3×10^4) were plated in triplicates to 70% confluency in 24-well culture plates (Corning Incorporated Life Sciences, Acton, MA) containing phenol red-free DMEM medium supplemented with 10% charcoal-stripped FCS and 1% L-glutamine for 24 hr. The cells were then co-transfected with 0.25 μg each of pCMV-hnRNPH1, pCMV-AR, and/or psPSA-luc plasmid using TransFast™ transfection reagent (Promega). An empty pcDNA3.1 plasmid was used as controls to adjust for amounts of transfected DNA. Luciferase activity was normalized by adding 5 ng of *Renilla* luciferase pRL-SV40 plasmid to the transfection mixture. A day later, synthetic androgen (10^{-8}M) or vehicle alone was added for an additional 24 hr period. Firefly luciferase assays were performed using a dual-luciferase report assay system (Promega Corporation, Madison, WI) as we described (25).

AR transactivation in each treatment group was expressed as a fold change relative light unit (RLU) in comparison to controls from three independent experiments.

Immunoblotting and Co-IP Assays

Unless otherwise indicated, Lamin B (Santa Cruz Biotechnology, Inc., Dallas, TX) and GAPDH (Santa Cruz Biotechnology) were used as a loading control. Blots were incubated with AR (Abcam), hnRNPH1 (Bethyl Laboratories, Inc.), NCOA3 (Gene Tex, Irvine, CA), and NCOA4 (Gene Tex) antibodies at recommended dilutions and subsequently developed using ECL kit as per manufacturer's instructions (Pierce, Rockford, IL, USA) as we described before (25). The hnRNPH1 interaction with AR and AR co-activators was determined using Pierce Classic Magnetic IP/Co-IP Kit (Thermo Fisher Scientic Inc, Rockford, IL) and Active Motif Nuclear Extraction Kits (Active Motif, Calsbad, CA). Briefly, protein A/G Magnetic Beads-precleared nuclear fraction (500 µg) or cytosolic fraction (500 µg) of treated cells were diluted (1:10) with a modified coupling buffer containing Pierce IP lysis/wash buffer (0.025M Tris, 0.15M NaCl, 0.001M EDTA, pH 7.4, 1%) NP40, 5% glycerol, and protease inhibitor cocktail (Santa Cruz Biotechnology), and then incubated overnight at 4°C with 2 µg of either normal rabbit IgG (Millipore Billerica, MA), anti-hnRNPH1 or anti-AR antibody. The immune complexes were pulled down by protein A/G magnetic beads (0.25 mg) followed by 4 hr incubation at 4°C. Bound proteins were then eluted in Pierce Classic Magnetic IP/Co-IP Kit elution buffer, and subsequently fractionated by SDS-PAGE. After semi-dry transfer, membranes were analyzed by immunoblotting using anti-AR, anti-hnRNPH1, anti-NCOA3, anti-NCOA4, anti-Lamin B, and anti-GAPDH antibodies at recommended dilutions. Immune complexes were detected with appropriate secondary antibodies and chemiluminescence reagents.

Electrophoretic Mobility Shift Assay (EMSA)

Control and treated cells' nuclear proteins were prepared by a nuclear extraction kit (Pierce Biotechnology, Rockford, IL) and DNA binding assays were carried out using DIG Gel Shift kit in accord with manufacturer's recommendation (Roche Applied Science, Indianapolis, IN) as we described before (26). Briefly, nuclear extracts (4 μg) were incubated for 30 min at room temperature with DIG-labeled oligonucleotide probes to detect hnRNPH1 binding to AREs on PSA gene. Three oligonucleotide sequences encompassing the promoter ARE I (-170) and ARE II (-394) and the enhancer ARE III (-4258) were used in EMSA analysis are described (Supplementary Table 4, available online) (27). Negative and positive controls were included in absence of nuclear extract and hormone treatment, respectively. For super shift assay, antibody (1 μg) was preincubated with nuclear extracts for 15 min prior to the addition of labeled probes. The reaction mixes were resolved onto 4% polyacrylamide nondenaturing gels and subsequently examined for protein/DNA binding and supershifts by a chemiluminescence detection kit (Roche Applied Science, Indianapolis, IN).

Chromatin Immunoprecipitation (ChIP) Assay

The hnRNPH1 *in vivo* binding to ARE within AR and PSA promoter, enhancer and exonic regions of PSA and AR genes was analyzed by ChIP assay as per manufacturer's instructions (Millipore). Briefly, DHT and vehicle control treated PC cells were fixed with 1% formaldehyde to preserve protein/DNA interactions for 10 min. The cells were washed in ice-cold PBS containing protease inhibitors, pelleted, resuspended in 0.5 ml of SDS lysis buffer, and incubated on ice for 10 min. The chromatin was sheared by sonicating the lysates eight times with 10 s pulses at energy level 4 (Sonic Dismembrator, Fisher Scientific), followed by 30 s of cooling after each burst. Debris was removed from samples by centrifugation for 10 min at 15,000 3 *g* at

4°C. An aliquot of the chromatin preparation was removed and designated as the Input fraction. The sonicated chromatin was diluted in immunoprecipitation buffer and precleared with protein A agarose (Santa Cruz Biotechnology) for 1 hr at 4°C. After centrifugation, the supernatants were incubated overnight at 4°C with 1 μg of anti-human hnRNPH1 antibody (Bethyl Laboratories, Inc.) or control normal rabbit IgG (Santa Cruz Biotechnology) to immunoprecipitate DNA/protein complex. After washing, Protein A immune complexes were eluted and cross-linking was reversed by NaCl and proteinase K treatment. The immunoprecipitated DNA was recovered by phenol/chloroform extraction and PCR analysis was performed using primer sets (Supplementary Table 5, available online) flanking AREs within the promoter (ARE I and II) and the enhancer element (ARE III) of PSA gene as shown before (28). Additionally, ChIP analysis was performed by PCR primer sets (Supplementary Table 5, available online) flanking exons B and H as well as exons D and E encompassing ARE-1 and ARE-2, respectively, of the AR gene using PCR conditions as described (29). PCR products were analyzed by agarose/ethidium bromide gel electrophoresis.

MircoRNA Analysis

Prostate cancer and normal adjacent epithelium were procured from tissue slides of AA and CA men by LCM. RNA was extracted from each sample using Arcturus PicoPure RNA isolation kit according to the manufacturer's instructions (Applied Biosystems, CA). The concentration of RNA was adjusted to 5ng/μl and cDNA was synthesized by mercury LNA™ Universal TR microRNA PCR kit (Exiqon Inc, MA). Based on miRNA target scan (http://www.targetscan.org) and miRanda (http://www.ebi.ac.uk/enright-srv/microcosm/htdocs/targets/v5/) analysis, qPCR was performed to analyze four miRNAs (miR-22, miR-122, miR-132, and miR-495) involved in

regulation of hnRNPH1 gene. Sample clinicopathological characteristics, miRNAs and their targeted sequences (Exiqon Inc, MA) are described in Supplementary Tables 6 and 7 (available online). The PCR conditions included polymerase activation/denaturation at 95^{o}C for 10 min followed by 45 amplification cycles at 95^{o}C for 10s and 60^{o}C for 1 min, ramp-rate 1.6^{o}C/s according to the manufacture's protocol (Exiqon Inc, MA). Fold change of miRNA was calculated using U6 snRNA as a reference control

Animal Studies

Animal studies were performed in accordance with the Institution Animal Care and Use Committee (IACUC) at Tulane University. C4-2B cells were transfected with a control or shRNA construct targeting the hnRNPH1 (OriGene, Rockville, MD) for 48 h using Lipofectamine^{TM} 2000 according to the manufacturer's protocol (Life Technologies, Grand Island, NY). Stable cell clones were selected with puromycin dihydrochloride (Santa Cruz Biotechnology). The hnRNPH1 protein levels in cell clones were assessed by Western blot analysis. Eight-week old severe combined immunodeficiency (SCID) male hairless congenic mice (Charles Rivers, Portage, MI) were maintained in microisolator cages with light-dark cycle set at 12-h intervals and provided with a commercial diet and water *ad libitum.* Control or hnRNPH1 transfected C4-2B cells (2×10^6) mixed (1:1) with Matrigel (BD Biosciences) were transplanted (100 µl) into the left and right flanks, respectively, of SCID mice, respectively. Animal weights were recorded weekly. Mice were sacrificed 4 weeks later and tumor sizes were measured by digital calipers using the formula: volume= width^2 × length × 0.4, where width represents the shorter dimension of the tumor.

Statistical Analysis

For microarray analysis, the intensity of each hybridization signal was evaluated photometrically by integrator software (GeneTAC), and normalized to the average signals of the housekeeping genes. Raw microarray measurements were typically normalized and the background-adjusted intensities were then log-transformed to reduce the dynamic range, achieve normality, and make the datasets from different hybridizations comparable. Fluorescence intensities of the two channels were balanced using Within-Array and Between-Array Normalization methods. Within-Array normalization allows for the comparison of the Cy3 and Cy5 channels while the normalized Between-Array compares the gene expression levels across slides or arrays**.** Linear regression of the two channels and of log ratio against average intensity (MA plots) was used for Within-Array normalization (30). Box-plot method for Between-Array normalization was used for comparing the distributions of log intensities or log ratios of genes on different arrays. For each array, the spot replicates of each gene were merged and expressed as median ratios ± SD. The ratios were log-transformed, and normalized using the local intensity-dependent algorithm. The evaluation of differential gene expression in AA and CA groups was approached as a collection of tests for each gene of the "null hypothesis" of no difference or alternatively as estimating the probability that a gene shows differential expression using a two-sided t-test statistic criterion with multiple testing adjustments and an overall level of significance of 5%. Genes with significant differential expression in tumor cells of AA men were reported in order of increasing *p*-value after a Bonfferoni adjustment procedure employed.

For IHC analysis, Chi-square test was used to examine if there were significant differences between AA and CA groups in hnRNPH1 protein expression, age at diagnosis, race, PSA at diagnosis, tumor size, TNM stage, Gleason score and grade, recurrence, and vital status

in TMA-4 slides. Likewise, Analysis of Variance (ANOVA) and Fisher's Exact test were employed to determine if there were significant differences between AA and CA on age at diagnosis, age at prostatectomy, Gleason score, and final score of hnRNPH1. Kaplan-Meier method was used to construct disease recurrence curves and to compare months to PSA recurrence free using Log-rank test. Correlation between hnRNPH1 and clinical parameters were tested using Pearson Correlation Coefficient. The study hypothesis was tested on the significance level of alpha = 5% throughout the analysis. All statistical analysis tests were performed with the Statistical Analysis Software 9.1 (SAS Institute, Cary, NC, U.S.A.) and graphs were plotted using R-software (The R Foundation for Statistical Computing). For *in vitro* experiments, data was analyzed by analysis of variance (ANOVA) or student *t*-test and significant difference between various groups was compared at *p*-values $\leq$ 5% level.

Results

Strategy to identify PC differentially expressed genes in AA men

The functional genomics approach employed for identification of differentially expressed genes is schematically depicted (Supplementary Figure 1A, available online). Each epithelial cell population harvested by LCM was estimated to be highly homogeneous as determined by microscopic visualization of the captured cells (Supplementary Figure 1B, available online). Our PCR analysis of cDNAs before and after *Rsa*I digestion and efficiency of adaptor ligation in forward hybridizations demonstrated that SSH analysis was carried out successfully (Supplementary Figure 2, A-D, available online). Subsequent cloning of cDNAs (200-900 bp) resulted in generation of SSH library ~1,500 race-related PC-specific cDNAs of unknown identity (Supplementary Figure 2E). The SSH cDNA libraries were exploited to custom construct cDNA array chip encompassing two super-grids of 750 PC-specific genes each for AA and CA patients. Initial hybridization analysis revealed that the custom arrays are reproducible and yield high signal to noise ratios.

Microarray screening and data analysis

*A*n RNA *in vitro* transcription strategy was employed to generate sufficient cRNA for microarray analysis. Total RNA was linearly amplified with T7 polymerase so that population skewing and the loss of quantification are minimal (31). Our use of aminoallyl derivatives obviates some of the complications generally seen in direct fluorescent labeling. Following image acquisition and normalization, the degree of variability and reproducibility among analyzed samples of various datasets was assessed. Statistical linear regression of Cy3 against Cy5 and the linear regression of log ratio against average intensity (MA plots) were used for Within-Array normalization (Figure 1A). Box-plot method for Between-Array normalization was used for comparing the

distributions of log intensities or log ratios of genes on different arrays (Figure 1B). With these approaches, minimal variability in gene expression was observed between normalized hybridizations.

hnRNPH1 correlates with AR expression and disease progression in AA men

The differential gene expression profile analysis in AA and CA groups was approached as a collection of tests for each gene based on the "null hypothesis" of no difference or, alternatively, as estimating the probability that a gene shows differential expression using *t*-test statistic criterion at 5% level. Our custom race-, PC-specific cDNA microarray and sequencing analyses revealed differential yet significant expression of a number of genes (Figure 1C). The hnRNPH1 was on the top of highly expressed genes ($p<0.001$) in AA prostate tumors compared to CA men. qRT-PCR analysis of in LCM-harvested cells showed a 6-fold ($p<0.001$) and 3-fold ($p<0.05$) increase in hnRNPH1 transcript levels in AA and CA prostate tumors, respectively, when compared to the matched normal epithelium in each group (Figure 1D). The differential hnRNPH1 expression was also examined in independent cohorts encompassing Affymetix array datasets either downloaded from NCBI Geo or mined using Oncomine (www.oncomine.com). In the first dataset (GSE17386) consisting of prostate tumor cells derived from AA (n=14) and CA (n=13) PC patients (32), the endogenous hnRNPH1 expression was significantly high ($P<0.0005$; 1.76 fold) in AA-men compared to CA-men (Figure 2A). In the second dataset encompassing 20 normal glands and 69 tumor tissues (33), the hnRNPH1 transcripts levels are significantly elevated in tumors versus normal epithelium and to a greater extent in AA ($P>0.0001$) tumors than in CA tumors ($P<0.018$), when compared to normal epithelium of the same ethnicity group (Figure 2, B and C). These findings were corroborated by TMA analysis. In comparison to neighboring stroma and normal epithelium (Figure 2, D-F) and BPH (Figure 2, G-I),

predominant nuclear hnRNPH1 immunoreactivity was detected tumor cores (Figure 2, D-F) in both race groups. Based on the histoscore, the hnRPH1 staining is significantly high in prostate tumors of AA-men compared with CA-men (Figure 2M). Collectively, the data strongly support selective endogenous elevation of hnRNPH1 transcripts in prostate tumors, especially among in AA-men.

Next, we examine whether hnRNPH1 expression correlates with PC progression. Of the clinicopathological variables studied (Supplementary Table 1, available online), the hnRNPH1 score positively correlated with Gleason score in both race groups, with significantly higher (p<0.01) levels in moderately differentiated (Gleason 6-7) tumors in AA men compared to CA men (Figure 2N). A second dataset (32) shows aberrant expression of hnRNPH1 in tumors with positive extraprostatic extension and high Gleason sum score (Figure 3, A and B). Similar finding were reported in a third independent dataset (33) (Figure 3C). Notably, hnRNPH1 expression also increases in five-year recurrent tumors (Figure 3 D). Furthermore, a direct correlation of hnRNPH1 and AR expression (p<0.0001; Pearson r=0.5174) and possible co-deregulation of these genes in PC tissues were observed (32) (Figure 3, E and F). This observation was further validated by qRT-PCT analysis of matched LCM procured normal epithelium and tumor cells from flash-frozen PC biopsies derived from a fourth ethnicity-based independent cohort of AA-men (n=13) and CA men (n=17). In addition to positive correlation with AR (r= 0.8323; p<0.0053), both hnRNPH1 and AR transcript levels were significantly elevated (P<0.005) in LCM procured prostate tumors of AA-men than CA-men (Figure 3, G and H). In addition a trend of positive correlation between hnRNPH1 staining and PSA recurrence-free was observed in AA men as opposed to CA men (*data not shown*), suggesting a trend

towards poor prognostic outcome in this ethnic group of patients. Together these findings suggest a potential role for hnRNPH1-AR axis in PC progression among AA-men.

Prostate tumor aberrant hnRNPH1 gene expression is regulated by miRNAs and promoter methylation

Prediction of miRNA target analysis has identified four miRNAs potentially involved in regulation of hnRNPH1 transcripts (Supplementary Figure 3A, available online). qRT-PCR analysis in LCM procured tumor cells, after normalization to matched adjacent normal prostate epithelium in each race group, revealed significant (p<0.05) down-regulation of miR-22 and miR-212 in tumor cells of AA men than in CA men (Supplementary Figure 3B, available online). The data suggest that aberrant expression of hnRNPH1 in prostate tumors of AA men may be attributed to down-regulation of miR-22 and miR-212. Next, we examined by combined bisulfite restriction analysis (COBRA) whether the high differential expression levels of hnRNPH1 in the MDA PCa-2b, originally derived from an AA-men, compared to the low expression in normal RWPE-1 cells is attributed to methylation in the promoter-CpG island**.** The hnRNPH1 promoter is embedded in a 1796 bp long CpG island (Supplementary Figure 4A, available online). Based on the amount of digestion it appears that region f (hg19:chr5:179051441-179051688 is about 50% more methylated in MDA PCa-2b cell line than in RWPE-1 cell line (Supplementary Figure 4B, available online). The COBRA results were validated by bisulfite genomic sequencing, in which multiple clones from the bisulfite PCR products from the two cell lines were sequenced and the number of CpGs methylated in the cloned products was determined for each CpG site (Supplementary Fig 4C, available online). The results summarized in Supplementary Fig 4D (available online) suggest that 14 out of 19

CpG sites investigated show >25% increase in methylation in DNA from MDA PCa-2b cell line, suggesting a positive correlation between DNA methylation in this region and hnRNPH1 expression. To test this possibility, MDA PCa2b cells were treated with 5-Aza-2′-deoxycytidine for six days and RNA samples were prepared from the treated cells and untreated control cells. The results depict ~1.7-fold decrease in the level of hnRNPH1 transcript levels in the cells treated with 5-Aza-2′-deoxycytidine (Supplementary Fig. 4, E and F, available online). Taken together, the results suggest that methylation of the proximal region of the promoter CpG island is associated with transcriptional upregulation of hnRNPH1 in prostate tumors, especially in AA-men.

hnRNPH1 promotes PC cell growth and sensitizes AR-expressing PC cells to bicalutamide

The basal transcript expression levels of hnRNPH1 was 3- and 6-fold higher ($p<0.01$) in AR-expressing MDA-PCa-2b and C4-2B cells, respectively, with predominant nuclear localization compared to the AR(-) PC-3 cells (Figure 4, A and B). Accordingly, these cell lines were exploited as a model to unravel the functional significance of hnRNPH1 in the AR-mediated prostate tumor cell growth and drug resistance. Initially, we examined by siRNA strategy whether hnRNPH1 is critical to proliferation of MDA-PCa-2b and PC-3 cells. Transfection, as optimized by GFP and siGLO Lamin A/C duplex siRNA, demonstrates > 95% transfection and silencing efficiencies in both cell lines (Figure 4, C and D). The hnRNPH1 siRNA down-regulated the target gene by at least 90% as opposed to cells transfected with non-targeting siControl duplexes (Figure 4, E and F). As shown in Figure 4G, a significant time-dependent growth inhibition was observed as early as 48 hr in MDA-PCa-2b cells transfected with hnRNPH1 siRNA in comparison to untrasfected or siControl transfected cells. In contrast, the growth kinetics was not affected in response to target gene silencing in AR-naïve PC-3 cells

under similar experimental conditions (Supplementary Figure 5, available online). Since androgen deprivation is the mainstay therapy for locally advanced and CRPC, we sought to examine whether modulation of endogenous hnRNPH1 levels would impact the sensitivity and/or therapeutic efficacy of the non-steroidal anti-androgen bicalutamide (BIC) in PC cells. MDA-2B-PCa and C4-2B cells pre-transfected with hnRNPH1 siRNA or siControl were subjected to various concentration of BIC in presence of dihydrotestosterone (DHT) or vehicle control. hnRNPH1 siRNA-silenced MDA-PCa-2b and C4-2B cells were sensitive to BIC cytotoxicity at 10 μM in absence and presence of DHT in cells ($p<0.05$) (Figure 4, H and I), suggesting a role for this NM protein in development of antiandrogen drug resistance.

The growth modulatory effect of hnRNPH1 was verified *in vivo*. Notably, whereas no change in body weight was observed (Figure 4J), silencing of hnRNPH1 was coupled with significant ($p<0.05$) growth inhibition of C4-2B tumor xenografts *in vivo* (Figure 4, J and K). In contrast, overexpression of hnRNPH1 stimulated growth of less tumorigenic AR-expressing LNCaP cells when compared to control plasmid transfected cells in vivo (Supplementary Figure 6, available online). Together, both *in vivo* studies attest to growth promoting ability of hnRNPH1 in AR-expressing PC cells.

hnRNPH1 confers androgen dependent and independent transactivation of the AR in PC cells

The growth inhibitory effects caused by hnRNPH1 siRNA silencing in MDA-PCa-2b cells prompted us to investigate whether these effects are mediated through modulation of AR activation. hnRNPH1 induced hormone independent AR activation in wtAR transfected COS-7 and CV-1 cells ($p<0.05$) when compared to negative controls or cells transfected with wtAR or

hnRNPH1 alone (Figure 4, M and N). Likewise, transfection of C4-2B cells with hnRNPH1 caused AR transactivation in a ligand-independent manner (Figure 4O). In contrast, DHT induced almost twice the level of AR activation following ectopic co-expression of hnRNPH1 and AR in COS-7 and CV-1 cells (Figure 4, M and N) and hnRNPH1-transfected C4-2B cells (Figure 4, O) as opposed either factor alone ($p<0.05$). Interestingly, DHT in absence of AR significantly increased ($p<0.05$) PSA promoter activity in hnRNPH1-transfected COS-7 and CV-1 cells. (Figure 4, J and K). Finally, these findings were confirmed by silencing hnRNPH1 in MDA-C4-2B cells with or without DHT (Figure 4P).

hnRNPH1 physically interacts with AR and SRC-3 and regulates transcription of androgen regulated genes in PC cells

The activation of AR by hnRNPH1 prompted us to investigate if these proteins physically interact in PC cells. Analysis of PC cell lysates immunoprecipitated (IP) with anti-hnRNPH1 demonstrates an increase in immunoblotted AR levels (Figure 5A). Conversely, immunoblotted hnRNPH1 increased in cell lysates reciprocally IP with AR antibody in comparison to control rabbit IgG, suggesting protein-protein interaction. The AR-hnRNPH1 interaction was further augmented in DHT-treated cells (Figure 5B). Immunocytochemical analysis demonstrated that the interacting proteins are primarily co-localized in the nucleus even in the absence of DHT, an effect that was enhanced by of DHT (Figure 5C).

Based on its role in mRNA biogenesis and AR interaction, we examined if endogenous expression of hnRNPH1 modulates transcriptional regulation of AR and androgen regulated genes (ARGs) in PC cells. qRT-PCR analysis reveals that siRNA silencing of hnRNPH1 (Figure 5, D and E) was coupled with a significant reduction in the basal transcript levels of PSA (Figure

5, F-G) and AR (Figure 5, H and I) under both DHT treatment and deprived conditions ($p<0.05$). These findings were confirmed by immunoblot analysis (Figure 5, J and K). In contrast, DHT increased nuclear hnRNPH1 protein levels in both cell lines (Figure 5, J and K), suggesting a positive feedback regulatory loop between androgens and hnRNPH1 in the transcriptional regulation of AR and PSA genes in PC cells. The nuclear interaction with AR and regulation of ARG by hnRNPH1 appears to be associated with recruitment of SRC-3 to the transcriptional complex as evidenced by Co-IP assays in PC cells (Figure 5, L and M).

hnRNPH1 mediates AR binding to AREs on target genes in ligand dependent and independent fashion

The hnRNPH1-AR physical interaction and its role in transcriptional regulation of PSA suggest that this NM protein possibly enhances AR binding to the AREs on ARGs. To this end, EMSA was employed to examine hnRNPH1 ability to modulate AR binding to three DIG-labeled ds oligonucleotides (oligo) encompassing the proximal promoter ARE-I (-170) and ARE-II (-394) and the enhancer element ARE-III (-4258) of PSA gene (Figure 6A). Nuclear extract (NE) proteins binding to all AREs on PSA gene was reduced (~ 50%) upon addition of anti-hnRNPH1 antibody (Figure 6B) in presence or absence of DHT (Figure 6C) in MDA-PCa-2b cells. Moreover, siRNA silencing of hnRNPH1 reduced such ARE binding with and without DHT (**Figure 6D**), attesting to the possibility of hnRNPH1 binding to AR/ARE complex *in vivo* in a hormone-dependent and independent manner.

Next, we examined by ChIP analysis if hnRNPH1 binds AR/ARE complex *in vivo*. Whereas no binding was detected with control IgG, hnRNPH1 was found to be part of auxiliary protein binding complex in all PSA AREs examined under hormone-treated and, but to a lesser

extent under DHT-deprived conditions in both AR-expressing PC cells (Figure 6E). Likewise, ChIP analysis demonstrates hnRNPH1 binding to AR on ARE-1 and ARE-2-containing exons D and E of the AR gene in both cell lines (Figure 6, F and G). Interestingly, we also observed hnRNPH1 binding to exon H but not to exon B of AG gene, both used as control non-ARE containing domains. Taken together, the results suggest a novel hormone-dependent and independent AR co-activation role for hnRNPH1, a previously uncharacterized mechanism in PC cells.

Discussion

Differences in underlying biological mechanisms and tumor immunobiological differences have been proposed as a possible explanation of the disproportionate burden and progression of PC in AA men (8, 33). Several lines of evidence lend credence to the fact that PC transforms more rapidly from an indolent to an aggressive phenotype in AA than CA men (35). However, elucidation of molecular events underlying the progression of PC in AA men has been hampered by the limitations inherent to both *in vitro* and *in vivo* experimental approaches. Our comparative *in vivo* gene expression profile analysis represents the first study of its kind where an integrated unbiased functional genomics approach encompassing a combined LCM/SSH on fresh specimens for custom construction of race-based, PC-specific DNA oligo arrays to examine whether AA men have unique *in vivo* gene expression profile compared to age and tumor stage-matched CA men. In this study, we demonstrated, for the first time, selective nuclear expression of hnRNPH1 in prostate tumors in comparison to normal epithelium, stromal cells, and BPH in both populations, but with higher expression in AA than CA men. Although not stratified based on race, elevated expression of hnRNPH1 has been shown predominantly in the nuclei of several human cancers, including, adenocarcinoma of the pancreas, hepatocellular carcinoma, gastric carcinoma, and head and neck cancer (18). Interestingly, the expression of hnRNP K, another member of hnRNP family, has been shown to be correlated with Gleason score and poor prognosis in PC patients (36). Importantly, we showed through multiple independent cohorts that the hnRNPH1 expression in prostate tumors correlates with AR expression, Gleason score, extraprostatic extensions, disease recurrence and poor clinical outcome, especially among AA men. Taken together, hnRNPH1 may have potential clinical utility as a biomarker, prognostic indicator, and/or therapeutic target in the management of PC.

The molecular mechanism(s) involved in transcriptional regulation of hnRNPs remain largely unknown (37). In the present study we demonstrate increased methylation of promoter CpG islands correlates with elevated endogenous levels of hnRNPH1 in PC cells. The down-regulation of hnRNPH1 transcripts by 5-Aza-2′-deoxycytidine suggest the aberrant expression of this NM protein in prostate tumors of AA-men may partially be attributed to promoter hypermethylation. Consistent with our findings, a number of studies demonstrate that promoter hypermethylation, especially at transcription repressor binding sites, is related to gene overexpression in cancer cells (37-39). However, based on miRNA target scan analysis, the hnRNPH1 transcriptional upregulation may also be ascribed to dysregulated miR-22 and miR-212 expression in tumor cells of AA men. Additionally, we also showed aberrant expression of hnRNPH1 in AR-expressing, but not AR naïve, PC cells, suggesting hnRNPH1 may be a transcriptional target of DHT/AR in PC cells, presumably through putative ARE on the promoter region. These findings suggest AR signaling, epigenetic alterations and/or dysregulation of miRNA expression as underlying molecular mechanisms governing transcriptional regulation of hnRNPH1 in prostate tumor cells, especially among AA-men.

The hnRNPH1 is one of the lesser known members of the hnRNP family in terms of its biological functions. The mutations, aberrant expression of AR gene, and activation of AR signaling have been implicated in growth and metastasis of PC and correlates with PSA elevation (40). Here we report that hnRNPH1 is involved in AR-expressing PC cells growth both *in vitro* and *in vivo,* even under hormone deprivation conditions, suggesting activation of AR signaling is critical in part to its growth stimulatory effects. This notion is further strengthened by the fact that hnRNPH1 require AR, regardless of its mutation status, to induce ligand dependent and independent activation of PSA promoter, primarily through transcriptional up-regulation of AR

in ligand dependent and independent manner. We also demonstrate that hnRNPH1 transcripts are partially upregulated by DHT, suggesting a positive feedback loop between AR and this NM protein. In agreement with our findings, ectopic expression of hnRNP K has been shown to enhance cell proliferation and anchorage-independent growth of breast cancer cells (41). In contrast to hnRNPH1 action, hnRNP A1 has been shown to inhibit PC cell growth through suppression of ARA54-enhanced AR transactivation (42), indicating that some members of hnRNP family have mutually antagonistic effects on tumor cell growth. Our data document, for the first time, a previously uncharacterized mechanism for hnRNPH1 in mediating selective transactivation of AR and aberrant expression of AR and ARGs in an androgen-dependent and independent manner. The hnRNPH1's new role in activation of AR signaling and ligand-dependent and independent transcriptional regulation of ARGs thus represents a novel mechanism by which prostate tumor cells may escape androgen dependence, especially in AA men.

That a number of coregulators interact directly or indirectly with AR and modulate its activity (43) prompted us to speculate that hnRNPH1 possibly mediate its ARGs promoter activation through AR binding. To this end, we demonstrated physical interaction between hnRNPH1 and AR, predominantly in the nuclei of PC cells. In agreement with our findings, direct cell-free binding studies showed the prostate NM to have acceptor sites for high AR binding (44). Regardless of hormone stimulation status, our EMSA and ChIP analyses revealed that hnRNPH1-AR binding was primarily observed on all AREs on the promoter and enhancer domains of the PSA gene and selective ARE-containing exons on AR gene, suggesting it may act as a coactivator of AR in PC cells. Our findings were corroborated by reports that AR coactivator Tip60, which is up-regulated by androgen deprivation therapy, has been shown to be

recruited to the promoter of the PSA in the absence of androgens (45). We also revealed simultaneous recruitment of AR-coactivator SRC-3 to the AR-hnRNPH1 complex. AR coactivators SRC-1 and TIF-2 have been shown to be up-regulated in tissue specimens of patients who failed PC endocrine therapy and that their selective expression is coupled with enhanced activation of the AR signaling in tumor cells (46). Taken together, our reporter assays, physical interactions with AR and SRC-3 and selective ARE binding suggest a new coactivation role for hnRNPH1 in AR regulation of ARGs in PC cells under hormone induced and deprived conditions.

We also observed AR-independent induction of PSA promoter activity by hnRNPH1 in the presence of DHT, indicating it may directly bind specific DNA sequences to regulate transcription. This finding is in line with the fact that hnRNPH1 is implicated as a *trans*-acting factor by direct binding to DNA sequences (16) and estrogen response element (47). This newly identified functional role for hnRNPH1 was also exhibited by other hnRNP family members, such as hnRNP A1 (48) and hnRNP K (49, 50). Moreover, several hnRNP family members have been shown to bind DNA Matrix Attachment Regions (MARs), a specific chromatin DNA sequences that interact with NM and initiate transcription (51). Thus hnRNPH1 binding to MARs may potentially modulate the chromatin state and induce transcription of ARGs possibly via modifications of RNA complexes and protein-protein interaction. Whether selective binding by DHT of the NM or nuclear ribonucleoprotein particles, leads to AR-independent transactivation of ARGs certainly warrant further investigation.

The nonsteroidal antiandrogen BIC is often used as monotherapy or in combination with androgen deprivation therapy (52) for locally advanced or biochemically recurrent PC to prevent androgen dependent activation of the AR and upregulation of ARGs (53) by binding to and

accelerating degradation of the AR in tumor cells (54**)**. Although this treatment regimen initially exhibits favorable responses, PC inevitably becomes refractory and develops resistance to BIC (55). As a suppressor of AR transcription and activation, we demonstrate that hnRNPH1 silencing sensitizes PC cells to the BIC-mediated growth arrest under DHT-deprived conditions--thus further augmenting AR-dependent growth inhibition by BIC in PC cells. This effect was partially ameliorated by DHT in AR-expressing, suggesting that hnRNPH1 overexpression may be associated with development of resistance to hormonal therapy via up-regulation of AR transcripts and amplification of AR signaling in tumor cells. Thus, targeting of hnRNPH1 may represent a novel form of hormone sensitization-based therapy in the clinical management of androgen-dependent and CRPC.

In conclusion, our study paves the way for further understanding of the complexity of the biology and molecular mechanisms involved in the disparity of PC. Given heterogeneity of PC and that AR is implicated in development of CRPC, the results suggest that selective expression of hnRNPH1 in a subset of tumor cells in AA men may confer disease progression and development of therapeutic resistance via enhancing transcription and activation of AR in a ligand dependent and independent manner. The hnRNPH1-AR axis may thus represent a previously unknown mechanism for disease progression, and development of hormone refractory disease in this ethnic group of patients. The results not only implicate racial differences in the biology of PC, but also suggest, for the first time, a new frontier for the development of diagnostic, preventive, and/or targeted therapeutic strategies to circumvent disease in this ethnic group of patients.

Acknowledgments

This work was partially supported from ASC grant #RSGTCCE-116942 (A.B.A), DOD grant # PC081598 (A.B.A.), and NIH grant # CA118767-01(A.B.A). We would like to thank Dr. Oliver O. Sartor for his critical review of the manuscript.

References

1. Horner MJ, Ries LAG, Krapcho M. et al. SEER Cancer Statistics Review, 1975-2006, National Cancer Institute. Bethesda, MD; 2009.
2. de Vere White RW, Deitch AD, Jackson AG. Radical differences in clinically localized prostate cancers of black and white men. *J Urol.* 1998;159(6):1979-1983.
3. Powell IJ, Banerjee M, Novallo M, et al. Prostate cancer biochemical recurrence stage for stage is more frequent among African American than white men with locally advanced but not organ-confined disease. *Urology.* 2000;55(2):246-251.
4. Whittemore AS, Wu AH, Kolonel LN, et al. Family history and prostate cancer risk in black, white, and Asian men in the United States and Canada. *Am J Epidemiol.* 1995; 141(8):732-740.
5. Cher ML, Lewis PE, Banerjee M, et al. A similar pattern of chromosomal alterations in prostate cancers from African-Americans and Caucasian Americans. *Clin Cancer Res.* 1998;4(5):1273-1278.
6. Haiman CA, Patterson N, Freedman ML, et al. Multiple regions within 8q24 independently affect risk for prostate cancer. *Nat Genet.* 2007;39(5):638-641.
7. Yeager M, Orr N, Hayes RB, et al. Genome-wide association study of prostate cancer identifies a second risk locus at 8q24. *Nat Genet.* 2007;39(5):645-649.
8. Epstein JI, Pizov G, Walsh PC. Correlation of pathologic findings with progression after radical retropubic prostatectomy. *Cancer.* 1993;71(11):3582-3593.
9. Chen CD, Welsbie DS, Tran C, et al. Molecular determinants of resistance to antiandrogen therapy, *Nat Med.* 2004;10(1):33-39.

10. Heemers HV, Tindall DJ. Androgen receptor (AR) coregulators: a diversity of functions converging on and regulating the AR transcriptional complex. *Endocr Rev.* 2007; 28(7):778-808.

11. Small D, Nelkin B, Vogelstein B. Nonrandom distribution of repeated DNA sequences with respect to supercoil loops and the nuclear matrix. *Proc Natl Acad Sci, USA*. 1982;79(19):5911-5915.

12. Leman ES, Getzenber RH. Nuclear structure as a source of cancer specific biomarekers. *J Cell Biochem.* 2008;104(6):1988-1993.

13. Krecic AM, Swanson MS. hnRNP complexes: composition, structure, and function. *Curr Opin Cell Biol*. 1999;11(3):363–371.

14. Siomi MC, Eder PS, Kataoka N, et al. Transporin-mediated nuclear import of heterogeneous nuclear RNP proteins. *J Cell Biol.* 1997;138(6):1181-1192.

15. Honoré B, Rasmussen HH, Vorum H, et al. Heterogeneous nuclear ribonucleoproteins H, H′, and F are members of a ubiquitously expressed subfamily of related but distinct proteins encoded by genes mapping to different chromosomes. *J Biol Chem.* 1995;270(48):28780–28789.

16. Alkan SA, Martincic K, Milcarek C. The hnRNPs F and H2 bind to similar sequences to influence gene expression. *J Biochem*. 2006;393(Pt1):361-371.

17. Holzmann K, Korosec T, Gerner C, et al. Identification of human common nuclear-matrix proteins as heterogeneous nuclear ribonucleoproteins H and H' by sequencing and mass spectrometry. *Eur J Biochem.* 1997;244(2):479-86.

18. Honoré B, Baandrup U, Vorum H. Heterogeneous nuclear ribonucleoproteins F and H/H' show differential expression in normal and selected cancer tissues. *Exp Cell Res.* 2004;294(1):199-204.

19. Liu J, Beqai S, Yang Y, et al. Heterogeneous nuclear ribonucleoprotein-H plays a suppressive role in visceral myogenesis. *Mech Dev*. 2001;104(1-2):79-87.

20. Epstein, JL, Carmichael, M, Partin, AW. OA-519 (fatty acid synthase) as an independent predictor of pathologic stage in adenocarcinoma of the prostate. *Urology.* 1995;45(1):81-86.

21. Gu, Z, Thomas, G, Yamashiro, J. et al. Prostate stem cell antigen (PSCA) expression increases with high gleason score, advanced stage and bone metastasis in prostate cancer. *Oncogene*.2000;19(10)1288-1296.

22. Borowczyk, E, Mohan KN, D'Aiuto L, et al. Identification of a region of the DNMT1 methyltransferase that regulates the maintenance of genomic imprints. *Proc. Natl. Acad. Sci.* 2009:106(49):20806-20811.

23. Yang L, Xie H, Jamaluddin MS, et al. Induction of androgen receptor expression by phosphatidylinositol 3-kinase/Akt downstream substrate, FOXO3a, and their rates in apoptosis of LNCaP prostate cancer cells. *J Biol Chem.* 2005;280(39):33558–33565.

24. Shin T, Sumiyoshi H, Matsuo N, et al. Sp1 and Sp3 transcription factors upregulate the proximal promoter of the human prostate-specific antigen gene in prostate cancer cells. *Arch Biochem Biophy.* 2005;435(2):291-302.

25. Graham T, Odero-Marah V, Chung LWK, et al. PI3K/Akt-dependent transcriptional regulation and activation of BMP-2-Smad signaling by NF-κB in metastatic prostate cancer cells. *Prostate.* 2009;69(2):168-180.

26. Abdel-Mageed, AB, Agrawal KC. Activation of nuclear factor kappa B: potential role in metallothionein-mediated mitogenic response. *Cancer Res*. 1998:58(11);2335-2338.

27. Cleutjens KB, van der Korput HA, van Eekelen CC, et al. An androgen response element in a far upstream enhancer region is essential for high, androgen regulated activity of the prostate specific antigen promoter. *Mol Endocrinol*. 1997;11(2):148-161.

28. Carpenter B, MacKay C, Alnabulsi A, et al. (2006) The roles of heterogeneous nuclear ribonucleoproteins in tumour development and progression. *Biochem Biophys Acta.* 2006;1765(2):85–100.

29. Lubahn DB, Brown TR, Simental JA, et al. Sequence of the intron/exon junctions of the coding region of the human androgen receptor gene and identification of a point mutation in a family with complete androgen insensitivity. *Proc Natl Acad Sci, USA*. 1989;86(23):9534-9538.

30. Smyth, GK, Speed, TP. Normalization of cDNA microarray data. *Methods. 2003;* 31(4):265-73.

31. Stears RL, Martinsky T, Schena M. Trends in microarray analysis. *Nat Med.* 2003;9(1):140-145.

32. Timofeeva, OA, Zhang, X, Ressom, HW, et al. Enhanced expression of SOS1 is detected in prostate cancer epithelial cells from African-American men. *Int. J. Oncol*. 2009; 35(4):751-760.

33. Wallace TA, Prueitt RL, Yi M, et al. Tumor immunobiological differences in prostate cancer between African-American and European-American men. *Cancer Res*. 2008;68(3):927–936.

34. Glinsky, GV, Glinskii, AB, Stephenson, AJ, et al. Gene expression profiling predicts clinical outcome of prostate cancer. *J. Clin. Invest*. 2004;113(6):913-923.

35. Powell, IJ, Bock, CH, Ruterbusch, JJ, et al. Evidence supports a faster growth rate and/or earlier transformation to clinically significant prostate cancer in black than in white American men, and influences racial progression and mortality disparity. *J. Urol.* 2010; 183(5)**:**1792-1796.

36. Barboro P, Repaci E, Rubagotti A, et al. Heterogeneous nuclear ribonucleoprotein K: altered pattern of expression associated with diagnosis and prognosis of prostate cancer. *Br J Cancer*. 2009;100(10):1608-1616.

37. Nabilsi, NH, Broaddus, RR, Loose DS. DNA methylation inhibits p53-mediated survivin repression. *Oncogene.* 2009;28(19):2046–2050.

38. Kim, TW, Kim, WJ, Lee, HJ, et al. Hs.137007 is a novel epigenetic marker hypermethylated and up-regulated in breast cancer. *Inter. J. Oncol*. 2010;36(5):1105-1111.

39. Guenin, S. *et al*. Aberrant promoter methylation and expression of UTF1 during cervical carcinogenesis. *PloS One. 2012;*7(8):e42704.

40. Chen Y, Sawyers CL, Scher HI. Targeting the androgen receptor pathway in prostate cancer. *Curr Opin Pharmacol*. 2008;8(4):440-448.

41. Mandal M, Vadlamudi R, Nguyen D, et al. Growth factors regulate heterogeneous nuclear ribonucleoprotein K expression and function. *J Biol Chem.* 2001;276(13):9699-9704.

42. Yang Z, Chang YJ, Miyamoto H, et al. Suppression of androgen receptor transactivation and prostate cancer cell growth by heterogeneous nuclear ribonucleoprotein A1 via

interaction with androgen receptor coregulator ARA54. *Endocrinology.* 2007;148(3):1340–1349.

43. Wang X, Yang Y, Guo X, et al. Suppression of androgen receptor transactivation by Pyk2 via interaction and phosphorylation of the ARA55 coregulator. *J Biol Chem*. 2002;277(18):15426– 15431.

44. Barrack ER (1983) The nuclear matrix of the prostate contains acceptor sites for androgen receptor. *Endocrinology*. 1983;113(1):430-432.

45. Halkidou K, Gnanapragasam VJ, Mehta PB, et al. Expression of Tip60, an androgen receptor coactivator, and its role in prostate cancer development. *Oncogene.* 2003;22(16):2466–2477.

46. Culig Z, Comuzzi B, Steiner H, et al. Expression and function of androgen receptor coactivators in prostate cancer. *J Steroid Biochem Mol Biol.* 2004;92(4):265-271.

47. Chen H, Hu B, Gacad MA, et al. Cloning and expression of a novel dominant-negative-acting estrogen response element-binding protein in the heterogeneous nuclear ribonucleoprotein family. *J Biol Chem*. 1998;273(47):31352–31357.

48. Donev RM, Doneva TA, Bowen WR, et al. HnRNP A1 binds directly to double-stranded DNA in vitro within a 36 bp sequence. *Mol Cell Biochem*. 2002;233(1-2):181-185.

49. Ostrowski J, Kawata Y, Schullery DS, et al. Transient recruitment of the hnRNP K protein to inducibly transcribed gene loci. *Nucleic Acids Res*. 2003;31(14):3954-3962.

50. Lynch M, Chen L, Ravitz MJ, et al. hnRNP K binds a core polypyrimidine element in the eukaryotic translation initiation factor 4E (eIF4E) promoter, and its regulation of eIF4E contributes to neoplastic transformation. *Mol Cell Biol*. 2005;25(15):6436-6453.

51. Barboro P, D'Arrigo C, Repaci E, et al. Proteomic analysis of the nuclear matrix in the early stages of rat liver carcinogenesis: Identification of differentially expressed and MAR-binding proteins. *Exp Cell Res*. 2009;315(2):226-239.

52. Blackledge G, Kolvenbag G, Nash A. Bicalutamide: a new antiandrogen for use in combination with castration for patients with advanced prostate cancer. *Anticancer Drugs*. 1996;7(1):27-34.

53. Furr BJ, Tucker H. The preclinical development of bicalutamide: pharmacodynamics and mechanism of action. *Urology*. 1996;47(A1 Suppl):13–25.

54. Waller AS, Sharrard RM, Berthon P, et al. Androgen receptor localization and turnover in human prostate epithelium treated with the antiandrogen, Casodex. *J Mol Endocrinol*. 2000;24(3):339–351.

55. Hodgson MC, Astapova I, Hollenberg AN, et al. Activity of androgen receptor antagonist bicalutamide in prostate cancer cells is independent of NCoR and SMRT corepressors. *Cancer Res.* 2007;67(17):8388-8395.

Figure legends

Figure 1. Construction of race-based PC-specific SSH libraries and cDNA arrays. **A)** Box-plot analysis to evaluate the degree of variability of analyzed samples from different hybridization experiments. Statistical linear regression of Cy3 against Cy5 and the linear regression of log ratio against average intensity (MA plots) were used for Within-Array normalization. **B)** Histogram plots are representation of Cy3 and Cy5 raw intensities and log transformation of Cy3 and Cy5 intensities of various spots in the chip demonstrating linear distribution of signal intensities. **C)** A representative fluorescence-stained custom array encompassing two supergrids of pooled PC-specific SSH-enriched cDNAs for AA and CA men. **D)** qRT-PCR analysis of hnRNPH1 gene expression relative to the β-actin in LCM-procured normal prostate epithelium (NE) and tumor cells (T) of AA and CA (n=24). * and ** denotes significant difference at $p<0.05$ and $p<0.01$, respectively, in comparison to controls.

Figure 2. Selective expression and correlation of hnRNPH1 to PC progression in AA men. Affymetix array datasets either downloaded from NCBI Geo or mined using oncomine and analyzed for differential hnRNPH1 expression. **A)** The first dataset (GSE17386) denotes significant expression of hnRNPH1 in prostate tumors in AA-men in comparison to CA-men. **B and C)** In the second dataset, the hnRNPH1 transcripts levels are significantly elevated in tumors (T) versus normal epithelium (NE) and to a greater extent in AA tumors than in CA tumors. **D, E** and **F)** A representative AA malignant prostate core from an ethnicity-based TMA-4 depicting intense nuclear immunoreactivity to hnRNPH1 (*arrow*) in comparison to stroma (*arrowhead*). A representative BPH **(G, H** and **I)** and normal prostate tissue **(J, K** and **L)** cores demonstrating weak nuclear immunoreactivity (*arrow*) in epithelial cells in comparison to

the adjacent stroma (*arrowhead*). **M)** Total IHC score of hnRNPH1 in tumors (T) relative to normal epithelium (NE) in AA (*n*=148) and CA men (*n*=152). **N)** hnRNPH1 IHC score stratified by Gleason scores. Scale bars represent 40 μm **(A, D, G** and **J)**; 20 μm **(B, E, H, J, K** and **L)**, and 10 μm **(C, F** and **I)**. * denote significant difference at P<0.05.

Figure 3: Aberrant hnRNPH1 expression is associated with disease progression, AR expression and recurrence. **A, B and C)** Affymetix array datasets (NCBI Geo A and Oncomine) show aberrant expression of hnRNPH1 in tumors with positive extraprostatic extension (EPE) and high Gleason sum score. **D)** The hnRNPH1 expression increases in five-year recurrent tumors in comparison to non-recurrent tumors. **E and F)** A positive correlation between gene expression of hnRNPH1 and AR in prostate tumors in comparison to normal epithelium. **G and H)** Ethnicity-based qRT-PCT analysis demonstrating transcriptional upregulation of hnRNPH1 and AR gene expression in LCM procured and tumor cells relative to their matched normal epithelium in AA-men compared to than CA-men. **I)** A trend of positive correlation between hnRNPH1 immunostaining and PSA recurrence-free in AA men as opposed to CA men. "a" and "b" denote significant difference (P<0.05) relative to NE and CA-men, respectively.

Figure 4. hnRNPH1 confers growth stimulation and hormone resistance through activation of AR in PC cells. **A)** qRT-PCR analysis of hnRNPH1 in AR-expressing (C4-2B and MDA-PCa-2B) and AR-naïve PC-3 cells. **B)** ICC analysis of hnRNPH1 in MDA-PCa-2b cells. **C and D)** Optimization of siRNA silencing and transfection efficiencies in PC cells by GFP and siGLO Lamin A/C, respectively. **E and F)** Endogenous mRNA and proteins levels of hnRNPH1, respectively, at 24 hr following siRNA transfection. **G)** Assessment of growth inhibitory effects

by a cell counting assay kit in hnRNPH1 siRNA-silenced MDA-PCa-2b cells cultured in complete medium for up to 120 hr. **H and I)** Cell growth of MDA-PCa-2b and C4-2B cells, respectively, pre-transfected with siControl or hnRNPH1 siRNA and cultured in RPMI containing charcoal-stripped serum and various concentrations of BIC with (+) or without (-) DHT for 24 hr (*n*=3). **J** and **K)** COS-7 and CV-1 cells, respectively, were cultured in charcoal-stripped FBS medium in absence (ethanol) or presence of DHT and co-transfected with hnRNPH1, pCMV-AR, and psPSA-Luc plasmids. **L)** C4-2B cells co-transfected with hnRNPH1 and psPSA-Luc plasmids and cultured with or without DHT. **M)** C4-2B cells co-transfected with siControl or siRNPH1 and psPSA-Luc reporter and cultured with or without DHT. For normalization all cells were co-transfected with 5 ng pRL-SV40. Activity was measured with dual luciferase system and the results were expressed as fold change of relative light units (RLU). * and ** denotes significant difference at $p<0.05$ and $p<0.01$, respectively, in comparison to controls (*n*=3).

Figure 5. AR-hnRNPH1 interaction and transcriptional regulation of AR and PSA in PC Cells. **A)** PC cell lysates cultured in complete medium were subjected to immunoprecipitation (IP) using anti-AR or anti-hnRNPH1 antibody, followed by immunoblotting (IB) with the indicated antibodies in a reversed order as shown. **B)** Lysates of PC cells cultured in charcoal-stripped medium with or without DHT were analyzed for AR-hnRNPH1 interaction by Co-IP analysis as shown above (*n*=3). **C)** Representative deconvolution photomicrographs (Leica DMRXA) Deconvolution image depicting endogenous expression and co-localization of AR and hnRNPH1 in PC cells under DHT treated and hormone-deprived conditions for 2 hr. Cells were fixed and stained with Dapi nuclear counterstain (blue) and then reacted with hnRNPH1 or AR specific antibody followed by a secondary antibody conjugated with Alexa Fluor 488 (green) or Alexa

Fluor 568 (red). Inset depicts hnRNPH1 not localized (*white arrow*) or weakly co-localizes with AR (*yellow arrow*) in the nucleus in absence of DHT. In merged microphotographs, DHT increases both expression and nuclear co-localization of hnRNPH1 and AR (*green arrow*) in PC cells. Scale bar, 10μm. qRT-PCR analysis of hnRNPH1 **(D** and **E)**, PSA **(F** and **G)**, and AR **(H** and **I)** transcripts in MDA-PCa-2b and C4-2B cells, respectively, cultured in phenol red-free, charcoal-stripped media and transfected with siControl (non-target siRNA) or hnRNPH1 siRNA (siRNPH1) with or without DHT (n=3). Immunoblot analysis of PSA, AR and hnRNPH1 in siRNPH1-silenced or siControl-transfected MDA-PCa-2b **(J)** and C4-2B **(K)** cells, respectively, with or without DHT. **L and M**, Immunoblot analysis depicting weak cytosolic and strong nuclear co-precipitation of SRC-3 with AR and hnRNPH1 in C4-2B cells, respectively. The purity of nuclear and cytoplasmic fractions was assessed by TATA binding protein (TBP), α-tubulin, GAPDH and lamin B, whereas actin was used as a loading control (n=3). * and ** denotes statistical significant difference at $p<0.05$ and $p<0.01$, respectively.

Figure 6. hnRNPH1 mediates hormone dependent and independent AR binding to AREs in PC Cells. **A)** Schematic representation of PCR-amplified AREs (*underlined*) on proximal promoter (ARE I and ARE II) and enhancer (ARE III) elements of PSA gene. **B)** Nuclear extract of MDA-PCa-2b cells cultured in complete medium was used for EMSA analysis with labeled ds oligonucleotides corresponding to PSA AREs in presence or absence of hnRNPH1 antibody. Specific AR-DNA binding was observed in all AREs (*arrowhead*), which was reduced by molar excess of cognate unlabeled ARE oligo. Binding of hnRNPH1 to ARE complex was evident by supershift (*arrow*) upon addition of a specific hnRNPH1 antibody (n=2). **C)** EMSA analysis of hnRNPH1 binding to PSA enhancer ARE-III domain in MDA-PCa-2b cells under DHT treated

or deprived conditions. Note addition of hnRNPH1 antibody markedly inhibited both hormone naïve and induced ARE-III binding (*n*=3). **D)** siRNA silencing of hnRNPH1 caused potent reduction of both hormone naïve and induced ARE-III binding in MDA-PCa-2b cells. **E)** ChIP assay performed using anti-hnRNPH1 and PCR amplification of sequences flanking AREs of PSA gene (Supplementary Table 4) in presence or absence of DHT (*n*=3). **F)** Depicts PCR amplified exon B, in the DNA-binding domain (DBD), and exons D, E, (containing ARE-1 and 2, respectively), and H in the hormone-binding domain (HBD) of AR gene. **G)** ChIP analysis of hnRNP H 1 binding to exons B, D, E, and H of AR gene as influenced by DHT in PC cells. Input DNA and rabbit control IgG were used as controls (*n*=3).

Figure 1

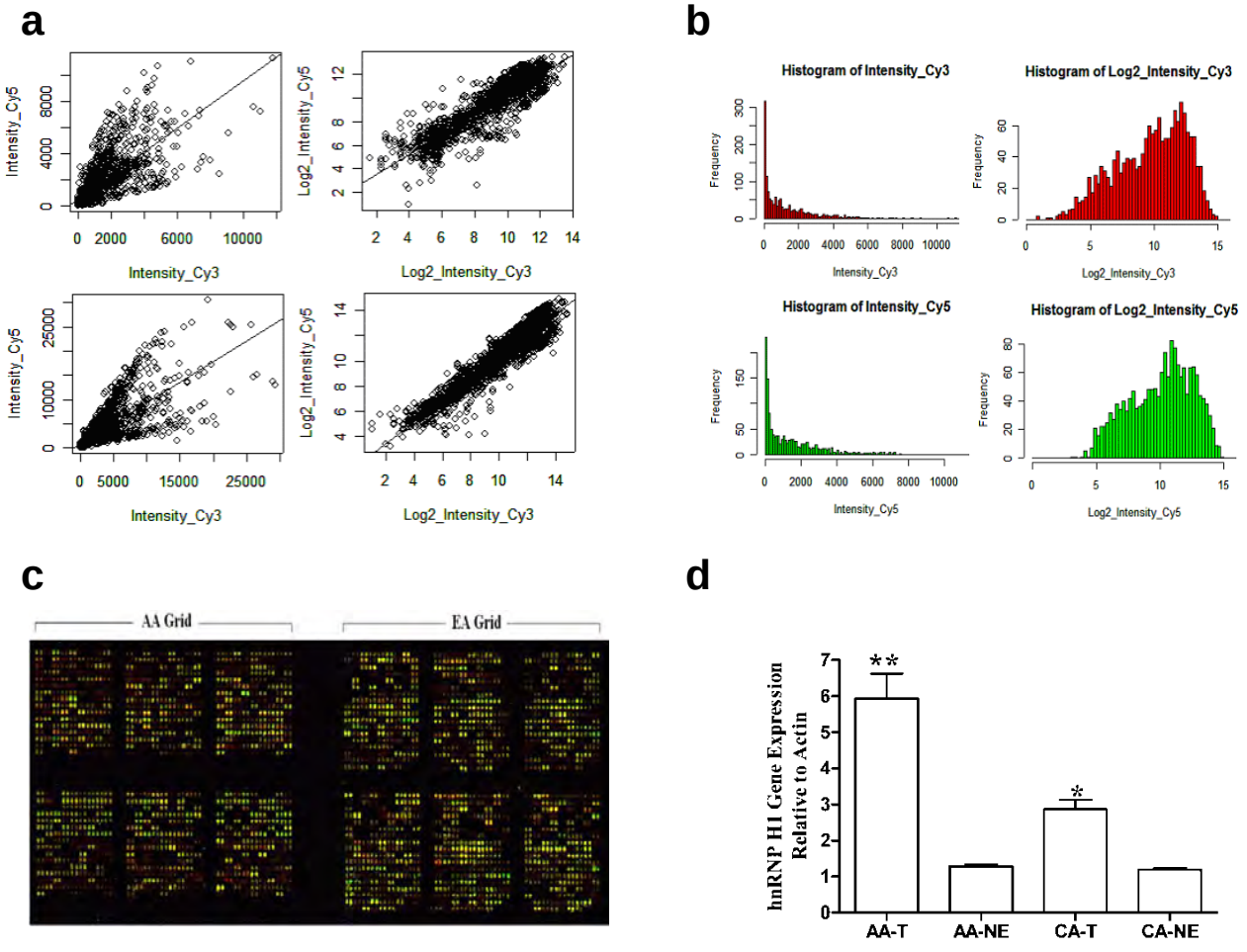
a
Intensity_Cy5
Intensity_Cy3
Log2_Intensity_Cy5
Log2_Intensity_Cy3
b
Histogram of Intensity_Cy3
Histogram of Log2_Intensity_Cy3
Histogram of Intensity_Cy5
Histogram of Log2_Intensity_Cy5
Frequency
c
AA Grid
EA Grid
d
hnRNP H1 Gene Expression Relative to Actin
AA-T
AA-NE
CA-T
CA-NE

Fig. 2

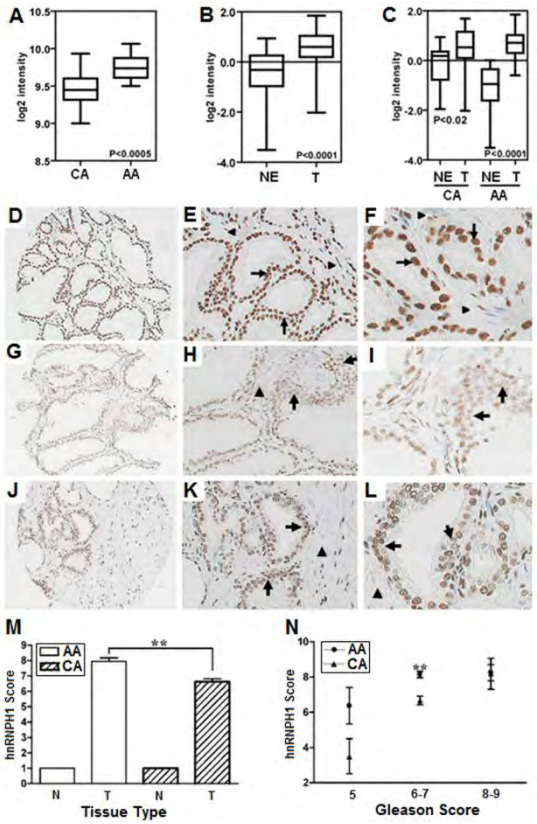
A
log2 intensity
10.5
10.0
9.5
9.0
8.5
P<0.0005
CA
AA
B
log2 intensity
2.0
0.0
-2.0
-4.0
P<0.0001
NE
T
C
log2 intensity
2.0
0.0
-2.0
-4.0
P<0.02
P<0.0001
NE T NE T
CA
AA
D
E
F
G
H
I
J
K
L
M
hnRNPH1 Score
AA
CA
**
N
T
N
T
Tissue Type
N
hnRNPH1 Score
AA
CA
**
5
6-7
8-9
Gleason Score

Fig. 3

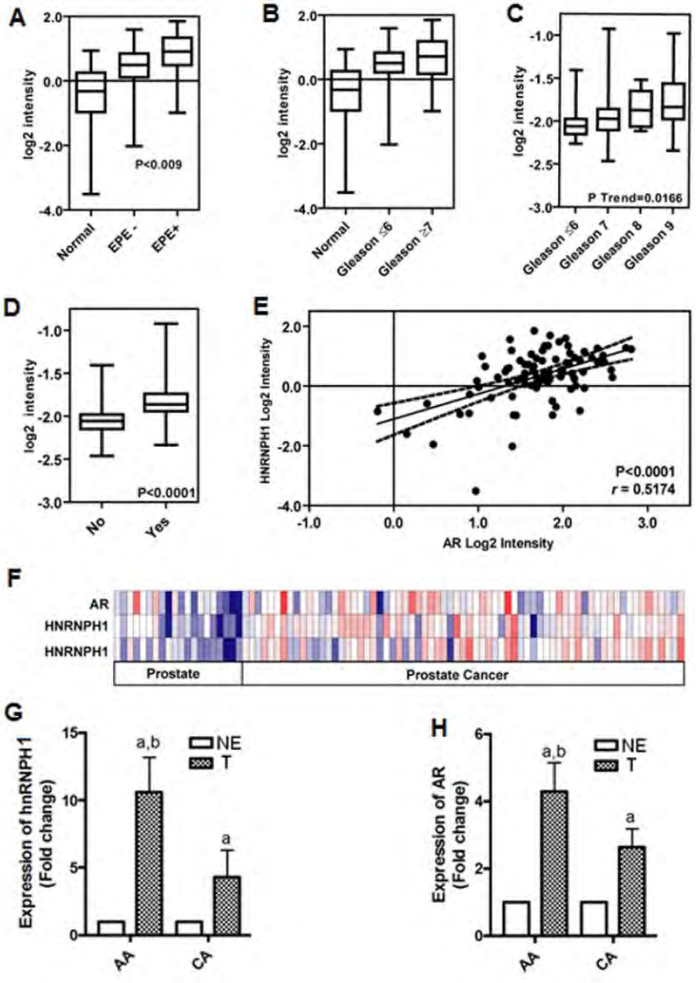
A
log2 intensity
P<0.009
Normal
EPE -
EPE+
B
log2 intensity
Normal
Gleason ≤6
Gleason ≥7
C
log2 intensity
P Trend=0.0166
Gleason ≤6
Gleason 7
Gleason 8
Gleason 9
D
log2 intensity
P<0.0001
No
Yes
E
HNRNPH1 Log2 Intensity
P<0.0001
r = 0.5174
AR Log2 Intensity
F
AR
HNRNPH1
HNRNPH1
Prostate
Prostate Cancer
G
Expression of hnRNPH1 (Fold change)
a,b
a
NE
T
AA
CA
H
Expression of AR (Fold change)
a,b
a
NE
T
AA
CA

Fig. 4

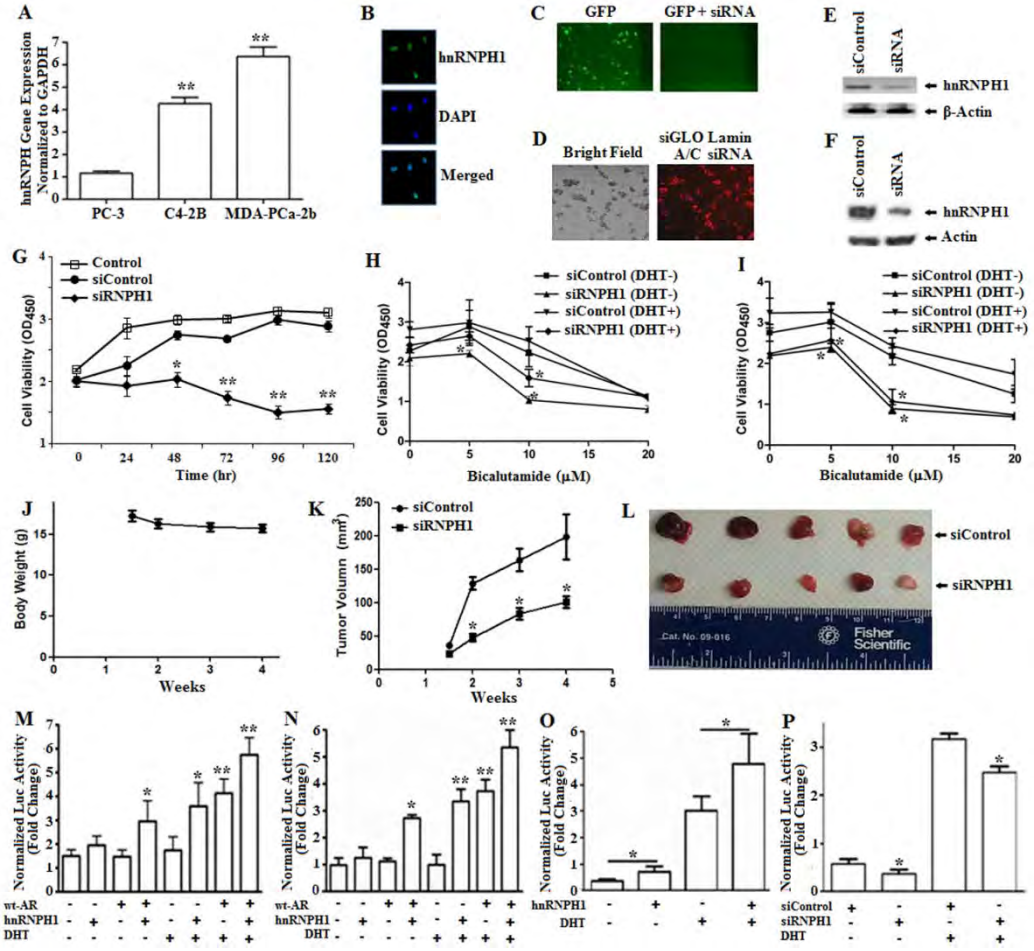
A
hnRNPH Gene Expression Normalized to GAPDH
PC-3
C4-2B
MDA-PCa-2b
B
hnRNPH1
DAPI
Merged
C
GFP
GFP + siRNA
D
Bright Field
siGLO Lamin A/C siRNA
E
siControl
siRNA
hnRNPH1
β-Actin
F
siControl
siRNA
hnRNPH1
Actin
G
Control
siControl
siRNPH1
Cell Viability (OD450)
Time (hr)
H
siControl (DHT-)
siRNPH1 (DHT-)
siControl (DHT+)
siRNPH1 (DHT+)
Cell Viability (OD450)
Bicalutamide (μM)
I
siControl (DHT-)
siRNPH1 (DHT-)
siControl (DHT+)
siRNPH1 (DHT+)
Cell Viability (OD450)
Bicalutamide (μM)
J
Body Weight (g)
Weeks
K
siControl
siRNPH1
Tumor Volumn (mm3)
Weeks
L
siControl
siRNPH1
Cat. No. 09-016
Fisher Scientific
M
Normalized Luc Activity (Fold Change)
wt-AR
hnRNPH1
DHT
N
Normalized Luc Activity (Fold Change)
wt-AR
hnRNPH1
DHT
O
Normalized Luc Activity (Fold Change)
hnRNPH1
DHT
P
Normalized Luc Activity (Fold Change)
siControl
siRNPH1
DHT

Fig. 5

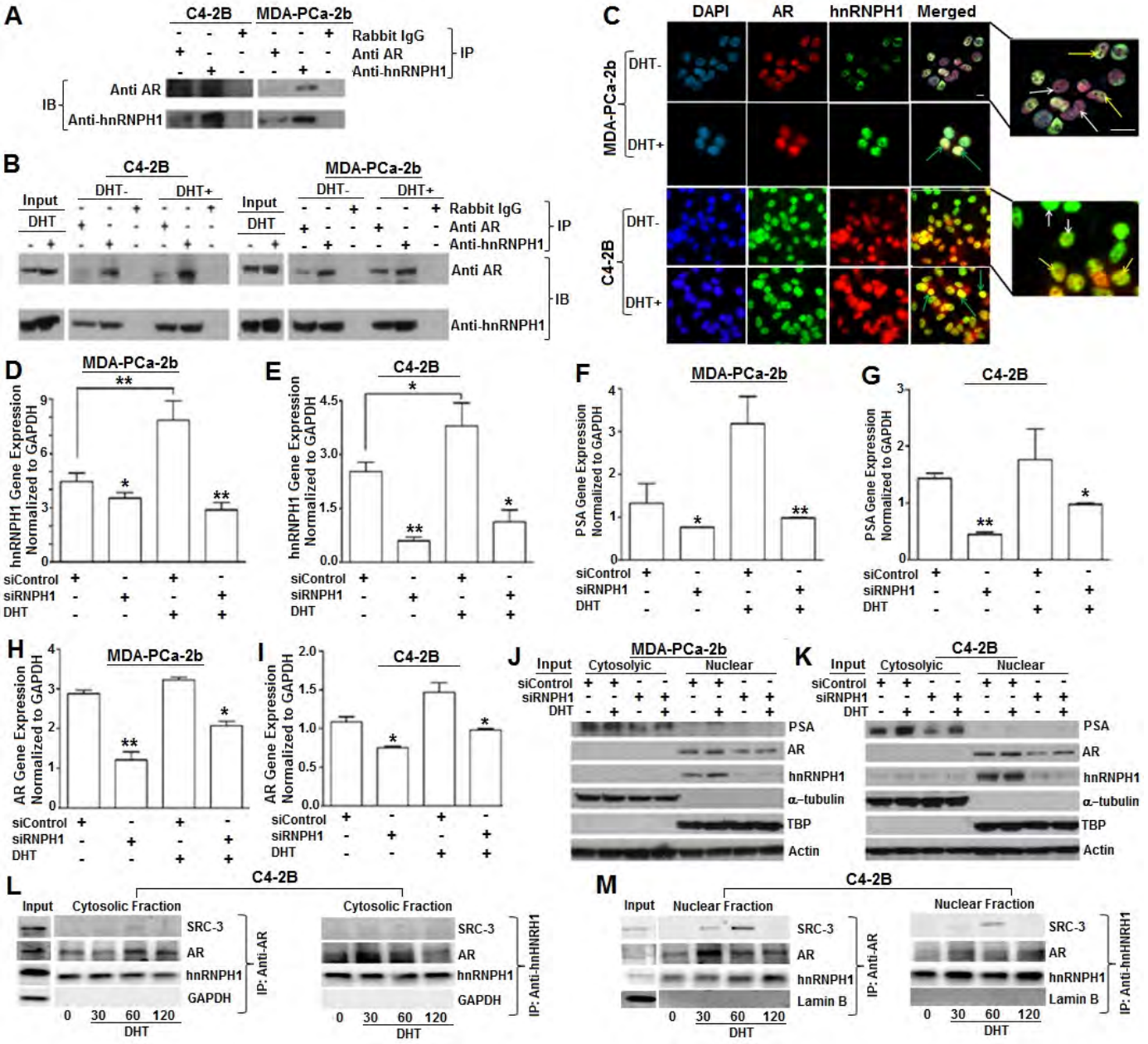
A
C4-2B
MDA-PCa-2b
Rabbit IgG
Anti AR
Anti-hnRNPH1
IP
IB
Anti AR
Anti-hnRNPH1
B
C4-2B
MDA-PCa-2b
Input
DHT
DHT-
DHT+
Rabbit IgG
Anti AR
Anti-hnRNPH1
IP
IB
Anti AR
Anti-hnRNPH1
C
DAPI
AR
hnRNPH1
Merged
MDA-PCa-2b
C4-2B
DHT-
DHT+
D
MDA-PCa-2b
hnRNPH1 Gene Expression Normalized to GAPDH
siControl
siRNPH1
DHT
E
C4-2B
hnRNPH1 Gene Expression Normalized to GAPDH
siControl
siRNPH1
DHT
F
MDA-PCa-2b
PSA Gene Expression Normalized to GAPDH
siControl
siRNPH1
DHT
G
C4-2B
PSA Gene Expression Normalized to GAPDH
siControl
siRNPH1
DHT
H
MDA-PCa-2b
AR Gene Expression Normalized to GAPDH
siControl
siRNPH1
DHT
I
C4-2B
AR Gene Expression Normalized to GAPDH
siControl
siRNPH1
DHT
J
MDA-PCa-2b
Input
Cytosolyic
Nuclear
siControl
siRNPH1
DHT
PSA
AR
hnRNPH1
α–tubulin
TBP
Actin
K
C4-2B
Input
Cytosolyic
Nuclear
siControl
siRNPH1
DHT
PSA
AR
hnRNPH1
α–tubulin
TBP
Actin
L
C4-2B
Input
Cytosolic Fraction
Cytosolic Fraction
SRC-3
AR
hnRNPH1
GAPDH
IP: Anti-AR
IP: Anti-hnHNRH1
0 30 60 120
DHT
M
C4-2B
Input
Nuclear Fraction
Nuclear Fraction
SRC-3
AR
hnRNPH1
Lamin B
IP: Anti-AR
IP: Anti-hnHNRH1
0 30 60 120
DHT

Figure 6

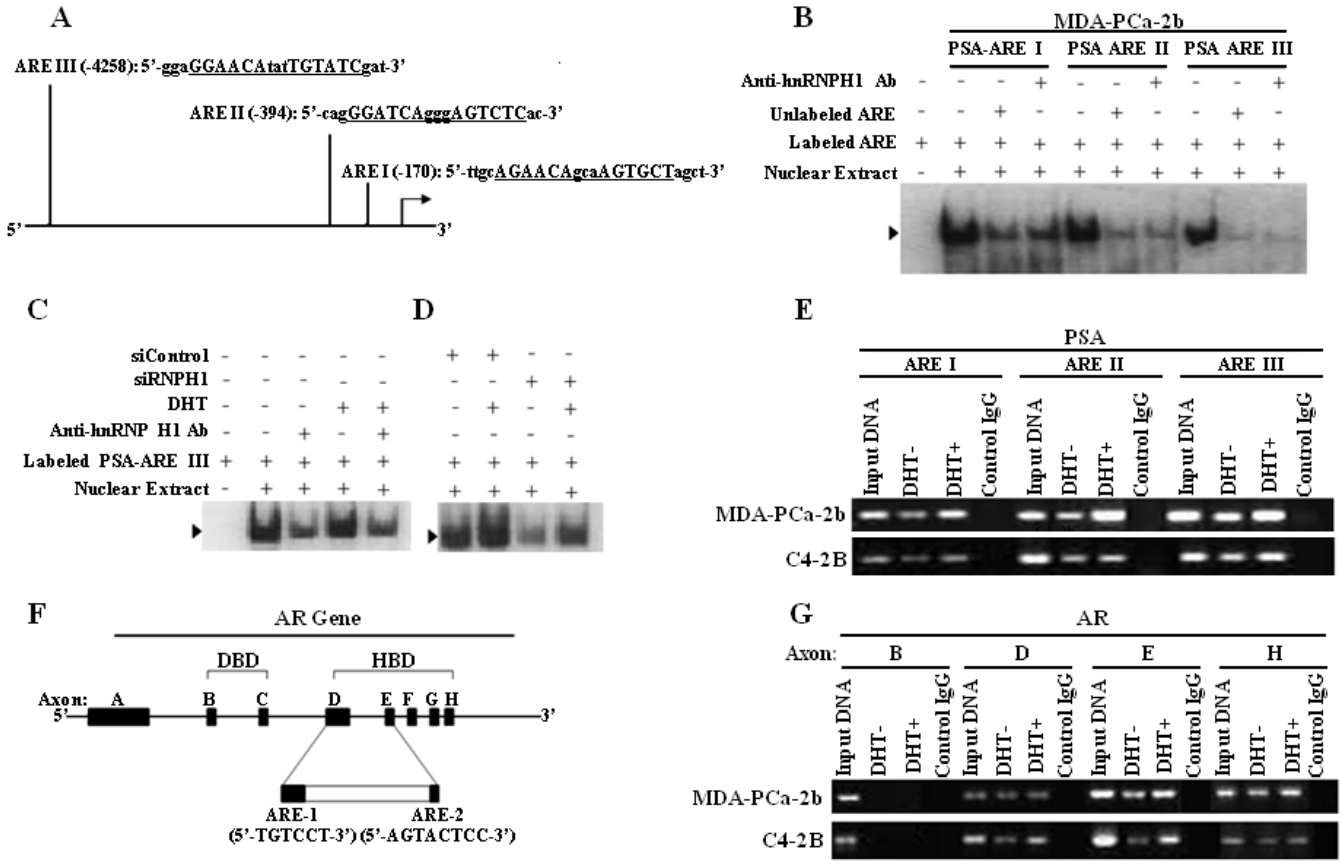
A
ARE III (-4258): 5'-ggaGGAACAtatTGTATCgat-3'
ARE II (-394): 5'-cagGGATCAgggAGTCTCac-3'
ARE I (-170): 5'-ttgcAGAACAgcaAGTGCTagct-3'
5'
3'
B
MDA-PCa-2b
PSA-ARE I
PSA ARE II
PSA ARE III
Anti-hnRNPH1 Ab
Unlabeled ARE
Labeled ARE
Nuclear Extract
C
D
siControl
siRNPH1
DHT
Anti-hnRNP H1 Ab
Labeled PSA-ARE III
Nuclear Extract
E
PSA
ARE I
ARE II
ARE III
Input DNA
DHT-
DHT+
Control IgG
MDA-PCa-2b
C4-2B
F
AR Gene
DBD
HBD
Axon:
A
B
C
D
E
F
G
H
5'
3'
ARE-1
(5'-TGTCCT-3')
ARE-2
(5'-AGTACTCC-3')
G
AR
Axon:
B
D
E
H
Input DNA
DHT-
DHT+
Control IgG
MDA-PCa-2b
C4-2B

Supporting Figures

hnRNPH1 Promotes Prostate Tumorigenesis and Hormone Resistance Through Transcriptional Upregulation and Activation of Androgen Receptor: Potential Role in Racial Disparities of Prostate Cancer

Yijun Yang*[1], Dingwu Jia*[1], Zakaria Y. Abd Elmageed[1], Hogyoung Kim[1], Kommu N. Mohan[1], Rodney Davis[6], Sudesh Srivastav[7], Krzysztof Moroz[2,5], Byron E. Crawford[2], Krishnarao Moparty[1,8], Raju Thomas[1,5], Robert S. Hudson[9], Stefan Ambs[9] and Asim B. Abdel-Mageed[1,3,5**]

[1]Department of Urology, [2]Department of Pathology, [3]Department of Pharmacology, [4]Department of Medicine, and [5]Tulane Cancer Center, Tulane University School of Medicine, New Orleans, LA 70112

[6]Department of Urology, **University of Arkansas for Medical Sciences, Little Rock, Arkansas 72205**

[7]Department of Biostatistics, Tulane University School of Public Health and Tropical Medicine, New Orleans, LA 70112

[8]Division of Urology, Southeast Louisiana Veterans Health Care System (SLVHCS), New Orleans, LA 70112

[9]Laboratory of Human Carcinogenesis, National Cancer Institute, NIH, Bethesda MD, 20892-4258

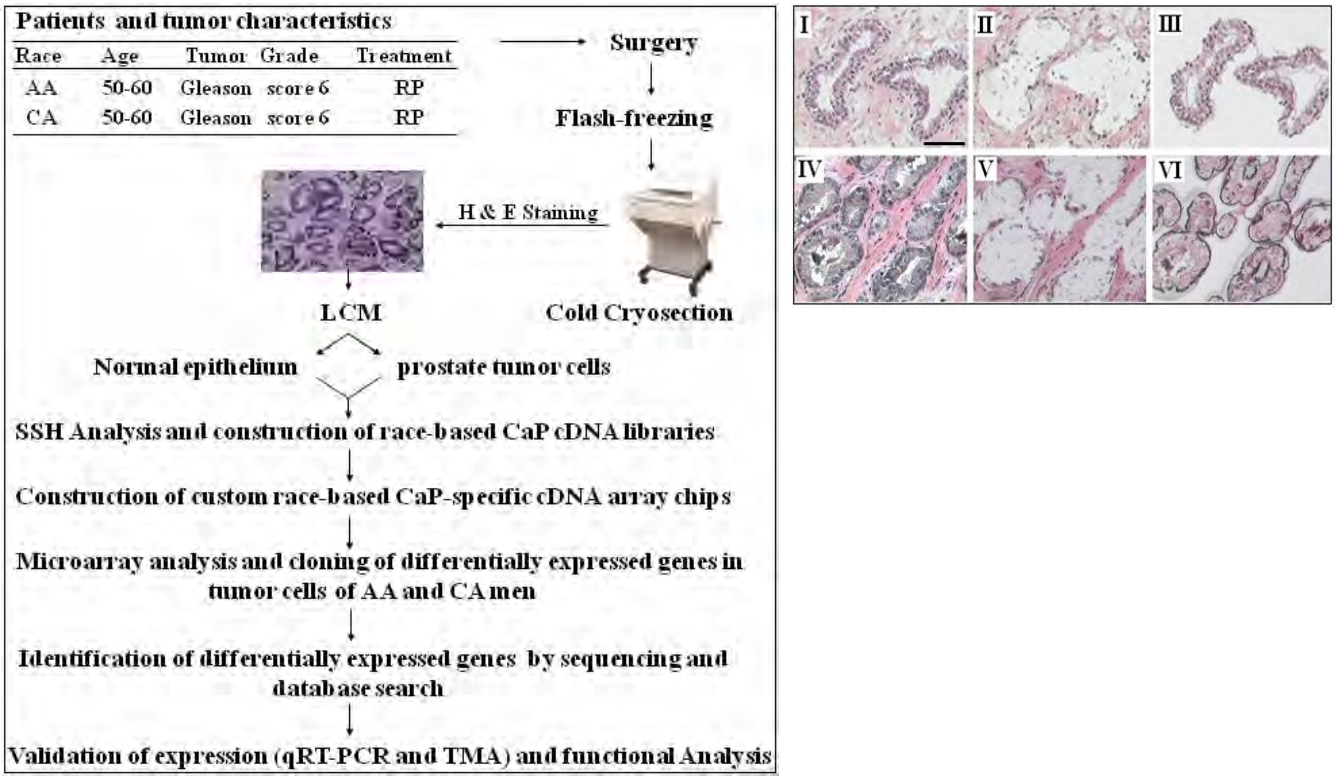

Figure S1. Schematic representation of the functional genomics approach employed. A) Schematic representation of the functional genomics approach employed for identification, and functional characterization of differentially expressed genes in prostate tumor cells of AA and CA men (n=10). To construct *in vivo* race-based, CaP-specific subtracted cDNA libraries, flash-frozen biopsies surgically derived from age (50-60 years) and tumor grade (Gleason 6)-matched AA and CA men who underwent radical prostatectomy (RP) were sectioned and H & E stained. Matched LCM-procured normal epithelium and tumor cells in each section were subjected to SSH analysis to generate cDNA libraries for construction of custom race-based, CaP-specific cDNA microarray chips. Differentially expressed genes were determined by microarray analysis using probes of LCM-harvested normal and tumor cells. Target genes were identified by cloning, sequencing and verified by qRT-PCR and TMA analyses. **B)** Representative high magnification digital images of H & E stained, flash-frozen sections used for orientation of morphologically identifiable normal epithelium (I) and prostate tumor cells (IV) before (II & V) and after (III & VI) LCM harvest. Scale bars represent 20 μm.

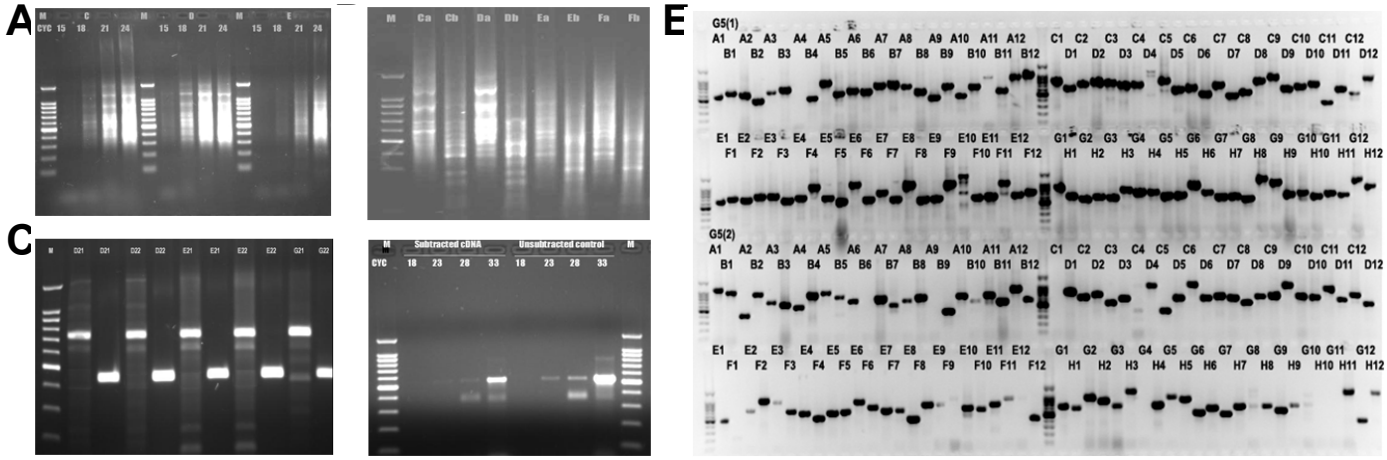

Figure S2. Suppressive subtractive hybridization (SSH) and construction of race-based prostate tumor specific cDNA libraries. **A**) cDNA synthesis and optimization of LD-PCR. **B**) ds cDNA synthesis before and after *Rsa*I digestion. **C**) Analysis of ligation efficiency using Adaptor 1 and 2R primers in presence of forward and reverse primers of GAPDH. **D**) Analysis of subtraction efficiency in prostate tumor cells versus unsubtracted controls. **E**) A representative stained gel depicting PCR amplification of subtracted library of LCM procured prostate tumor cells of each AA and CA tissue section utilized in the study.

A

Gene	GenBank	3'UTR position on mRNA	Target Site	Score	Prediction algorism
hnRNPH1	NM_005520	22-28	3' ugucaagaaguugacCGUCGAa 5' hsa-miR-22 5' aaggagcagugaacaGCAGCUa 3' HNRNPH1	0.7739	TargetScan Ver. 6.2, microRNA.org & MicroCosm Targets Ver. 5
		331-337	3' ccggcacugaccucUGACAAu 5' hsa-miR-212 5' cugaguaaacuauaACUGUUa 3' HNRNPH1	0.5759	
		331-337	3' gcugguaccgacaucUGACAAu 5' hsa-miR-132 5' gcugaguaaacuauaACUGUUa 3' HNRNPH1	0.5759	
		548-555	3' uucuUCACGUGGUACAAACAAa 5' hsa-miR-495 5' aaacAUUUUGGCAUGUUUGUUa 3' HNRNPH1	0.6341	

B

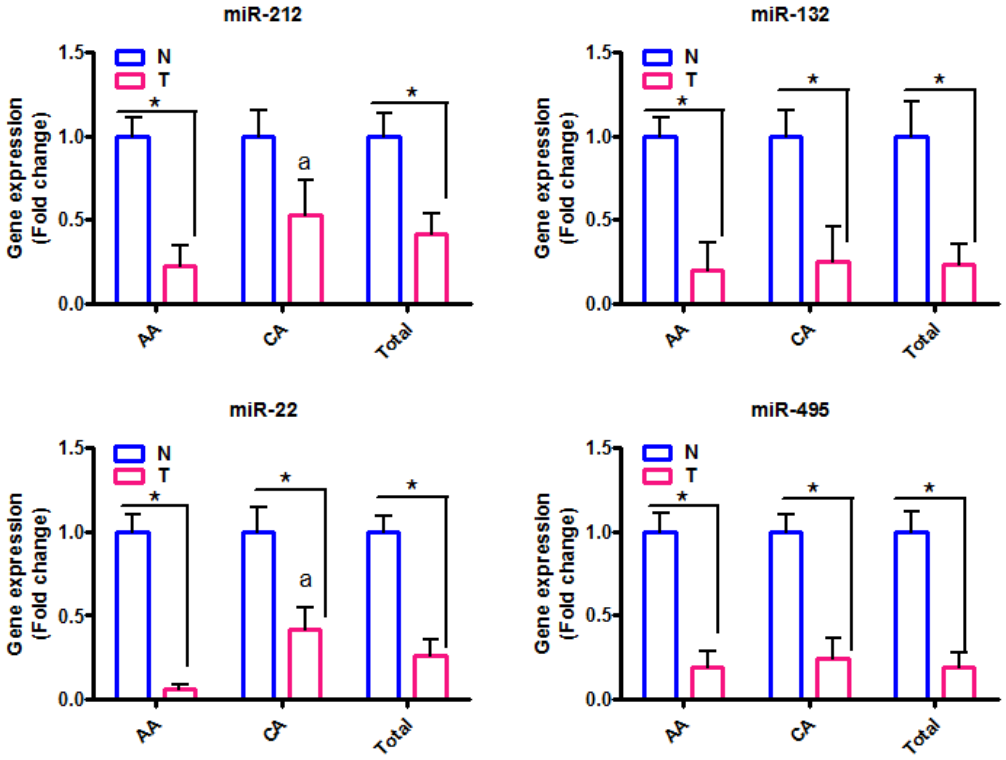

Figure S3. hnRNPH1-related microRNA expression in human PC human speciemns. A) List of putative binding sites on hnRNP H1 by four miRNAs (miR-22, miR-122, miR-132, and miR-495) based on miRNA target scan and miRanda analyses. **B**) RNA was extracted from 12 flash-frozen microdissected prostate tumors and normal adjacent gland, analyzed for miRNA expression by qRT-PCR and compared among AA and CA men. Fold change was calculated relative toU6 as an internal control. * and "a" denote significance at $P<0.05$ in tumor cells relative to control glands and AA tumor cells, respectively.

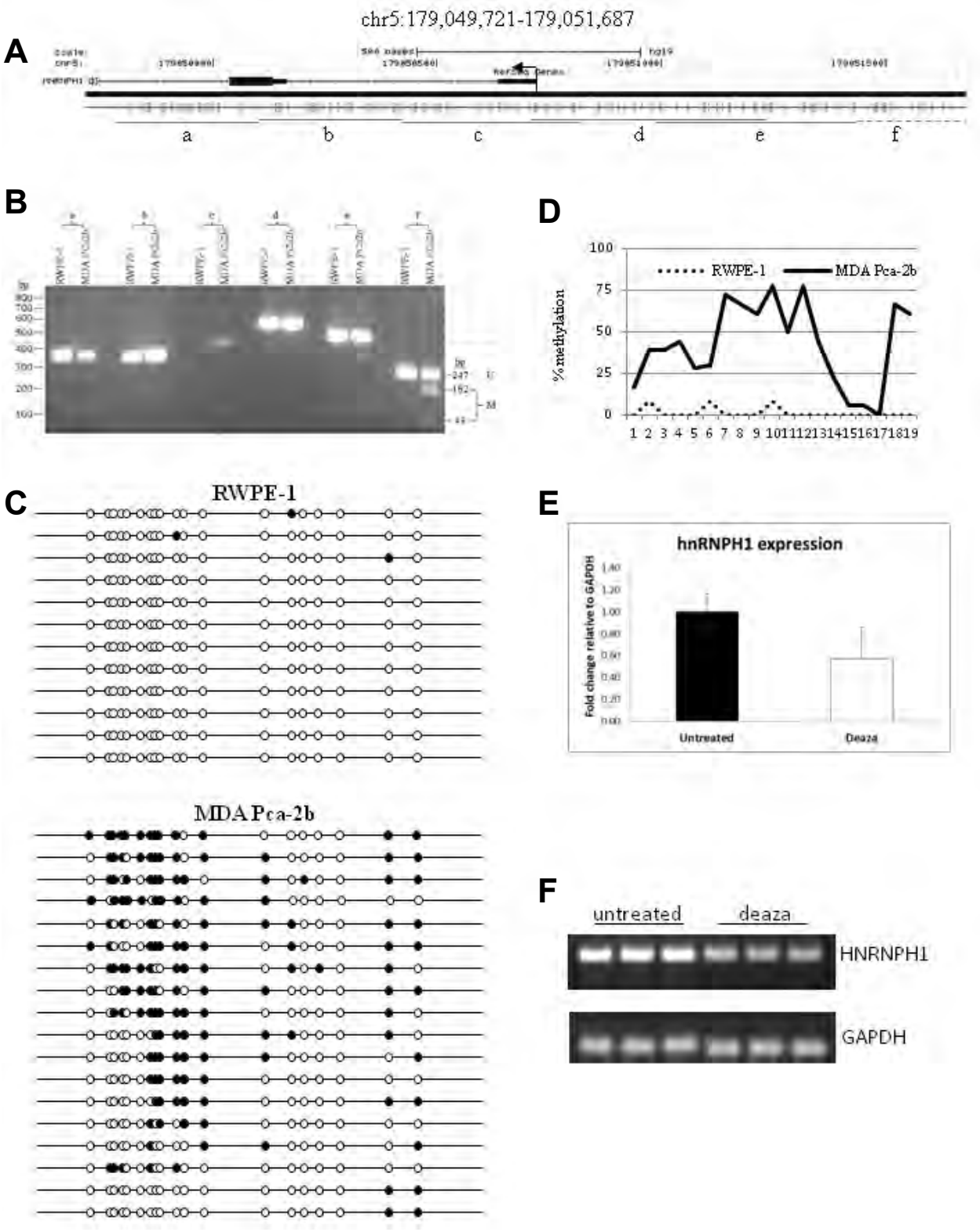
A
chr5:179,049,721-179,051,687
a
b
c
d
e
f
B
C
RWPE-1
MDA Pca-2b
D
RWPE-1
MDA Pca-2b
% methylation
E
hnRNPH1 expression
Fold change relative to GAPDH
Untreated
Deaza
F
untreated
deaza
HNRNPH1
GAPDH

Figure S4. Analysis of DNA methylation in the hnRNPH1 promoter-CpG island. A) Organization of the hnRNPH1 promoter CpG island. The CpG island is 1796 bp long (hg19; Chr5: 179049816-179051611) with the transcription start site located approximately in the middle. Lines named a-f display the regions of amplification by bisulfite PCRs for studying methylation using combined bisulfite restriction analysis (COBRA) and bisulfite genomic sequencing. Region f, shown as dashed line shows a difference in methylation between MDA PCa-2b and RWPE-1 cell lines. **B**) COBRA of different regions of the hnRNPH1 promoter-CpG island in MDA PCa-2b and RWPE-1 cell lines. About half of the product from region f is digested by *Bst*UI in MDA PCa-2b but not in RWPE-1, suggesting that this region is hypermethylated in the former. No significant difference was observed for the other regions. U: unmethylated DNA, M: fragments from methylated DNA. For more details on fragment sizes for all the regions, see Supplementary Table 1. **C**) Bisulfite genomic sequencing of region f from MDA PCa-2b and RWPE-1. This region (247 bp) contains 19 CpGs shown as vertical lines at the top. Twelve clones from RWPE-1 and 18 clones from MDA PCa2 were sequenced. Methylated CpGs are shown as filled circles and unmethylated CpGs as clear circles. **D**) Summary of bisulfite genomic sequencing data for the two cell lines. Fourteen out of 19 CpGs studied show more than 25% increase in methylation for MDA PCa2-b cell line. **E**) qRT-PCR analysis of GAPDH and hnRNPH1 in untreated MDA PCa2b control cells and cells treated with 5-Aza-2′-deoxycytidine (Deaza).

.

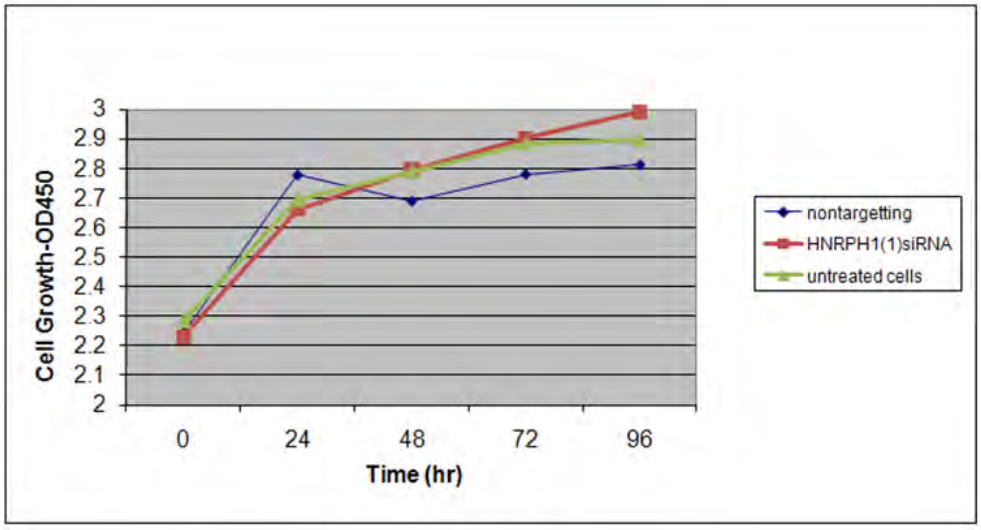

Figure S5. Growth of hnRNP H1 siRNA-silenced PC-3 cells. The cells were transfected with siControl or hnRNP H1 siRNA and subsequently cultured in RPMI-1640 medium supplemented with 10% FBS. Cell growth was monitored by a cell counting (WST) assay kit for up to 120 hr.

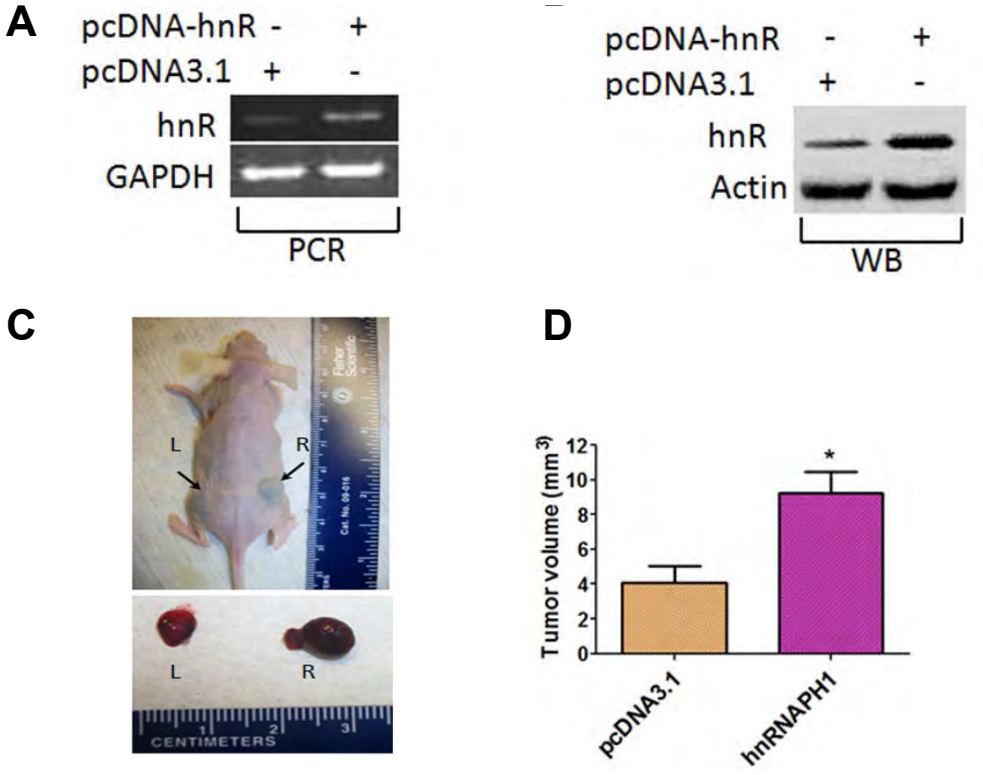

Figure S6. hnRNP H1 promotes tumor formation by LNCaP cells in nude mice. The androgen dependent LNCaP cells were transfected with control pcDNA3.1 or hnRNPH1 expression plasmid and stable cell clones were examined for hnRNPH1 expression by PCR (**A**) and immunoblot (**B**) analyses. **C**) Four-week old BALB/cAnNCr-*nu*/*nu* mice (*n*=5) were transplanted s.c. with control plasmid (left flank) and hnRNPH1-expressing LNCaP (right flanks) cells. **D**) Animals were sacrificed and resected tumor volumes were measured. * denotes significance at $P<0.05$ relative to control tumors.

Supporting Tables

hnRNPH1 Promotes Prostate Tumorigenesis and Hormone Resistance Through Transcriptional Upregulation and Activation of Androgen Receptor: Potential Role in Racial Disparities of Prostate Cancer

Yijun Yang*[1], Dingwu Jia*[1], Zakaria Y. Abd Elmageed[1], Hogyoung Kim[1], Kommu N. Mohan[1], Rodney Davis[6], Sudesh Srivastav[7], Krzysztof Moroz[2,5], Byron E. Crawford[2], Krishnarao Moparty[1,8], Raju Thomas[1,5], Robert S. Hudson[9], Stefan Ambs[9] and Asim B. Abdel-Mageed[1,3,5**]

[1]Department of Urology, [2]Department of Pathology, [3]Department of Pharmacology, [4]Department of Medicine, and [5]Tulane Cancer Center, Tulane University School of Medicine, New Orleans, LA 70112
[6]Department of Urology, University of Arkansas for Medical Sciences, Little Rock, Arkansas 72205
[7]Department of Biostatistics, Tulane University School of Public Health and Tropical Medicine, New Orleans, LA 70112
[8]Division of Urology, Southeast Louisiana Veterans Health Care System (SLVHCS), New Orleans, LA 70112
[9]Laboratory of Human Carcinogenesis, National Cancer Institute, NIH, Bethesda MD, 20892-4258

Table S1. Patient characteristics and histopathological features of the ethnicity-based TMA-4 tissue cores

Race	Age (years)					Total Number
	Range			Mean		
AA	45-74			59.6		148
CA	49-73			62.7		152
	Stage (*n*)					
	pT1		pT2		pT3	
AA	2		122		24	
CA	2		98		52	
	Gleason Score (*n*)					
	5	6	7	8	9	
AA	5	45	84	8	6	
CA	2	49	89	6	8	
	PSA Recurrence-Free (Ave Months)					
AA			35.9			
CA			45.6			

Table S2: Primers for Combined Bisulfite Restriction Analysis of hnRNP H1 promoter-CpG island

Forward	Reverse	Amplified Region	Size
GGTTTTGATTGTTTTGGGGT	TCTTAAATTTTAAACAATACTACTAAAA	>hg19;chr5:179051441-17905168	247bp
TTTTTATGGGATTGTATAGGAGTTT	CCCCAAAACAATCAAAACCTAC	>hg19;chr5:179051013-179051462	449bp
TAATTTAAATAAGGTTTTTTGTG	ACAATCTACAACTAACCAACTTC	>hg19;chr5:179050688-179051214	526bp
AAAGTTGTTTTGAGTAATAGTTGT	AAAAAACCTTATTTAAATTAC	>hg19;chr5:179050322-179050712	397bp
TTTTAGTTTTAATTTATTAGAAAAA	ACTCAAAACAACTTTAAAAATCC	>hg19;chr5:179050019-179050340	321bp
AAAAAGATATTTATAAAAGAAAAGTTGGTG	TTTTCTAATAAATTAAAACTAAAAC	>hg19;chr5:179049720-179050045	325bp

Table S3: qRT-PCR primers

Name	Forward	Reverse
hnRNP H1	5'-GGTGAAGCAGATGTCGAG-3	5’-GCTCCTTGGTTACCTATGC-3’
AR	5'-CCTGGCTTCCGCAACTTACAC-3'	5'-GGACTTGTGCATGCGGTACTCA-3'
PSA	5’-CCTCCTGAAGAATCGATTCCT-3	5’-CGTCCAGCACACAGCATGAA-3’
β-actin	5’- GCCGATCCACACGGAGTACT-3	5'-GGCACCCAGCACAATGAAG-3
GAPDH	5’-GAGTCAACGGATTTGGTCGT-3’	5’-TTGATTTTGGAGGGATCTCG -3’

Table S4. Double-stranded oligonucleotides used in gel retardation analysis

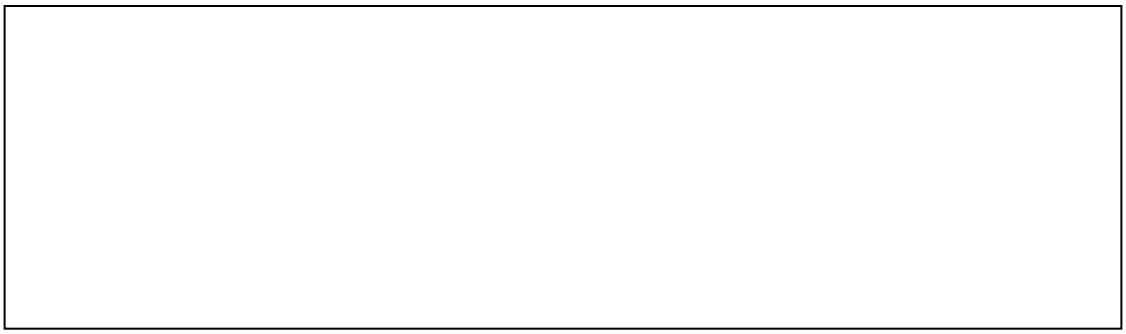

Table S5. PCR primer sets used in ChIP analysis.

Name	Forward	Reverse
PSA-ARE I (Proximal promoter)	5'-TCTGCCTTTGTCCCCTAGAT-3'	5'- AACCTTCATTCCCCAGGACT-3'
PSA-ARE II (Distal Promoter)	5'-CCACAAGATCTTTTTATGATGACAG-3'	5'-GCTCATGGAGACTTCATCTAG-3'
PSA-ARE III (Enhancer)	5'-GGTGACCAGAGCAGTCTAGGTG-3'	5'-TGTTTACTGTCAAGGACAATGGAT-3'
AR-Exon B	5'-CCTAAGTTATTTGATAGGGCCTTG-3'	5'-GCCTGCAGGTTAATGCTGAAGACC-3'
AR-Exon D	5'-GATCCCCCTTATCTCATGCTCCC-3'	5'-GGAGTTTAGAGTCTGTGACCAGG-3'
AR-Exon E	5'-AGCTTCACTGTCACCCCATCACCATG-3'	5'-CAACCCGTCAGTACCCAGACTGACG-3'
AR-Exon H	5'-GGAACATGT TCATGACAGACTGTA-3'	5'- GAG GCC ACG TCG TTG TCA CTG- 3'

Table S6: Patient characteristics and histopathological features of specimens used for analysis of miRNA expression by qRT-PCR analysis

		AA	CA	Total
Age (year)	Mean ± SD	56.14 ± 5.87	59.47 ± 6.48	57.96 ± 6.34
	N	13	17	30
Gleason score	<7	4	3	7
	7	5	7	12
	>7	5	6	11
PSA	Mean ± SD	5.07 ± 2.19	4.43 ± 1.86	5.66 ± 2.36
Tumor grade	T2b	1	1	2
	T2c	10	7	17
	T3a	2	5	7
	T3b	1	3	4

Table S7: miRNA primer sets

	miRNA	Target Sequence
1	hsa-miR-22	AAGCUGCCAGUUGAAGAACUGU
2	hsa-miR-132	UAACAGUCUACAGCCAUGGUCG
3	hsa-miR-212	UAACAGUCUCCAGUCACGGCC
4	hsa-miR-495	AAACAAACAUGGUGCACUUCUU